Zentrum
für Biodiversität und Nachhaltige Landnutzung

Sektion
Biodiversität, Ökologie und Naturschutz

– Centre of Biodiversity and Sustainable Land Use –
Section: Biodiversity, Ecology and Nature Conservation

Long-term vegetation dynamics along altitudinal and longitudinal gradients in the Hyrcanian forest region (northern Iran)

The role of climate, fire and anthropogenic impacts during the late Quaternary

Dissertation
for the award of the degree
"Doctor of Philosophy" (Ph.D. Division of Mathematics and Natural Sciences)
of the Georg-August-Universität Göttingen

within the doctoral program Biodiversity and Ecology

Submitted by

Leila Homami Totmaj
from Tehran (Iran)
Göttingen, 2021

Thesis committee

Prof. Dr. Hermann Behling
(Department of Palynology and Climate Dynamics / Albrecht-von-Haller Institute for Plant Sciences)

Prof. Dr. Erwin Bergmeier
(Department of Vegetation and Pyhtodiversity Analysis / Albrecht-von-Haller Institute for Plant Sciences)

Dr. Thomas Giesecke
(Department of Palynology and Climate Dynamics / Albrecht-von-Haller Institute for Plant Sciences)

Members of the examination committee

Prof. Dr. Hermann Behling
(Department of Palynology and Climate Dynamics / Albrecht-von-Haller Institute for Plant Sciences)

Prof. Dr. Erwin Bergmeier
(Department of Vegetation and Pyhtodiversity Analysis / Albrecht-von-Haller Institute for Plant Sciences)

Dr. Thomas Giesecke
(Department of Palynology and Climate Dynamics / Albrecht-von-Haller Institute for Plant Sciences)

Prof. Dr. Daniela Sauer
(Department of Geography - Section Physical Geography)

Prof. Dr. Alexander Schmidt
(Department of Geobiology / Evolution of Landplants & Development of Terrestrial Ecosystem)

Prof. Dr. Dirk Hölscher
(Tropical Silviculture and Forest Ecology, Burckhardt Institute)

Date of oral examination: 16.12.2021

With LOVE dedicated to my beloved soulmate

Hamid Moradian

Acknowledgments

Studying PhD in the Department of Palynology and Climate Dynamics was a remarkable opportunity in my life, and I owe this opportunity to Professor Hermann Behling. I would like to send my endless gratitude to my best supervisor “Prof. Behling” for all his patience, support, and guidance. During these three years, I learned a lot about palaeoecology and palynology. Besides study, I also learned a lot from his humility, patience, and kindness, and I thank you, dear Professor, for your amiable attitude and constant support.

I also would like to express my gratitude to my Bachelor, Master, and forever supervisor “Prof. Shahin Zarre” from the University of Tehran, who helped me get on this path.

A special thanks also goes to Dr. Sina Alizadeh for all the support, help, and encouragement for my work and private life. I am very much appreciative that you introduced palaeoecology into my life. Your patience and constant support helped me to develop a scientific way of thinking and working in the last three years.

I would also like to mention my appreciation for Dr. Panthea Giahchi and Mr. Pouya Amani, from the Ministry of Industries and Mines Geological Survey of Gilan, for their kindness on our excursions, which was not possible to do coring without their help.

I also, give thanks to my co-supervisor, Dr. Thomas Giesecke, for his scientific helps on R software and Prof. Erwin Bergmeier for his support and to the Deutsche Forschungsgemeinschaft (DFG) for the financial supports provided throughout my PhD.

I would also like to acknowledge my colleagues, especially Ekaterina Lukanina, Dr. Kartika Anggi Hapsari, and Caio Alves de Moraes for the wonderful memories and hard work put in together, it was a lovely time with all of you. I am so happy to have met you all and very much grateful that you were always open to discussions as well as scientific and non-scientific activities.

I would also like to express my gratitude to my lovely family, who is far away, but who I miss deeply, beyond words can express. I have so much appreciation for my mother “Vida Nejati Namin” my father “Hashem Homami Totmaj” and my lovely brothers “Mohammad and Hamed” for their endless love and support.

To continue, I would like to express my gratitude to my little angel “Sogand”, born in the middle of my PhD journey and lighten up my life. Whenever I got tired, her beautiful eyes gave me extra power to continue. SOGAND MOMMY LOVES YOU

Finally, these last words are dedicated to my beloved soulmate “Hamid” who helped and supported me endlessly during my PhD journey. Hamidam (My Hamid), it is impossible to find the proper words to appreciate you and thank you. Simply and honestly, without you coming all this way would not have been possible. LOVE YOU.

Summary

As an Arcto-Tertiary species refugium, the Hyrcanian forest region of Iran, may play an important role in investigating paleoclimatic and palaeoecological changes. This narrow belt, located between the biggest lake of the world, the Caspian Sea, and the northern slopes of the Alborz Mountains, has distinctive biodiversity compared to other geographical parts of Iran. Although the uniqueness and importance of this region are not hidden to anyone, this region was not sufficiently investigated. Hopefully, paleoclimatologists and paleobotanists have increased their investigations on this area since the last decade while focusing more on the eastern and central parts. The Gilan province, the western part of the Hyrcanian region, is the least studied province, while is of high importance due to:

i) the extensive forests and wetlands which make an appropriate area to carry out palaeoecological studies

ii) the importance of its vegetation history that can provide new insights into the refugium hypothesis for the west Eurasian temperate deciduous forest as is the corridor that connects the isolated southern coast of the Caspian Sea to western Eurasia

iii) being the wettest among the Hyrcanian provinces, and its palaeoecology allows the comparison on an east-western precipitation gradient during the past

iv) having the largest remnant of the coastal fluvial forest

v) being home of the most ancient known human settlements in Iran

This multi-proxy paleoenvironmental research was carried out on three different areas from mid-elevated to high elevated areas of the Gilan province. Besides, paleoenvironmental studies of the modern vegetation in two different altitudinal gradients were investigated, utilizing palynology and DNA metabarcoding approaches.

The first record named Pounel (PNL) was retrieved from a mire in the highlands of the Gilan province (2280 m a.s.l.) located above the Hyrcanian forest. This study, which provides the oldest record from Gilan province, dates back to 4300 cal yr BP. The study represented the dominance of the steppe vegetation around the study area throughout the recorded period. Also, indicated wet climatic conditions between 4300 to 1700 cal yr BP. After 1700 cal yr BP until 1000 cal yr BP, vegetation cover was reduced with increased Cichorioideae and Amaranthaceae while trees decreased significantly at lower elevations. Together with increased values of K and Ti, drier conditions and/or increment of the anthropogenic activities are suggested. Since the last 1000 years, the higher frequency of Poaceae and Cyperaceae as well as the recovery of

forest suggested wetter conditions. However, the still frequent Cichorioideae and *Plantago lanceolata* along with *Sordaria* may reflect continued intense livestock grazing at this study area.

The second record investigated the Kholash-Kouh lake (KHL), located above the forest line (at 2000 m a.s.l.), reconstructed the vegetation, climate changes, local fire history, and anthropogenic role activities for the past 1245 cal yr BP. Based on the palynological reconstruction, the lake's surrounding (between ca. 1245-1030 cal yr BP) was covered mostly by Poaceae, *Artemisia*, and Amaranthaceae, indicative of open vegetation. The strong environmental disturbance is reflected by the high representation of human indicators and coprophilous spores. The high amount of macro-charcoal particles suggests widespread fire, resulting in a low proportion of arboreal vegetation. The dominance of the forest vegetation and the warmest condition are the most important characteristics of the period between 1030-730 cal yr BP. Lastly, between ca. 730-50 cal yr BP, arboreal vegetation replaced by herbs and evidenced the more open vegetation that may correlate with the Little Ice Age's cold and dry condition and/or the increased anthropogenic activities which occurred precisely during that period.

The third record, as the first report from the western mid-elevated area, applied multi-proxy studies to reconstruct environmental changes, represents a high-resolution study of Annal Lake (ANL) for the late Holocene period. The lake located at 700 m elevation in the Hyrcanian forest of the Gilan province recovered the last 1690 years ago. Based on the multi-proxy analysis, a mixed forest with *Alnus*, *Carpinus*, *Quercus*, and *Fagus* were present, as well as patches of grassland areas around the lake between ca. 1690-1450 cal yr BP. At ca. 1450 cal yr BP, the forest expanded and reduced the open grassland areas until 65 cal yr BP. Different proxies indicated that humans were present in the studied area since the beginning of the recorded period. However, since 65 cal yr BP, human impact increased markedly by deforestation and cattle grazing, and settlers probably changed from pastoralism to more farmers. Ratios of geochemical elements such as V/Cr, K/Al, Rb/Al, Si/Fe, and Ca/K suggested the warmest period with more rainfall and detrital inputs forming a shallow lake between ca. 1690 – 580 cal yr BP. In contrast, warm and wet conditions changed to cold and dry conditions after around 580 cal yr BP and remained prevailed until 250 cal yr BP. Finally, due to the XRF results, the last ca. 250 cal yr BP at ANL surroundings, was experienced the wettest and relatively stable climatic conditions.

The fourth and the last study investigated the modern pollen rain and forest inventory through altitudinal gradients in two different transects, from lowlands up to the slopes of the Alborz Mountains in Gilan province for the first time. The new method of DNA metabarcoding complemented the modern pollen rain data hired to investigate the representation of the vegetation along the two altitudinal transects. The capability of the DNA metabarcoding for vegetation survey was examined in this study, which emphasizes using a combination of the multi-locus approach of ITS2 and rbcL. Comparing the DNA base and pollen analytical results on the vegetation abundances around the collected samples indicated that a higher proportion of microscopy results was affected by the wind-pollinated families (such as Betulaceae and Fagaceae) due to their higher pollen production. While the results derived from DNA barcoding were more relevant to the actual vegetation cover.

Outline of the chapters

This thesis comprises five chapters:

Chapter 1

This chapter includes an introduction to the Hyrcanian region and previous studies related to the objectives of the current study. Also, it represented an overview of the study sites, a description of the methods, and the multi-proxy palaeoecological analyses.

The aims of this research were developed into four separate manuscripts to be published in peer-reviewed scientific journals. The published and submitted manuscripts are presented in Chapters 2 - 5:

Chapter 2

Four millennia of vegetation and environmental history above the Hyrcanian forest, northern Iran

This study provided the first study on the highlands of the Gilan province. With the help of the multi-proxy analysis, vegetation changes of the mire were examined for the last 4,300 years ago, under the influence of human activities and climate changes.

Chapter 3

Late Holocene paleoenvironmental changes inferred from multi-proxy studies of the Kholasht-Kouh Lake sediments in the Gilan mountains, northern Iran

The vegetation dynamics and climate changes were reconstructed using the palynological and geochemical records of the lake sediment core. In addition, the effects of the past climatic changes as well as anthropogenic activities on the south-eastern highlands of the Gilan province were reconstructed using palaeoecological proxies.

Chapter 4

Late Holocene Hyrcanian forest and environmental dynamics in the mid-elevated highland of the Alborz Mountains, northern Iran

The past vegetation, fire, climate dynamics, and human impact on the western mid-elevated area of the Hyrcanian forest were investigated applying the multi-proxy analysis for the last ca. 1700 cal yr BP.

Chapter 5

The contemporary vegetation of the western Hyrcanian forests was investigated in two different altitudinal transects for the first time utilizing the novel DNA metabarcoding technic and traditional pollen counting.

Chapter 6

In the final chapter, the main findings of the research synthesized, and future possible research aspects expressed.

Chapter 1: Introduction

1. Hyrcanian region

The Hyrcanian forest of Iran occurs between the northern slopes of Alborz and the southern coast of the Caspian Sea (CS) forming the 820 km long narrow belt which occupies 6% of the area in Iran. This region extends from the coastal area up to > 2000 m a.s.l. (Sabeti 1994; Talebi et al. 2014). However, above 2,000 m, the forests are mostly replaced by forest/steppe or steppe vegetation. The area covers approximately 1.9 million ha and consists of three provinces from west to east, namely Gilan, Mazandaran, and Golestan. This small belt hosts 3234 plant species, including ca. 500 endemic plants, and accounts for 44% of plant diversity (Akhani et al. 2010). Along with the forests of northern Anatolia, Hyrcanian forests constitute the most important refugia and the last relicts of broad-leaved deciduous forests that covered the temperate zones of the northern hemisphere before the Quaternary (Leroy and Roiron 1996; Ramezani et al. 2008). During the Pliocene, the Arcto-Tertiary flora covered the entire temperate zone of the northern hemisphere. This flora, however, became extinct in Europe and northern Asia during the Pleistocene. Studies suggest that the northern Iran, Caucasus, and the southern coast of the Black Sea, might act as a refugium for Arcto-Tertiary species (Browicz 1989). Therefore, this unique flora attracted many floristic researchers such as Rechinger (1963-1999, http://www.iranicaonline.org/articles/flora-iranica), who introduced many of the taxa in that area in Flora Iranica (in 178 volumes).

As the restricted area between mountains and Sea, the upper forest line and coastal vegetation have been subjected to pronounced changes due to temperature fluctuations, changes in the rainfall regime, and CS level changes, respectively, in space and time. In addition, due to extensive anthropogenic forces during the last centuries, vegetation has been modified significantly. Occurring in such changeable environmental conditions, investigating the Hyrcanian environmental history, including vegetation, plant diversity, climate, fire, and human impact, are of crucial importance. Unfortunately, so far, only a few palaeoecological records have been reported from the Hyrcanian region.

1.1. Palynological and palaeoecological research on the Hyrcanian region

The former studies on the environmental history of the area around the Caspian Sea (CS) can be categorized into five main topics. First, investigations on sea level are important for archaeology, palaeoecology, and the economy. Also, the large area of the coastal plain can be

inundated during high stands leading to disruption of coastal settlements and vegetation. Hence the most discussed topic has been referring to the **CS level changes**.

The **vegetation history of the coastal area**, as the second topic, has been investigated on the same palynological records used for sea-level changes. These studies provide insights into the changes in vegetation communities after sea-level fluctuations as well as the timing and effects of the early and the recent (intensified) human activities.

The third topic referred to the **vegetation history of the Alborz Mountains** to detect the dynamics of vegetation zones through altitudinal gradients under natural and anthropogenic forces. This topic has only been addressed in the central Hyrcanian region.

The fourth topic focuses on **the marine record from CS** available only from one study in the southern basin. This record contributed to a more regional understanding of the past environmental changes around the CS.

The last topic is **investigating modern vegetation/climate – pollen relationships** with palynological studies on surface samples that provide information on pollen productivity and dispersal of the main Hyrcanian arboreal taxa and afford an efficient tool for the interpretation of pollen records.

These studies are also essential to reconstruct a more reliable climatic condition based on palynological data. The main studies implemented are discussed below.

Sea level changes: The Caspian Sea Level (CSL) changes have been substantial in annual, decadal, and millennial scales. The annual rate of changes in CSL (ca. 34 cm) is 100 times higher than in the oceans (Kroonenberg et al. 2000). In only six decades, CS experienced a full sea-level cycle by the magnitude of 3 m (Cazenave et al. 1997). On a millennial scale, the change was about 160 meters between ca. +50 and ca. -110 m a.s.l. (during the Early Khvalynian-high stand and the Mangyshlak-low stand, respectively) (Rychagov 1997; Leroy et al. 2013a; Kakroodi et al. 2015). After the Mangyshlak low stand, the early to mid-Holocene CSL showed major fluctuations across different records with different timing. However, all records agree that the average CSL during the early to mid-Holocene was higher than its current level (-27 m a.s.l.). Rychagov (1997) recognized three transgressions with the magnitude of 2-7 m during the early to mid-Holocene as revealed by geological studies on deltas and terraces adjacent to the Azerbaijani coast of the CS. Similar trends have been inferred from palynological studies in the Volga Delta (Richards et al. 2014) and dinocysts and

sedimentological multi-proxy analyses on the sediments recovered from the south-eastern corner of the CS (Leroy et al. 2013a; Kakroodi et al. 2015). However, the two latter studies did not report the high stand of the CSL between ca. 6000 and 5000 uncal yr BP as reported by (Rychagov 1997). The dinocysts analysis on a marine core from the southern basin of CS (Leroy et al. 2013b) recognized the highest CSL between 8400 and 4400 cal yr BP that is partly in agreement with (Rychagov 1997) but almost is in contradiction to records from the south-eastern corner of the CS.

During the late Holocene, the CSL has experienced at least five sea-level cycles since the past 3260 years (Kakroodi et al. 2015), as reported from the Gomishan area in the south-eastern corner of CS. Among these fluctuations, however, two transgressions at ca. 2600 cal yr BP (Kroonenberg et al. 2007; Kakroodi et al. 2012, 2015) and during the Little Ice Age (Leroy et al. 2011; Kakroodi et al. 2012, 2015; Beni et al. 2013; Haghani et al. 2015; Ramezani et al. 2016) and a regression (Derbent low stand) during the Medieval Climate Anomaly (Hoogendoorn et al. 2005; Kakroodi et al. 2012; Beni et al. 2013; Richards et al. 2014) are the most agreed sea-level oscillations. The high stand during the Little Ice Age caused brackish water incursion 10 km inland in Gilan province. Consequently, soil salinization created a very narrow coastal plain, increased the abundance of steppe-type vegetation, and reduced the Hyrcanian forests (Haghani et al. 2015).

Oscillation in the discharge of the Volga river (which currently accounts for over 80% of the water influx into the CS), changes in evaporation from the sea surface, solar forcing, and tectonic movements have been introduced as the main drivers of CSL changes (Kroonenberg et al. 2007; Richards et al. 2014).

As this short review shows, long records covering the Holocene CSL changes are missing from central and western areas of southern CS coasts. In Gilan, with the old evidence of human settlement (Fallahian 2013), such long records of CSL changes can provide helpful information for archaeological and palaeoecological studies.

Vegetation history of the coastal plain: is subdivided into western, central, and eastern coasts. Western coast (Gilan province): Two short cores with approximately 350 years of age have been recovered from Anzali and Amirkola lagoons (Leroy et al. 2011). The pollen diagram of Anzali starting at ca. AD 1670 illustrates a stable vegetation history around the lagoon with some representatives of the lower slopes of the Alborz Mountains. Slight but continuous human activities are detectable in the Anzali record. In the small lagoon of Amirkola, the dense alder

(*Alnus glutinosa*) wetland forest has been temporarily disturbed by fire, followed by the expansion of rice fields from AD 1720 to 1800, indicating more extensive human activities near this lagoon.

An approximately 650-year old sediment core was recovered from Langarud wetland located 10 km inland (Haghani et al. 2015). The record indicated the reduction of the alder swamp after the brackish water incursion at the early Little Ice Age. Also, it indicated unsuitable conditions for agriculture activities due to the salinity of the soils.

Another report published recently (Gu et al. 2021) has applied multiproxy analysis, such as pollen, macro-charcoal, and X-ray fluorescence analysis on Zarbijar wetland with the aim of past vegetation reconstruction, regional climate dynamics, fire events, and anthropogenic effects on the coastal region of Gilan. The mentioned study provided evidence of the ecosystems affected extremely by the anthropogenic activities on the coastal plain of the south-western Caspian Sea during the last 600 years. Intensified anthropogenic activities during the past centuries, such as agriculture, construction, and human-induced fires, played an important role in the decline of the Hyrcanian forest.

Central Coast (Mazandaran province): The Mazgah mire documented the last 3000 years' vegetation dynamics of the central Caspian lowlands and Alborz foothills (Ramezani et al. 2016). The high values of *Alnus* pollen together with diverse non-pollen palynomorphs indicated that wet eutrophic to mesotrophic alder swamp was present mostly during the record. However, tree growth was hampered by inundation due to the CSL high stand at ca. 2600 cal yr BP. After ca. 1200 cal yr BP, pollen grains of the major component in the vegetation composition of the Caspian lowland (Wingnut (*Pterocarya fraxinifolia*)) strongly decreased, most probably due to a drier or colder climate. The first signal of anthropogenic activity in the area can be inferred from the pollen of *Juglans regia* at ca. 2350 cal yr BP and slightly later of *Fagopyrum esculentum*. A marked decrease in arboreal pollen during the last centuries suggests that both lowland and upland forests near the mire have been replaced by open vegetation, most probably by humans.

Eastern Coast (Golestan province): A sediment core collected by (Leroy et al. 2013a) from the southeast corner of the CS allows reconstruction of vegetation history in CS coastal plain and Alborz foothills since 10640 cal yr BP. The record demonstrates a delay in woodland expansion at the beginning of the Holocene. The succession of the main tree species out of their refugia has been established as deciduous *Quercus*, *Carpinus betulus*, *Parrotia persica*, *Fagus*

orientalis, and *Pterocarya fraxinifolia*. This succession presents a close relation to the south European interglacial of the Early Pleistocene and suggests a similarity in climate. The decline in *Pterocarya* is documented since ca. 1500 cal yr BP. The human activities during the Sasanian Empire and the subsequent drier climate contributed to the contraction of the *Pterocarya* population (Leroy et al. 2013a).

A sediment core, taken from the Kongor Lake (Shumilovskikh et al. 2016) in the center of eastern Gorgan Plain covering 6100 to 800 cal yr BP, suggests a dry period between 5900 and 3900 cal yr BP and an increase in regional humidity afterward with a maximum between 2700 and 700 cal yr BP. The study indicates that the eastern part of the Gorgan Plain was characterized by open steppe landscapes during the last 6000 years. The most extensive human influence on the landscapes around the Kongor site is documented during the Parthian and Sasanian Empires (200 BC–651 AD) and the Islamic era until the attack of the Mongol people.

The latest report from the eastern coast (Leroy et al. 2019) provides comprehensive investigation, including palynology, archaeology, CSL changes, and faunal and botanical evidence back to the Pleistocene-Holocene transition. The sequences of Shahkileh and Gharasoo represented a period of high CS levels for the Late Pleistocene. The Shahkileh core evidenced a decline in herbivore grazing indicators, high CS levels, and abundant freshwater, specifically in the Allerød Interstadial. This evidence supports the first part of McBurney's hypothesis that when CS levels were high and the coastal plain was narrow, Mesolithic hunters were reliant on seals and deers. Also, the sequences documented three low-stands CSL for the Last Glacial Maximum, the Mangyshlak, and the 4 ka event, before the local infilling of the lagoon.

A combination of palynology, anthropology, and plant macro-remains allowed vegetation reconstruction. Different proxies indicated the continuous presence of wetlands. In addition, the diverse range of deciduous trees that persisted in this region, during the Younger Dryas, indicated favorable climatic conditions for a variety of plant and animal food resources, and hence for human survival.

Vegetation history of Alborz Mountains: Only at the central Hyrcanian forests are palaeoecological records available through an altitudinal transect on slopes of the Alborz Mountains. Records from three peatlands at 550 m a.s.l. (Muzidarbon, (Ramezani et al. 2008)), 1080 m a.s.l. (Tepe Kelar, (Ramezani 2013)) and 1475 m a.s.l. (Veisar, (Khakpour Saeej et al.

2013)) reconstructed the vegetation history, climatic condition, and anthropogenic influence through the past 1500 years. These records show that:

I. During the whole studied period *Alnus, Fagus, Carpinus, Quercus,* have been present near the sites.

II. The pollen from *Pterocarya fraxinifolia* became rare since 900-800 cal yr BP more probably owing to the Medieval Climate Anomaly.

III. The number of *Fagus, Quercus* and some other forest trees gradually declined more likely due to human impact and also climatic factors.

IV. Pollen of cultivated plants like walnut, hazelnut, and wheat and plants indicated open landscapes such as *Plantago, Sambucus, Polygonum* increased especially during the last few centuries.

and V. charcoal particles increased through the Veisar record that implies the extensive human activities.

Vegetation history inferred from deep-sea sediment cores: The 11800 years of vegetation history was inferred from marine sediment records retrieved from the southern basin of CS (Leroy et al. 2013c). The study demonstrated that an open woodland partially replaced the Late-Pleistocene deserts and steppes in CS coastal plain with *Pinus, Juniperus-Hippophae-Elaeagnus,* and even *Alnus-Quercus-Pterocarya* and *Fraxinus* plant communities. *Artemisia* reached a maximum in Younger Dryas chronozone. From 11500 to 8400 cal yr BP, shrubs such as *Ephedra* dominated prepared open landscape dominated by, also *Quercus* increased progressively. Probably the dry climate in the early Holocene, the final expansion of mixed evergreen and deciduous forests was delayed until 8400 cal yr BP.

Investigating modern vegetation/climate – pollen relationships: The first study was implemented over a forest-steppe transect in Golestan National Park, NE Iran, in 18 sampling points applying descriptive and numerical approaches (Djamali et al. 2009). The second study explored the pollen–vegetation relationships along an altitudinal transect in the central Caspian forests of northern Iran (Ramezani et al. 2013). The pollen percentages of the most abundant plant taxa were compared with the vegetation abundances in the pollen plots.

The main results of these two studies are:

i) Hyrcanian lowland forests are characterized by pollen assemblages dominated by *Quercus* and *Carpinus betulus*

ii) *Parrotia persica* and *Zelkova carpinifolia* and many insect-pollinated taxa are under-represented in pollen assemblages that should be considered in the interpretation of fossil pollen diagrams.

iii) transitional communities between the forest and steppe are more difficult to distinguish by pollen assemblages.

iv) a higher proportion of light pollen grains in the samples, such as those for *Quercus* and *Carpinus*, arrive from outside of the area covered by the vegetation analysis. In contrast, heavier pollen grains or those with a patterned exine, such as *Diospyros*, *Parrotia*, *Acer*, and *Hedera*, are opposite.

2. Aims and objectives

This research aims to investigate the long-term dynamics of vegetation and biodiversity in the western part of the Hyrcanian forest using an innovative multi-proxy approach. Also, discovering the role of climatic changes and human activities is an important goal of this study. These above aims raise the following research objectives:

- Understanding the relationship between modern pollen spectrum and the current vegetation structure in different landscapes.
- The relationship between plant diversity in the landscape and diversity of pollen in the assemblage.
- The dynamics of vegetation and plant biodiversity through altitudinal and longitudinal gradients in Gilan province during the late Quaternary.
- The role of climate and humans on the Hyrcanian vegetation dynamics during the late Quaternary.
- Detecting the resilient/sensitive vegetation types regarding past climatic changes.

The output of this study is of especial importance for nature conservation, forest and rangeland management, archaeology, agriculture, and sustainable development.

3. Study sites - an overview

3.1. Location

The first two core sites are located in the southwestern and southeastern highlands of the Gilan province above the Hyrcanian forest line on the Alborz Mountains. However, the third core site

is located at the mid-elevated altitude of the Hyrcanian forest. Thus, the two altitudinal transects of the pollen traps were settled from the lowlands up to the highlands of the Alborz Mountains in two different geographical directions of Asalem-Khalkhal and Shanderman- Masal (Fig.1.1). Detailed information on the coring sites is given in Table 1.1.

	High-altitude (above forest line)		Mid-altitude (center of forest)
Name	Pounel mire (PNL)	Kholash-Kouh Lake (KHL)	Annal Lake (ANL)
Location	37° 34′ 3.80″ N 48° 40′ 45.98″ E	36° 45' 43.49" N 49° 53' 42.79" E	37° 31' 44.83" N 48° 53' 13.99" E
Altitude (m a.s.l.)	2280	2000	700
Average precipitation (mm)	376 mm	260	792
Average Temperature (°C)	8.9	11.5	21
Core length (cm)	128	135	272
Age (cal yr BP)	4300 ± 35	1245± 30	1690 ± 30
Proxies	Pollen, Spore, NPPs, Charcoal, XRF	Pollen, Spore, NPPs, Charcoal, XRF, LOI	Pollen, Spore, NPPs, Charcoal, XRF, LOI
Chapter	II	III	IV

Table 1.1. Information of the coring sites

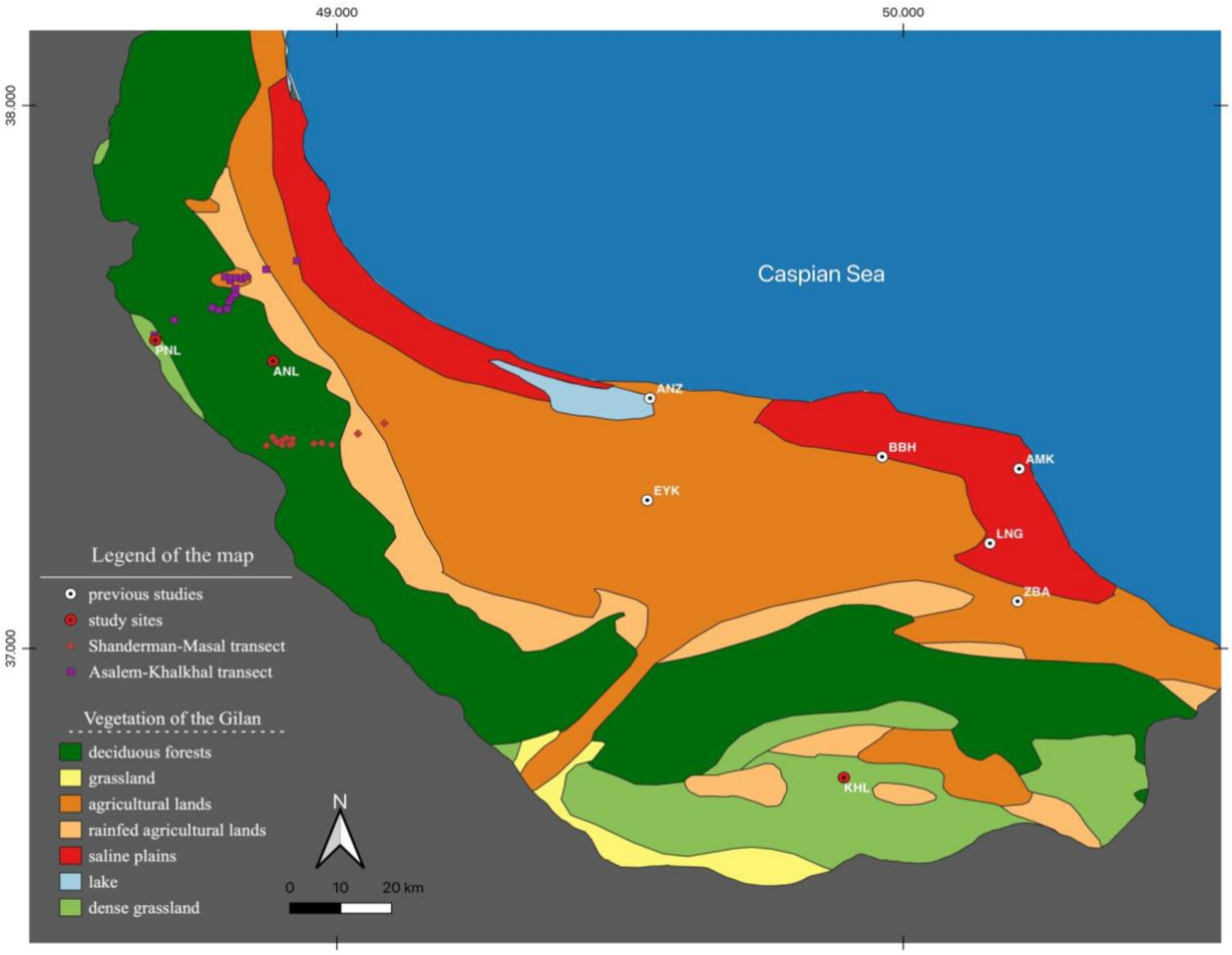

Fig. 1.1. Map of the coring sites and the distributed collected pollen rain samples, besides the past studies site (Leroy et al. 2011; Haghani et al. 2015; Gu et al. 2020, 2021)

3.2. Climate

Different components of the regional atmospheric circulation patterns control the climate in northern Iran (Akhani et al. 2010). The high amount of moisture from the mid-latitude westerlies of the North Atlantic Ocean, Black Sea, and the Mediterranean Sea transport to the western part of Asia, contributing to the autumn-winter spring precipitation of the southern Caspian region (Alijani and Harman 1985). The high amount of rainfall during summer and autumn in coastal areas of the CS is caused due to the Siberian Anticyclone, which flows over the north of Eurasia and extends into Central Asia, blocking the eastern penetration during the autumn and winter months (Khalili 1973; Alijani and Harman 1985). The western and eastern parts of the Hyrcanian region are significantly different in terms of precipitation regime (cf. (Domroes et al. 1998). In total, precipitation from west to east and from lowlands to highlands decrease significantly. The western part stands top of the north-easterly winds originating from the Siberian Anticyclone or polar front. The winds sweep the Caspian Sea surface and bring

much of the moisture to the south of the Caspian region (Khalili 1973). The other important rainfall mechanism in the Hyrcanian region is the precipitation from the Caspian Sea (Alijani and Harman 1985), which minimizes the length of the summer and suppresses dry conditions (Akhani et al. 2010) (Fig.2). The average annual precipitation of each coring site is based on the nearest meteorological station shown in Table 1.

3.3. Vegetation

Several studies have classified the modern vegetation of the Hyrcanian region into different zones (e.g. (Akhani et al. 2010; Ramezani et al. 2013). However, the investigation of (Ramezani et al. 2013) gives the best view of the vegetation in the Hyrcanian region. It provided some information about pollen-vegetation relationships along an altitudinal transect in the central region of the Hyrcanian forest. Based on this study, *Carpinus betulus*, *Parrotia persica*, and *Buxus hyrcana* are the main forest taxa of the lowland forests (< 550 m elevation). In the lower mountains (1,300–550 m), *Fagus orientalis*, *Alnus subcordata*, *Acer velutinum*, *C. betulus*, *Diospyros lotus*, and *Pterocarya fraxinifolia* are the most abundant trees. Also, in the upper mountains (1,300–2,400 m), the most dominant forest taxa were *F. orientalis*, *C. betulus* (lower than 1,550 m), *C. orientalis*, *Sorbus torminalis*, *Pyrus*, *Acer campestre*, and *Quercus macranthera*. (Ramezani et al. 2013) argued that the wind-pollinated (anemophilous) taxa show relatively more pollen abundance than the corresponding taxon abundance (taxa like *Quercus*, *Fagus*, *Carpinus*, and *Fraxinus*). However, it is not the case for the insect-pollinated (entomophilous) taxa (like *Tilia*, *Acer*, *Parrotia*, *Diospyros*, and *Ilex*).

4. Multi-proxy approach - General aspects on methods and applications

4.1. Fieldworks

To achieve the aims of this study, coring of sediment archives in Gilan was obtained from one mire (Pounel - PNL) and two lakes (Annal Lake - ANL and Kholasht Kouh Lake - KHL) at high and mid-elevated areas. The 128 cm-long sediment core of PNL from the Pounel mire was collected with the Russian corer (50 cm length, 5 cm diameter) in September 2016. While the rest two lakes sediments of the ANL core in 272 cm-long and KHL core in 135 cm-long were retrieved with the modified Livingstone corer (Livingstone 1955) in September 2018. All the recovered sediments were sealed and taken to the Department of Palynology and Climate Dynamics of the Göttingen University and stored under dark and cold conditions.

4.2. Chronology

In total, ten samples were taken from the sediment cores for radiocarbon dating with the Accelerator Mass Spectrometry (AMS) (Table 1.2). The calibrated ages and the age-depth models have been done with the R-Studio data platform, using RBacon package 2.4.3 (Blaauw and Christeny 2011). All the samples were calibrated based on the linear extra- and interpolation using the IntCal13-curve (Reimer et al. 2013).

4.3. Pollen, Spores and Non-pollen palynomorphs (NPPs) analysis

Based on the unique shapes of the pollen and spores, it is possible to identify their productive source (Faegri and Iversen 1989). The changes in pollen and spore assemblage can reflect the changes in vegetation composition as well as in climate and environment (Braak and Prentice 1988). The pollen analysis is often combined with the study of other microfossils called non-pollen palynomorphs (NPPs). To distinguish the changes in the past vegetation of the study areas, we applied the standard pollen and spore extraction methods followed by Faegri and Iversen (1989), including 40% HF treatment, acetolysis sieved with 120 μm mesh size. Prior to the extraction process, *Lycopodium* spore tablets were added to each subsample to determine pollen concentration and influx. The extracted pollen and spores were counted for almost all subsamples up to the minimum of 300 pollen grains. The pollen, spores, and NPPs identification were done using the reference collection of the Department of Palynology and Climate Dynamics, University of Göttingen, and literature (Beug 2004). In total, 86 pollen, and ten spore types were distinguished, mostly to family or genus level and rarely to the species level. Also, several pollen types remained unknown.

4.4. Macro-charcoal analysis

Incomplete combustion of organic matter leads to charcoal particles production (Whitlock and Larsen 2002). Based on their size, these particles are distributed as the smaller ones reflect more regional fire while the bigger particles consider reflecting the local fire events (Whitlock and Larsen 2002). Therefore, charcoal particles in different studies are classified into two different groups based on their size: micro-charcoal with the size <125 μm and macro-charcoal with the size >125 μm (e.g. (Swain 1973; Millspaugh and Whitlock 1995; Long et al. 1998; Hallett and Walker 2000). The charcoal analysis is used to reconstruct long-term variations in fire occurrence. Furthermore, palaeoecologists used the pollen and charcoal data of the same core to reconstruct the climate, vegetation, fire, and human activities (Whitlock and Larsen 2002).

In order to understand the past local fire regime of the study areas, a macro-charcoal analysis was performed. Subsamples were taken continuously from the cores and prepared following Stevenson and Haberle (2005). Samples were placed in 10% KOH for 12 h, and then placed for 24 h in the weak hydrogen peroxide (6% H_2O_2) to remove the organic matter of the samples. Afterward, the samples were sieved using a mesh size of 125 μm. Charcoal particles were counted under a stereomicroscope.

4.5. Geochemical contents (XRF analysis)

The non-destructive X-ray fluorescence (XRF) scanning is a powerful method for tracing the elemental variations (Croudace et al. 2006). In the XRF profile, the results are shown based on the counted element per second, which prepared the relative changes of the elements in the profile rather than the absolute values of element concentration. The X-ray fluorescence (XRF) analysis for all three cores has been carried out at GEOPOLAR, University of Bremen (Germany) using Cr-tube on the ITRAX XRF-core scanner COX analytical system (Croudace et al. 2006). The scanner detected 40 elements for each core that selected specific elements reported in their XRF profiles.

4.6. Loss on Ignition (LOI)

The Loss on ignition (LOI) analysis is a standard method for determining the content of the organic and carbonate matter in the sediment core. In the current study, this analysis was obtained only for the KHL and ANL sediment cores. The subsamples preparation followed the procedure used by (Heiri et al. 2001). The wet subsamples were weighted, then dried at 105 °C for 24 h and weighed again. The subsamples were then combusted at 550 °C for 4 h. The combusted subsamples were also weighed. Finally, subsamples were combusted at 950 °C for 2 h and afterward weighted. The organic and the carbonate matter content of each subsample was calculated using the following equations, respectively:

$$\frac{\text{dry weight after 105 °C} - \text{dry weight after 550 °C}}{\text{dry weight after 105 °C}} \times 100$$

$$\frac{\text{dry weight after 550 °C} - \text{dry weight after 950 °C}}{\text{dry weight after 105 °C}} \times 100$$

4.7. Metabarcoding

DNA metabarcoding is a novel method of assessing biodiversity wherein samples can be taken from different environments such as water, sediment, or even air. Within this method, DNA is extracted and then amplified using general or universal primers in a polymerase chain reaction (PCR) and sequenced using next-generation sequencing (NGS) to generate extensive reads (thousands to millions of reads). Afterward, species presence can be determined and expanded to the overall biodiversity condition. However, as a unique method, metabarcoding is an interdisciplinary method that still needs to be developed well to become standardized (Ruppert et al. 2019).

To provide the current forest inventory, we used the evidence of the pollen rain through altitudinal transects in two different landscapes, from coastal fluvial forests to the slopes of Alborz Mountains in Gilan province for the first time. DNA metabarcoding as the supplementary method with the pollen counting hired to fill the gaps between investigations on long-term biodiversity dynamics.

In the beginning, 40 pollen traps (Jantz et al. 2013) were distributed for one year from September 2019 to 2020 (see Fig. 5.1 and Table 5.2 for details). However, only 18 samples were found. Therefore, wherever was applicable, mosses samples were collected (for 14 samples) as the replacement of the missing pollen traps. In total, 32 samples were collected for further analysis.

After the fieldwork, the samples were shipped to Germany and stored at 4 ^{o}C in the Department of Palynology and Climate Dynamics, University of Göttingen. After primary preparation, the samples were sent to the “lifeprint DNA Analysis GmbH” for molecular analysis.

DNA extraction and amplification

The DNA extraction was done with the help of explained instruction manual, using NucleoSpin Food Prep Kit from Macherey-Nagel (Düren, Germany). Amplification was performed for two target regions ITS2 and rbcL. The modified sequences of the standard primers for ITS2 (Chen et al. 2010; White et al. 1990) and rbcL (Erickson et al. 2017) were prepared to fit the dual-indexing metabarcoding strategy (Sickel et al. 2015). To reduce PCR bias, two separate reactions (25 µl in each) were performed. Also, negative and positive controls with the known species mixture were included in the run. The PCR mixture contained 12.5 µl AccuStart II PCR ToughMix (Quantabio), 1.25 µl 20x EvaGreen (Biotium), 1.25 µl of each ITS2 primer (10µM,

biomers), 0.75 µl of each rbcL primers (10 µM, biomers), 2.25 µl PCR grade water and 5 µl DNA (about 20 ng/µl). For the sample-specific labeling, the dual indexing primers with different forward/reverse index combinations were used for each sample. PCR under the following conditions was conducted with the Applied Biosystems 7300 Real-Time PCR System: initial denaturation at 95 °C for 10 min, 35 cycles of denaturation at 95 °C for 45 s, annealing at 52 °C for 60 s, and elongation at 72 °C for 60 s; followed by a final extension step at 72 °C for 10 min. Afterward, a dissociation curve was used as the control for amplification.

Altitude	"Asalem-Khalkhal" samples condition	"Shanderman-Masal" samples condition
2300	Trap (dry)	
2200		
2100		
2000	Trap (moist)	
1900		
1800	Mosses	
1700	Trap (liquid)	Mosses
1600	Trap (moist)	
1500		Mosses
1400	Trap (moist)	Trap (moist)
1300	Mosses	Trap (liquid)
1200	Mosses	Trap (dry)
1100	Mosses	Trap (liquid)
1000		Trap (liquid)
900	Mosses	Trap (liquid)
800		Trap (liquid)
700	Mosses	Trap (liquid)
600	Mosses	Mosses
500	Mosses	
400	Mosses	Trap (liquid)
300	Mosses	Mosses
200	Trap (liquid)	Trap (liquid)
100	Trap (moist)	Trap (liquid)

Table 1.2. List of elevation and condition of the collected modern pollen rain samples (gray cells indicate lost traps)

Sequencing

After PCR, 40 µl AMPure beads were added to 50 µl of the mixed PCR product to combine and purify each duplicated sample with magnetic beads (AMPure XP, Beckmann Coulter). Then samples were washed with 80% ethanol twice, and DNA was eluted in 30 µl of 10 µMTris (pH 8.5) while the concentration of the mixture was measured by applying a Qubit fluorometer. All samples with equal concentrations were pooled in the 4 nM library. Lastly, the library was diluted to 7 pM, denatured, and spiked with 15% of the denature d PhiX Control (Illumina) as

described in the 16S Metagenomic Sequencing Library Preparation workflow (Illumina). Finally, sequencing was performed on the Illumina MiSeq using 2 × 250 cycles v2 chemistry as described in Sickel et al. (2015).

Data analysis

The subsets of the ITS2 and rbcL markers were split up by applying the BLASTn, to estimate the first ten base pairs of each read, which are conserved for each marker and thus are a good discriminator. Then, forward and reverse reads of each marker were quality filtered, dereplicated, denoised, and finally merged to amplicon sequence variants (ASVs) using the DADA2 pipeline (Callahan et al. 2016a,b). The quality filtering parameters were set according to the ITS pipeline (Callahan et al. 2016 a,b) and pipeline for rbcL diatoms (Keck et al. 2019). The below parameters were set with the same values for both markers:

maxN = 0, maxEE = c (2, 2), truncQ = 2, rm.phix = TRUE

As reads belonging to ITS2 show natural length variation between 200-600 base pairs (bp), in order to obtain the maximum sequence diversity, the truncation was not applied to them. Instead, the minimum accepted length of sequences (minLen) was set to 50. Both forward and reverse reads from rbcL were truncated at 240. These numbers were gained from a quality profile plot. ASVs were classified taxonomically against the nr/nt databases of Genbank using the BLASTn (Benson et al. 2009). The order of criteria for selection was minimum E-value = 1e-50, maximum identity = 99%, and coverage = 99%. If more than one hit has the same quality metrics, the one with the taxon that has higher frequency among the hits for that sequence was selected.

Species selection

All assigned taxa were checked in the reference book of the flora of Iran (Rechinger 1963), as well as the recently reported paper of Ghorbanalizadeh and Akhani (2021) to find the taxa that are endemic or characteristic for Gilan province.

References

Akhani H, Djamali M, Ghorbanalizadeh A, Ramezani E (2010) Plant biodiversity of Hyrcanian relict forests, N Iran: an overview of the flora, vegetation, palaeoecology and conservation. Pakistan Journal of Botany 42:231–258

Alijani B, Harman JR (1985) Synoptic Climatology of Precipitation in Iran. Annals of the Association of American Geographers 75:404–416. https://doi.org/10.1111/j.1467-8306.1985.tb00075.x

Behling H, Cohen MCL, Lara RJ (2001) Studies on Holocene mangrove ecosystem dynamics of the Bragança Peninsula in north-eastern Pará, Brazil. Palaeogeography, Palaeoclimatology, Palaeoecology 167:225–242

Beni AN, Lahijani H, Harami RM, et al (2013) Caspian Sea-level changes during the last millennium: Historical and geological evidence from the south Caspian Sea. Climate of the Past 9:1645–1665. https://doi.org/10.5194/cp-9-1645-2013

Benson DA, Karsch-Mizrachi I, Lipman DJ, et al (2009) GenBank. Nucleic acids research 37:26–31

Beug HJ (2004) Leitfaden der Pollenbestimmung für Mitteleuropa und angrenzende Gebiete. Verlag Friedrich Pfeil, Munich

Blaauw M, Christeny JA (2011) Flexible paleoclimate age-depth models using an autoregressive gamma process. Bayesian Analysis 6:457–474. https://doi.org/10.1214/11-BA618

Browicz K (1989) Chorology of the Euxinian and Hyrcanian element in the woody flora of Asia. Plant Systematics and Evolution 162:305–314

Callahan BJ, Sankaran K, Fukuyama JA, et al (2016) Bioconductor workflow for microbiome data analysis: from raw reads to community analyses. F1000Research 5

Cazenave A, Bonnefond P, Dominh K, Schaeffer P (1997) Caspian Sea level from Topex-Poseidon altimetry: Level now falling. Geophysical Research Letters 24:881–884

Chen S, Vargas YN (2010) Improving the performance of particle swarms through dimension reductions—A case study with locust swarms. In: IEEE Congress on Evolutionary Computation 1–8

Croudace IW, Rindby A, Rothwell RG (2006) ITRAX: description and evaluation of a new multi-function X-ray core scanner 267(1):51-63

Djamali M, de Beaulieu JL, Campagne P, et al (2009) Modern pollen rain-vegetation relationships along a forest-steppe transect in the Golestan National Park, NE Iran. Review of Palaeobotany and Palynology 153:272–281. https://doi.org/10.1016/j.revpalbo.2008.08.005

Domroes M, Kaviani M, Schaefer D (1998) An analysis of regional and intra-annual precipitation variability over Iran using multivariate statistical methods. Theoretical and Applied Climatology 61:151–159

Erickson DL, Reed E, Ramachandran P, et al (2017) Reconstructing a herbivore's diet using a novel rbc L DNA mini-barcode for plants. AoB Plants 9 (3):1-17

Faegri K, Iversen J (1989) In: Faegri K, Kaland PE, Krzywinski K. Textbook of Pollen analysis

Ghorbanalizadeh A, Akhani H (2021) Plant diversity of Hyrcanian relict forests: An annotated checklist, chorology and threat categories of endemic and near endemic vascular plant species. Plant Diversity. https://doi.org/10.1016/j.pld.2021.07.005

Gu F, Ramezani E, Alizadeh K, Behling H (2021) Vegetation Dynamics, Environmental Changes, and Anthropogenic Impacts on the Coastal Hyrcanian Forests in Northern Iran. Journal of Coastal Research 37:611–619. https://doi.org/10.2112/JCOASTRES-D-20-00033.1

Haghani S, Leroy SAG, Khdir S, et al (2015) An early 'Little Ice Age' brackish water invasion along the south coast of the Caspian Sea (sediment of Langarud wetland) and its wider impacts on environment and people. Holocene 26:3–16. https://doi.org/10.1177/0959683615596835

Hallett D, Walker R (2000) Paleoecology and its application to fire and vegetation management in Kootenay National Park, British Columbia. Journal of Paleolimnology 24:401–414

Heiri O, Lotter AF, Lemcke G (2001) Loss on ignition as a method for estimating organic and carbonate content in sediments: reproducibility and comparability of results. Journal of paleolimnology 25(1):101-110

Hoogendoorn RM, Boels JF, Kroonenberg SB, et al (2005) Development of the Kura delta, Azerbaijan; a record of Holocene Caspian Sea-level changes. In: Marine Geology 222:359–380

Jantz N, Homeier J, León-Yánez S, Moscoso A, Behling H (2013) Trapping pollen in the tropics—Comparing modern pollen rain spectra of different pollen traps and surface samples across Andean vegetation zones. Review of Palaeobotany and Palynology 193: 57-69.

Kakroodi AA, Kroonenberg SB, Hoogendoorn RM, et al (2012) Rapid Holocene sea-level changes along the Iranian Caspian coast. Quaternary International 263:93–103. https://doi.org/10.1016/j.quaint.2011.12.021

Kakroodi AA, Leroy SAG, Kroonenberg SB, et al (2015) Late Pleistocene and Holocene sea-level change and coastal paleoenvironment evolution along the Iranian Caspian shore. Marine Geology 361:111–125. https://doi.org/10.1016/j.margeo.2014.12.007

Keck F, Rimet F, Vasselon V, Bouchez A (2019) GitHub - fkeck/DADA2_diatoms_ pipeline: DADA2 Custom Pipeline for rbcL Diatoms. In: https://github.com/fkeck/DADA2_diatoms_pipeline

Khakpour Saeej M, Ramezani E, Siyab Ghodsy A, et al (2013) Palynological reconstruction of 1500 years of vegetation history of Veisar (N Iran). Rostaniha 14:135–148

Khalili A (1973) Precipitation patterns of central Elburz. Archiv für Meteorologie, Geophysik und Bioklimatologie, Serie B 21:215–232

Kroonenberg SB, Abdurakhmanov GM, Badyukova EN, et al (2007) Solar-forced 2600 BP and Little Ice Age highstands of the Caspian Sea. Quaternary International 173–174:137–143. https://doi.org/10.1016/j.quaint.2007.03.010

Kroonenberg SB, Badyukova EN, Storms JEA, et al (2000) A full sea-level cycle in 65 years: barrier dynamics along Caspian shores. Sedimentary Geology 134:257–274

Leroy SAG, Amini A, Gregg MW, et al (2019) Human responses to environmental change on the southern coastal plain of the Caspian Sea during the Mesolithic and Neolithic periods. Quaternary Science Reviews 218:343–364. https://doi.org/10.1016/j.quascirev.2019.06.038

Leroy SAG, Kakroodi AA, Kroonenberg S, et al (2013a) Holocene vegetation history and sea level changes in the SE corner of the caspian sea: Relevance to SW Asia climate. Quaternary Science Reviews 70:28–47. https://doi.org/10.1016/j.quascirev.2013.03.004

Leroy SAG, Tudryn A, Chalié F, et al (2013b) From the Allerød to the mid-Holocene: palynological evidence from the south basin of the Caspian Sea. Quaternary Science Reviews 78:77–97

Leroy SAG, Tudryn A, Chalié F, et al (2013c) From the Allerød to the mid-Holocene: Palynological evidence from the south basin of the Caspian Sea. Quaternary Science Reviews 78:77–97. https://doi.org/10.1016/j.quascirev.2013.07.032

Leroy SAG, Lahijani HAK, Djamali M, et al (2011) Late Little Ice Age palaeoenvironmental records from the Anzali and Amirkola Lagoons (south Caspian Sea): Vegetation and sea level changes. Palaeogeography, Palaeoclimatology, Palaeoecology 302:415–434. https://doi.org/10.1016/j.palaeo.2011.02.002

Leroy SAG, Roiron P (1996) Latest Pliocene pollen and leaf floras from Bernasso palaeolake (Escandorgue Massif, H6rault, France). Review of paleobotany and palynology 94:295-328

Livingstone DA (1955) A Lightweight Piston Sampler for Lake Deposits

Long CJ, Whitlock C, Bartlein PJ, Millspaugh SH (1998) A 9000-year fire history from the Oregon Coast Range, based on a high-resolution charcoal study. Canadian Journal of Forest Research 28:774–787

Millspaugh SH, Whitlock C (1995) A 750-year fire history based on lake sediment records in central Yellowstone National Park, USA. The Holocene 5:283–292

Ramezani E (2013) Palynological reconstruction of late-Holocene vegetation, climate, and human impact in Kelardasht (Mazandaran province, N Iran). Iranian Journal of Forest and Poplar Research 21(1):48-62. https://doi.org/10.22092/ijfpr.2013.3338

Ramezani E, Marvie Mohadjer MR, Knapp HD, et al (2013) Pollen-vegetation relationships in the central Caspian (Hyrcanian) forests of northern Iran. Review of Palaeobotany and Palynology 189:38–49. https://doi.org/10.1016/j.revpalbo.2012.10.004

Ramezani E, Marvie Mohadjer MR, Knapp HD, et al (2008) The late-Holocene vegetation history of the Central Caspian (Hyrcanian) forests of northern Iran. Holocene 18:307–321. https://doi.org/10.1177/0959683607086768

Ramezani E, Mrotzek A, Marvie Mohadjer MR, et al (2016) Between the mountains and the sea: Late Holocene Caspian Sea level fluctuations and vegetation history of the lowland forests of northern Iran. Quaternary International 408:52–64. https://doi.org/10.1016/j.quaint.2015.12.041

Rechinger KH (1963) Flora Iranica, Flora des iranischen Hochlandes und der umrahmenden Gebirge. Graz/Wien: Akademische Druck- u. Verlagsanstalt, und Naturhistorisches Museum Wien.

Reimer PJ, Bard E, Bayliss A, et al (2013) IntCal13 and Marine13 radiocarbon age calibration curves 0–50,000 years cal BP. radiocarbon 55:1869–1887

Richards K, Bolikhovskaya NS, Hoogendoorn RM, et al (2014) Reconstructions of deltaic environments from Holocene palynological records in the Volga delta, northern Caspian Sea. The Holocene 24:1226–1252

Ruppert KM, Kline RJ, Rahman MS (2019) Past, present, and future perspectives of environmental DNA (eDNA) metabarcoding: A systematic review in methods, monitoring, and applications of global eDNA. Global Ecology and Conservation 17:e00547

Rychagov GI (1997) Holocene oscillations of the Caspian Sea, and forecasts based on palaeogeographical reconstructions. Quaternary International 41:167–172

Sabeti H (1994) Forest, trees and bushes of Iran

Shumilovskikh LS, Hopper K, Djamali M, et al (2016) Landscape evolution and agro-sylvo-pastoral activities on the Gorgan Plain (NE Iran) in the last 6000 years. Holocene 26:1676–1691. https://doi.org/10.1177/0959683616646841

Sickel W, Ankenbrand MJ, Grimmer G, et al (2015) Increased efficiency in identifying mixed pollen samples by meta-barcoding with a dual-indexing approach. BMC ecology 15:1–9

Stevenson J, Haberle S (2005) Palaeoworks Technical Papers 5. Macro Charcoal Analysis: A modified technique used by the department of Archaeology and Natural History. Department of Archaeology & Natural History, Australian National University, ACT 200

Swain AM (1973) A history of fire and vegetation in northeastern Minnesota as recorded in lake sediments. Quaternary Research 3:383–396

Talebi KS, Sajedi T, Pourhashemi M (2014) Forests of Iran: A Treasure From the Past, a Hope for the Future. Springer 10

Braak CJF, Prentice IC (1988) A theory of gradient analysis. Advances in ecological research 18:271–317

White TJ, Bruns T, Lee S, Taylor J (1990) Amplification and direct sequencing of fungal ribosomal RNA genes for phylogenetics. PCR protocols: a guide to methods and applications 18:315–322

Whitlock C, Larsen C (2002) Charcoal as a fire proxy. In: Tracking environmental change using lake sediments. Springer 75–97

Chapter 2: Paper I

Four millennia of vegetation and environmental history above the Hyrcanian forest, northern Iran

Leila Homami Totmaj[1*], Elias Ramezani[2], Kammaledin Alizadeh[1], Hermann Behling[1]

[1]University of Goettingen, Department of Palynology and Climate Dynamics, Albrecht-von-Haller Institute for Plant Sciences, Untere Karspüle 2, 37073 Goettingen, Germany

[2] Department of Forestry, Faculty of Natural Resources, Urmia University, Sero Boulevard, Nazloo, P.O. Box: 165, Urmia, Iran

Published (2020) in "Vegetation History and Archaeobotany 30(5), pp.611-621"

doi.org/10.1007/s00334-020-00813-y

Abstract

Past vegetation, fire, and climate dynamics, as well as human impact, have been reconstructed for the first time in the highlands of the Gilan province in the Alborz mountains (above the Hyrcanian forest) for the last 4300 cal yr BP. Multi-proxy analysis, including pollen, spores, non-pollen palynomorphs, charcoal, and geochemical analysis, has been applied to investigate the environmental changes at 2280 m elevation above the Hyrcanian forest. Dominant steppe vegetation occurred in the study area since the recorded period. The formation of the studied mire deposits, as well as vegetation composition, suggest a change to wetter climatic conditions after 4300 cal yr BP until 1700 cal yr BP. The fire was frequent, which may imply long-lasting anthropogenic activities in the area. Less vegetation cover with a marked decrease of the Moisture Index (MI) suggests drier conditions between 1700 to 1000 cal yr BP. A high proportion of Cichorioideae and Amaranthaceae, as well as the reduction of trees, in particular *Fagus* and *Quercus*, in lower elevations, indicate human activities such as intense livestock grazing and deforestation. Soil erosion as the result of less vegetation due to dry conditions or/and human activities reconstructed from a marked increase of *Glomus* spores and high values of K and Ti. Since 1000 cal yr BP, the increasing MI, as well as the rise of Poaceae and Cyperaceae together with forest recovery, suggest a change to wetter conditions. The occurrence of still frequent Cichorioideae and *Plantago lanceolata* along with *Sordaria* reflect continued intense grazing of the human's livestock.

Introduction

Between the northern slopes of the Alborz Mountains and the southern coast of the Caspian Sea (CS) is a narrow belt, 20-70 km wide and ca. 800 km long, which is covered by broad-leaved deciduous Hyrcanian forest. It is extending from the lowland up to >2000 m elevation (Sabeti 1994; Sagheb-Talebi et al. 2014). However, above 2000 m elevation, mostly forests replaced by forest/steppe or steppe vegetation. The area is covering approximately 1.9 million ha and from west to east, consists of three provinces, namely Gilan, Mazandaran, and Golestan (Fig. 2.1-II). Some of the Arcto-Tertiary species occurred in the Hyrcanian forest. *Pterocarya fraxinifolia*, *Parrotia persica,* and *Zelkova carpinifolia* are those refugia from the Quaternary glaciations which grew in the southern part of Europe (e.g. Zohary 1973; Leroy and Roiron 1996; Ramezani et al. 2008; Leroy and Arpe 2007; Leroy et al. 2013a, b). The history of the Hyrcanian region can provide important insight into the past Quaternary vegetation history.

The palynological studies in Iran began by Van Zeist and Wright (1963). Since then, there are still a few palynological studies throughout the country. Also, most of the studies focused

mainly on the Zagros Mountains (e.g., Van Zeist and Bottema 1977; Wasylikowa 2005; Djamali et al. 2009b), and only a few investigated the northern part of Iran. So far from those available studies, only Leroy et al. (2011) and Haghani et al. (2015) investigated the palynological aspects of the southwestern part of the CS; while the other studies mostly focused on the central and eastern part (e.g., Djamali et al. 2009a; Leroy et al. 2013a, b; Leroy et al. 2019; Ramezani et al. 2008, 2013, 2016; Shumilovskikh et al. 2016).

The multidisciplinary study of Leroy et al. (2019) in the south-eastern of the CS investigated the human responses to environmental alterations during the late Pleistocene and early Holocene. According to their palynological evidence, cool and dry climatic conditions of the Younger Dryas period did not affect this area immensely. Also, their analyses on botanical, faunal, and archaeological remains showed gradually and low-cost adaptation to an early process of Neolithization in the southern Caspian basin.

Leroy et al. (2011) studied two lagoons Anzali and Amirkola (also known as Amirkelaye). They indicated that during the Little Ice Age (LIA), the sea level increased as a result of more rainfall in the basin of the CS. Besides, due to anthropogenic activities, the dense alder forests have been disturbed by fire and expansion of rice paddies between 1720 to 1800 AD. Later Haghani et al. (2015) investigated the Langroud wetland. They showed that during the LIA, the high stand of CS caused brackish water incursion 10 km inland in Gilan province. As a result of the invasion, soil salinisation increased the abundance of steppe type vegetation, reduced the agricultural activities, and damaged the alder swamp, which is very sensitive to saltwater.

There are only three studies from different elevations in the central part of the Hyrcanian Forest that allowed preparing altitudinal transect record in the Hyrcanian forest. Those records from three peatlands at 550 m a.s.l. (Muzidarbon, Ramezani et al. 2008), 1080 m a.s.l. (Tepe Kelar, Ramezani 2013a) and 1475 m a.s.l. (Veisar, Khakpour et al. 2013) reconstructed the vegetation history, climatic condition, and anthropogenic influence through the past 1500 years. These studies show that I) during the last 1500 years, *Alnus, Fagus, Carpinus*, and *Quercus* have been present near the sites, II) *Pterocarya fraxinifolia* became rare since 900-800 cal yr BP more probably owing to the Medieval Climate Anomaly, III) *Fagus, Quercus*, and some other forest trees gradually declined more likely due to human impact and also climatic factors, IV) pollen of cultivated plants like *Juglans, Corylus*, and Cerealia besides the pollen of the plants such as *Plantago, Sambucus, Polygonum* indicating open landscapes especially for the last few centuries and V) charcoal particles increased through the Veisar, record that implies the extensive human activities.

The current study is the first and longest palynological record of the highlands of Gilan province. We aim to investigate past vegetation and climate changes as well as fire and human impacts above the western part of the Hyrcanian forest, with the help of the multi-proxy analysis. The main research questions are:

1) How did vegetation and climate change during the last 4300 years?
2) What was the role of fire on the vegetation dynamics?
3) How strongly anthropogenic activities affected the western part of the Hyrcanian forest ecosystems?
4) How natural are the modern vegetation?

Study area

Geographical setting

The Alborz Mountains, located in the south of the CS, is a barrier between the northern and the central parts of Iran (Fig. 2.1-I). The study area located in the western part of the Alborz Mountains between Gilan and Ardabil provinces. The elevation ranges between -26 m (in the coastal area) up to 2872 m a.s.l. in Sonbol Kūh (Forest Rangelands and Watersheds Management Organization 2003). The sediment core was collected from a mire in a small basin located near the Pounel-Khalkhal road, of the so-called Pounel area (37° 34'3.80 "N, 48° 40'45.98 "E, 2280 m elevation). The site is a 35 km distance to the CS. The nearest village, Majareh, located in Ardabil province, and is 5.7 km distant from the coring site (Fig. 2.1-III).

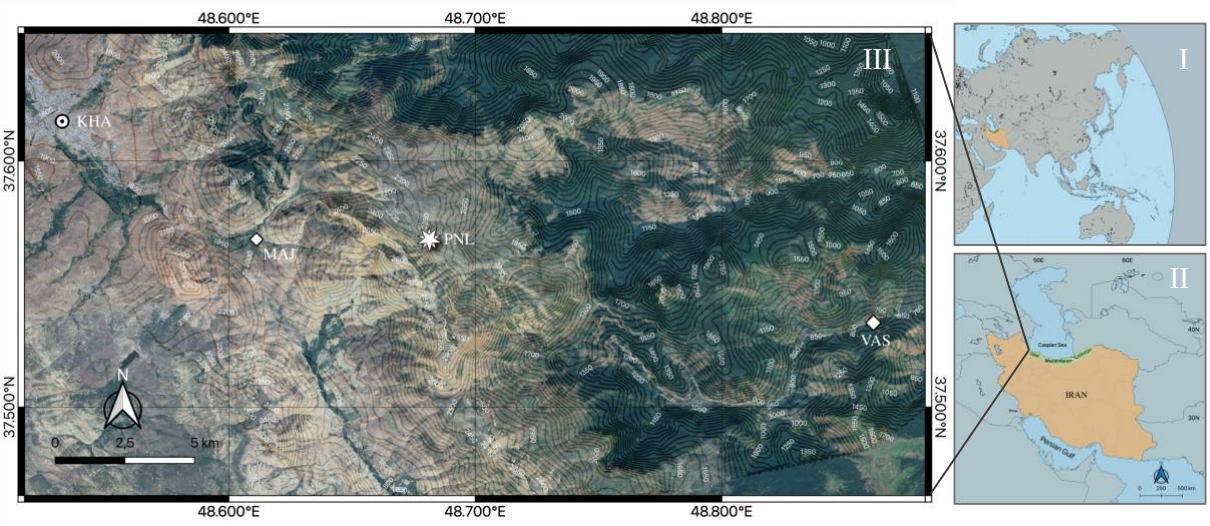

Fig. 2.1 Locations: I Geographical position of Iran; II Geographical distribution of the Hyrcanian forest in the northern part of Iran (in green); III location of the study area along with other places discussed in this study. The Pounel coring site (PNL) is marked with a white asterisk. Vaske village (VAS) and Majareh village (MAJ) are marked with white diamonds. The meteorological station of Khalkhal (KHA) is marked with a circled dot. The map was produced using natural earth data in a QGIS 3.14 environment

Climate

The climate in northern Iran controls by different components of regional atmospheric circulation patterns (Akhani et al. 2010). The mid-latitude westerlies transport a high amount of moisture from the North Atlantic Ocean, Black Sea, and the Mediterranean Sea to the western part of Asia, contributing to the autumn-winter-spring precipitation of the southern Caspian region (Kendrew 1961; Alijani and Harman 1985). The Siberian Anticyclone, which flows over the north of Eurasia and extends into Central Asia, blocks the eastern penetration during the autumn and winter months and causes high rainfall during summer and autumn in coastal areas of the CS (Alijani and Harman 1985; Khalili, 1973). According to the spatial analysis of precipitation seasonality (cf. Domoers et al. 1998), the western and eastern parts of the Hyrcanian region are significantly different in terms of precipitation regime. The west part is standing at the head of the north-easterly winds emanating from the Siberian Anticyclone or polar front. The winds sweep the CS surface and bring much of the moisture to the south of the Caspian region (Khalili 1973). The second most important mechanism of rainfall in the Hyrcanian region is the precipitation of the CS (Alijani and Harman 1985), which causes to minimise the length of the summer and suppress the dry condition (Akhani et al. 2010).

Khalkhal station is the nearest weather forecast station to the Pounel area (Fig. 2.1-III). The station located at 1797 m a.s.l. and in 13 km distance from the coring site. Based on the last 30 years records of this site, there is a four-month dry period extending from June to September (Moradi et al. 2019). Also, the average annual temperature and precipitation reported at 8.9 °C and 376 mm, respectively.

Vegetation

Several studies classified the modern vegetation of the Hyrcanian region into different zones (e.g., Akhani et al. 2010; Ramezani et al. 2013; Heshmati 2012; Dehshiri 2018). However, the Ramezani et al. (2013) investigation suits best with the aim of this study, as they provided some information about pollen-vegetation relationships along an altitudinal transect in the central of the Hyrcanian forest.

Based on this study, *Carpinus betulus*, *Parrotia persica,* and *Buxus hyrcana* were the main forest taxa of the lowland forests (<550 m elevation). In the lower mountains (1300-550 m), *Fagus orientalis*, *Alnus subcordata*, *Acer velutinum*, *C. betulus*, *Diospyros lotus* and *Pterocarya fraxinifolia* were the most abundant trees. Also, in the upper mountains (1300-2400 m) the most dominant forest taxa were, *F. orientalis*, C. betulus (lower than 1550 m), *C. orientalis*, *Sorbus torminalis*, *Pyrus*, *Acer campestre*, and *Quercus macranthera*. Ramezani et

al. (2013) interpreted that for the wind-pollinated (Anemophilous) taxa the ratio of the pollen abundance into the corresponding taxon abundance, are relatively large (taxa like *Quercus*, *Fagus*, *Carpinus*, and *Fraxinus*). However, for the insect-pollinated (entomophilous) taxa, the ratio, as mentioned earlier is relatively low (taxa like *Tilia*, *Acer*, *Parrotia*, *Diospyros*, and *Ilex*).

Vegetation around the site: Herbaceous plants cover the vegetation of the study site Pounel. The dominate species are Poaceae, Asteraceae, Amaranthaceae, and *Artemisia* species. Other frequent taxa that are growing in the surrounding of the coring site include *Taraxacum*, *Ranunculus*, *Carex*, *Lythrum*, *Nasturtium officinalis*, and *Veronica*. Furthermore, at the same elevation of the coring site on the adjacent slopes, such taxa as *Alchemilla*, *Geranium*, *Plantago lanceolata*, *Achillea*, and *Trifolium* grow. The upper mountain forest occurs at around 2000 m elevation, fewer than 800 m down to the coring site.

Human settlement

The most important six empires in Iran were: Elam (5000-2800 yr BP), Medes (2700-2500 yr BP), Achaemenids (2550-2280 yr BP), Partians (2240-1700 yr BP), Sasanians (224-651 AD), and Safavids (1501-1736 AD). Arabs and Mongols Conquered Iran around 1300 and 700 yr BP, respectively (Daryaee 2011).

Archaeological evidence suggests that at least in the last 4000 years, humans lived in the region of the Pounel site (Fallahian 2013). Vaske is an ancient village, a 14 km distance from the study site (Fig. 2.1-III) at an altitude of around 1000 m (Fallahian 2013). Several artefacts have been found in this village and refer to the Iron-Age. Most of the inhabitants were engaged in farming and animal husbandry at least since 1700 yr BP (Alizadeh 2014). Nowadays, human activities (e.g., livestock grazing and road construction) changed the vegetation of the Pounel region substantially.

Materials and methods

Sampling

A 128 cm-long sediment core of a mire area, called Pounel (PNL), was collected with a Russian corer (50 cm length, 5 cm diameter) in September 2016. The recovered three sections of the sediment core were wrapped in plastic film, placed in split PVC tubes, and stored in a cold room with +4 ^{o}C.

Radiocarbon dating and age-depth modelling

According to the lack of plant remains, four samples from the bulk sediment took for radiocarbon dating with accelerator mass spectrometry (AMS) at Poznan Radiocarbon

Laboratory in Poland. Based on the HCl test, which shows no reaction, and also the meagre amount of the Ca in the sediment core (see later in Fig. 2.5), the probable reservoir effect is very low or not existent. The surface dating assigned to the year of coring, which was in 2016 (-66 cal yr BP). An age-depth model in R-studio constructed (Fig. 2.2), using the BACON version 2.2 (Blaauw and Christen 2011) with linear interpolation, using the Northern Hemisphere terrestrial calibration curve IntCal13 from Reimer et al. (2013).

Pollen analysis

For palynological analysis, 33 samples of 0.5 cm^3 were taken mostly in intervals of 4 cm along the entire core. Samples processed by pollen analytical methods, including acetolysis (Faegri and Iversen 1989) and 40% HF treatment, and sieved with 120 µm mesh size. Each sample contains an exotic *Lycopodium* spore in order to determine pollen concentration and influx. Beug (2004) and the reference collection of the Department of Palynology and Climate Dynamics in Goettingen used as the references for pollen and spores identification. For each spectrum, the minimum of 300 pollen grains counted. Pollen sum includes arboreal pollen (AP), non-arboreal pollen (NAP), and unknown pollen types. Pollen types attributable to aquatic plants, along with Cyperaceae (due to its local high frequencies), spores, and non-pollen palynomorphs (NPPs), were excluded from the pollen sum.

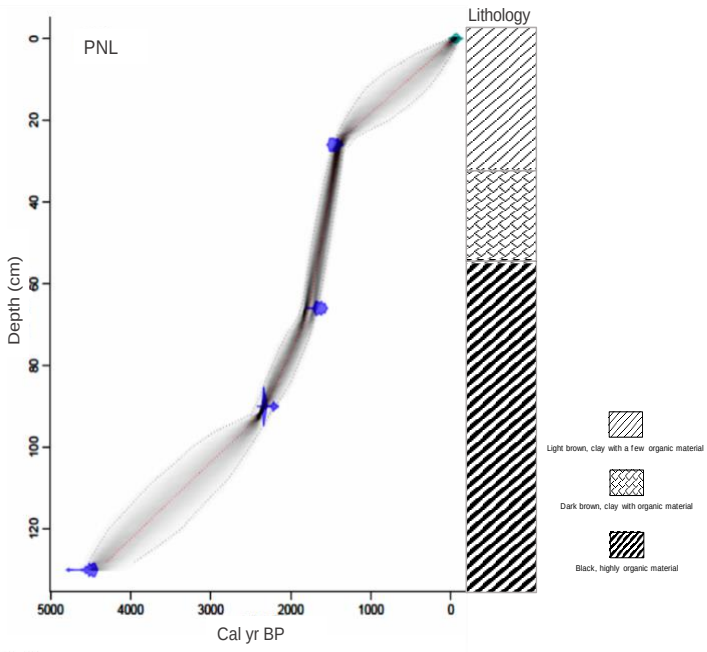

Fig. 2.2 Age-depth model for the PNL sediment core plotted by linear interpolation in BACON

Percentages of all the pollen taxa, as well as other taxa and NPPs, were calculated based on the pollen sum. The moisture index (MI), which is a ratio of (*Artemisia* + Poaceae)/Chenopodiaceae (Shumilovskikh et al. 2016), were calculated to identify changes in the climatic conditions. The former family name Chenopodiaceae will be in the paper with its approved new name Amaranthaceae.

TILIA and TILIAGRAPH program 2.1.1 used to illustrate the pollen, spore, and NPP data. A cluster analysis was performed by CONISS (Grimm 1987) on the pollen sum to establish pollen zones (Fig. 2.5).

Laboratory name	Core depth, cm	Dated material	Age ^{14}C	Calibrated age, (% probability)
Poz-107800	26	Bulk	1560 ± 30	465-631 AD (93.7) 442-452 AD (1.7)
Poz-107801	66	Bulk	1730 ± 30	322-417 AD (68.2) 250-305 AD (27.2)
Poz-107802	90	Bulk	2300 ± 30	321-211 BC (56.3) 399-346 BC (39.1)
Poz-85946	128	Bulk	4030 ± 30	2631-2471 BC (93.8) 2832-2821 BC (1.6)

Table 2.1 Results of radiocarbon dating and calibrated ages of the Pounel (PNL) core

Macro-charcoal analysis

For charcoal analysis, 0.5 cm^3 samples were taken continuously along the PNL core at intervals of 1 cm down to 126 cm depth (126 samples). All samples processed according to the method of Stevenson and Haberle (2005). Samples placed into the 10% KOH for 12 hours, and then in 6% H_2O_2 for 24 hours. Afterwards, the samples were sieved using a mesh size of 125 μm. Charcoal particles counted with the binocular microscope.

Geochemistry

X-Ray Fluorescence (XRF), using an ITRAX XRF-core scanner COX analytical system (Croudace et al. 2006), has been carried out at GEOPOLAR, University of Bremen (Germany). The XRF measurements were taken at 1 mm intervals down core by using a Cr tube. Determined main elements were Fe, Ti, Rb, K, and Ca. Ti and K are detrital fraction indicators, while the Fe/Ti ratio mirrors redox conditions (Croudace and Rothwell 2015). Also, Rb/K ratio and Ca respectively were analysed to track chemical weathering (Croudace and Rothwell 2015) and the occurrence of carbonate (Shumilovskikh et al. 2016) (Fig. 2.5).

Results

Lithology

The PNL sediment core consists mainly of organic material (Fig. 2.2). Based on the colour and the material of the sediment, the core contains three different units. The first unit (128–58 cm) is composed of black and compact, highly decomposed organic material. The second unit (58-35 cm) consists of dark brown compact clay with organic material. Finally, the last unit (35-0 cm) contains light brown clay with a few organic materials.

Chronology and sedimentation rate

The age-depth model prepared based on the four radiocarbon dates of the PNL core (Table 2.1, Fig. 2.2). The base of the PNL core dated to 4303 +/- 35 cal yr BP. There is no indication of a possible hiatus in the core. For the core depth of 128 to 92 cm, the calculated sedimentation rate is low (0.02 cm/yr), and in the middle part between 92 to 68 cm, it increases slightly (0.04 cm/yr). A marked increase in sedimentation rate occurs between 68 to 28 cm (0.11 cm/yr). In the uppermost part between 28 to 0 cm, it decreases again to a low rate (0.02 cm/yr).

Description of the pollen, spores, and NPP data

The pollen diagram illustrates 44 pollen taxa (excluding aquatic taxa and indeterminate pollen types) and ten different NPP types (Fig. 3 and 4). The CONISS analysis applied on AP and NAP taxa suggests two pollen zones with five subzones.

Pollen concentration from the bottom to the top of the core shows a decreasing trend. The influx values are low in the first two subzones (PNL-Ia and Ib), while values increase markedly through the PNL-IIa and IIb. Finally, during the last subzone (PNL-IIc), decreases to its lowest value.

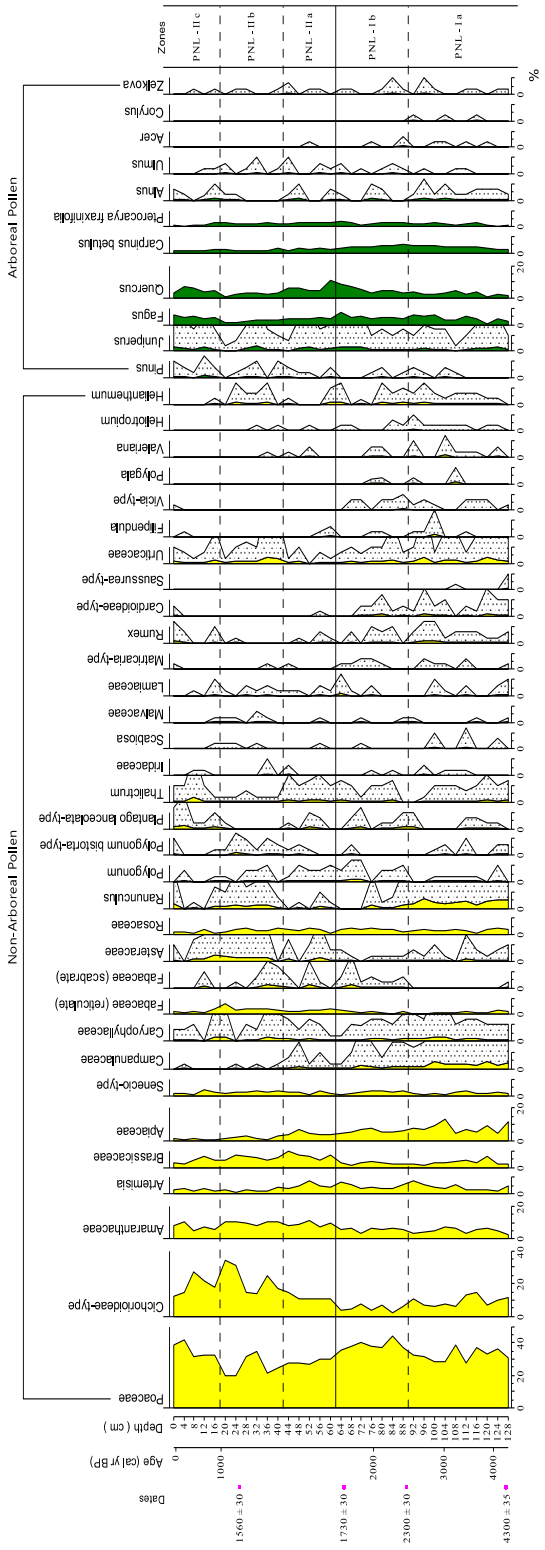

Fig. 2.3 Percentage pollen diagram of the PNL core. Non-Arboreal Pollen (NAP) in yellow and Arboreal Pollen (AP) in green. Stippled curves are exaggerated 10 ×

4.3.1. Subzone PNL-Ia (128-90 cm; ca. 4300-2330 cal yr BP)

The proportions of NAP (herbs) are higher than AP (shrubs and trees). NAP, in particular Poaceae (28–38%), Asteraceae subfamily Cichorioideae-type (6–14%), Apiaceae (4–13%), and *Artemisia* (2-8%) are the most frequent taxa. Amaranthaceae (3–8%) has its lowest values in this subzone, while *Ranunculus* (2–6%) and Campanulaceae (1–5%) have their highest values. The most frequent AP taxa are *Quercus*, *Fagus*, *Carpinus betulus,* and *Pterocarya fraxinifolia*. In this subzone, *Carpinus betulus* (2-5%) has its highest percentages. Pollen grains of *Corylus* are also present. *Alnus* pollen grains are present since the beginning of the record. A few *Pinus* pollen occur in this subzone. *Lemna* pollen grains are rare. Fern spores are present. Spores of *Glomus* and coprophilous fungi are also present. Besides, the spores of various algae observed. The MI index shows some fluctuations and in comparison, to the second zone (PNL-II) has relatively high values (Fig. 5).

4.3.2. Subzone PNL-Ib (90-62 cm; ca. 2330-1700 cal yr BP)

In this subzone, Poaceae pollen (44-30%) decreases slightly, but in comparison to PNL-Ia, it has higher proportions (average 37%). Other NAP keeps their previous trend or decreases slightly. Due to the increasing values of *Quercus*, *Fagus,* and other trees and shrubs, the average amount of AP increases to some degree (15% in PNL-Ia to 24% in PNL-Ib). Cyperaceae reaches its highest proportions. Fern spores decrease to their lowest values. *Glomus* falls in comparison to the previous subzone. The MI index shows small fluctuations, but it shows the highest value throughout the entire record.

4.3.3. Subzone PNL-IIa (62-42 cm; ca. 1700-1580 cal yr BP) and PNL IIb (42 – 18 cm; ca.1580-1000 cal yr BP).

The most characteristic feature of these two subzones is the relatively low values of Poaceae pollen, but it is remaining the most frequent taxon (20-35%). Some of the pollen taxa, e.g., Cichorioideae-type, Amaranthaceae, and Brassicaceae, increase and reach their highest values in the record. *Artemisia* pollen increases in subzone PNL-IIa but decreases in PNL-IIb. AP decrease in particular by *Quercus*, *Fagus,* and *Carpinus betulus*. *Alnus*, *Acer*, *Corylus,* and *Zelkova* become very rare since the end of PNL-IIa. *Lemna* pollen reaches its maximum amount in PNL-IIb throughout the whole core. Fern spores increase slightly. NPPs, which had constant values in the previous subzones, show some changes in these two subzones. *Glomus* reaches maximum values in PNL-IIb. Hdv-731 shows a peak in PNL-IIb. The MI index decreases to its lowest values in these two subzones.

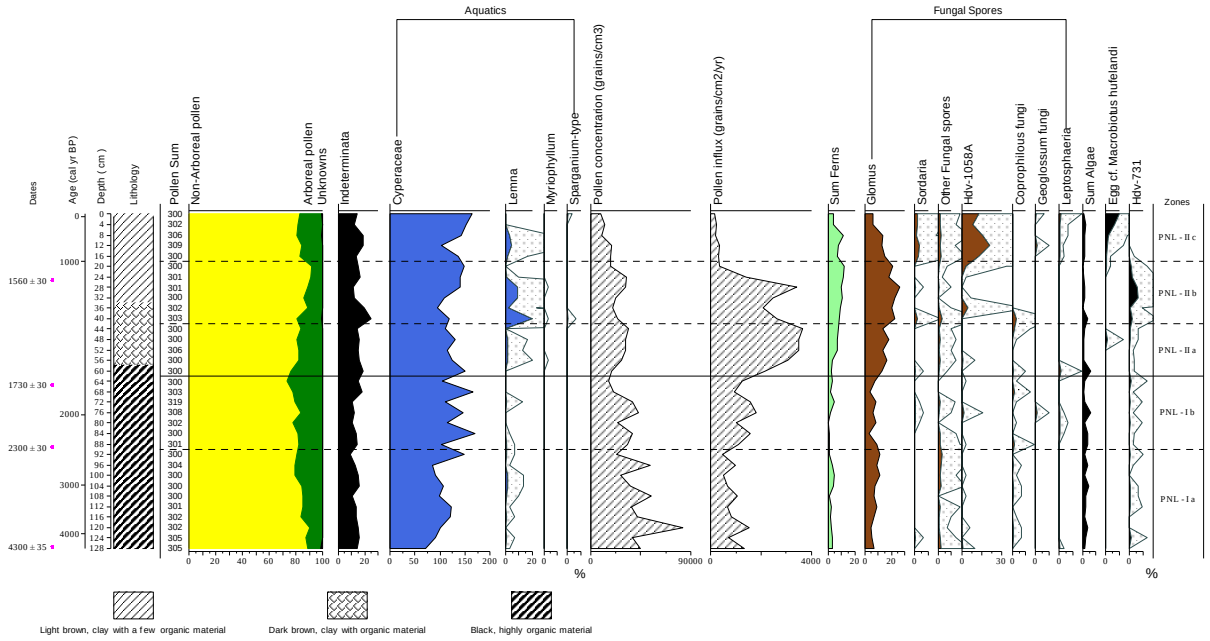

Fig. 2.4 Diagram with the results of the lithology, pollen summary diagram with the sum of NAP (in yellow), AP (in green) and Unknowns (in black), Aquatics (in blue), Pollen concentration and influx (hatched curves), sum of the Ferns (in pale green), Fungal spores (in brown) and other NPPs (in black). Stippled curves are exaggerated 10x

4.3.4. Subzone PNL-IIc (18-0 cm; 1000 to -66 cal yr BP)

Poaceae pollen increases and reaches to their previous values in PNL-Ib. *Thalictrum*, *Plantago lanceolata*-type, and *Rumex* are higher than the earlier subzones. However, other herbaceous taxa decrease. Among the AP, *Pterocarya fraxinifolia* represents lower values, while *Fagus* and *Quercus* show higher proportions. *Lemna* pollen is still present but falls in comparison to PNL-IIb. *Glomus* is also present but shows a decreasing trend. *Sordaria* and *Hdv-1058A* have become more abundant. The eggs of the *Macrobiotus hufelandi* increase in the upper part of this subzone. The MI index increases in comparison to the previous two subzones (PNL-IIa and IIb), but it shows still lower values in comparison to the first zone (PNL-I).

Charcoal data

Charcoal concentration and influx show their highest values in subzone PNL-Ia and decrease with some fluctuations since the beginning of PNL-Ib. Charcoal influx becomes very low from the end of the PNL-IIb up to the end of PNL-IIc.

XRF data

According to the geochemistry, main elements (K, Ca, Ti) and the ratio of Rb/K, as well as Fe/K, show relatively stable values in zone PNL-I. In zone PNL-II above 60 cm core depth up

to the end of the zone, K and Ti increase while the Rb/K ratios decrease. Ca and the Fe/Ti ratio are almost stable in PNL-IIa and IIb, but increase markedly in the upper part of PNL-IIc.

Interpretation and discussion

Local environment

The studied region is a mire that located in a small basin. It seems sediments started to accumulate in this area at least since 4300 cal yr BP. Multi-proxy analysis suggests, prevailed wetter conditions for the small basin of the Pounel from 4300 to 1700 cal yr BP. It also suggests drier conditions between 1700 to 1000 cal yr BP, which later shift to wetter conditions for the last 1000 years.

Frequency of Cyperaceae may suggest local changes in the moisture content of the mire area. Based on the current investigation, Cyperaceae, with some oscillations, were the most frequent plant through the recorded periods. Their least frequency was from 4300 to 2330 cal yr BP (PNL-Ia). However, the highest frequency was between 2330 - 1700 (PNL-Ib) and 1000 cal yr BP up to the present (PNL-IIc). *Lemna*, the aquatic plant, was frequent from 1580 to ca. 1200 cal yr BP (upper and middle part of PNL-IIb), which may suggest shallow and more open water in the mire area. Although the XRF results indicated stable sediment composition, a higher proportion of Ti and K from 1700 to 1000 cal yr BP (PNL-IIa and IIb) stating an increase of erosion (Croudace and Rothwell 2015).

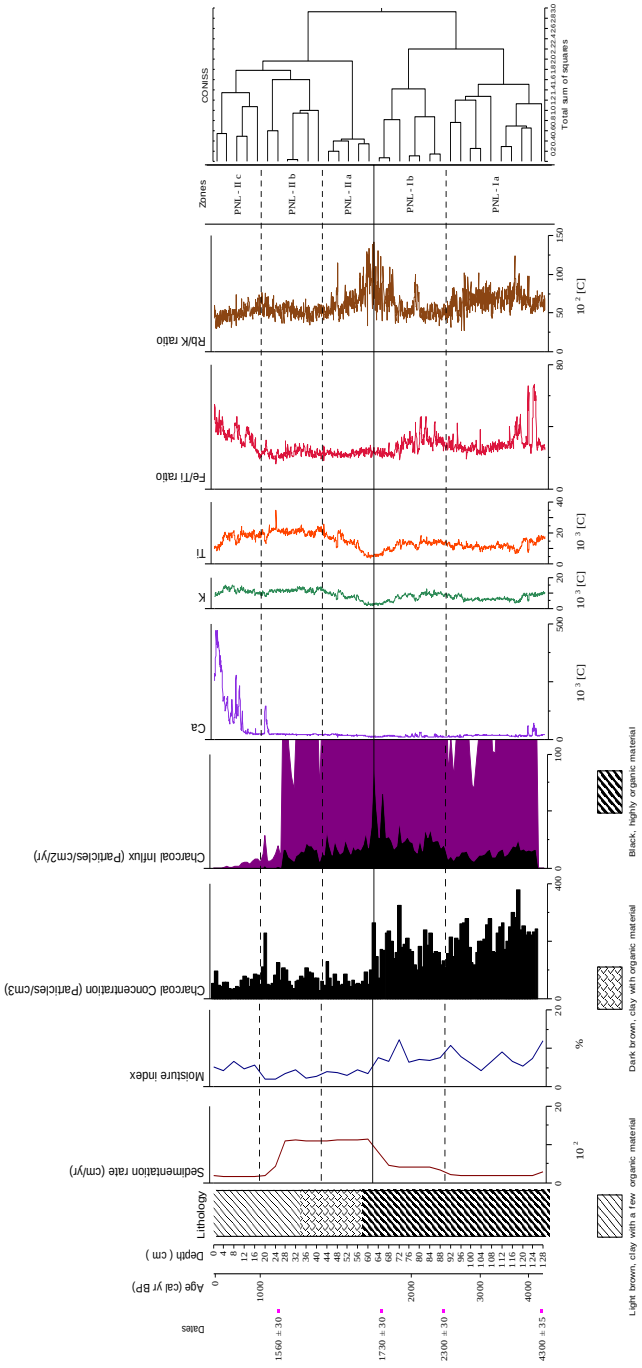

Fig. 2.5 Diagram with the results of the lithology, sedimentation rate, Moisture Index, charcoal concentration and influx, selected geochemical elements (based on counts per second), and CONISS of the pollen data (excluding Aquatics). 10 × exaggerated charcoal influx curve shown in purple

Also, *Glomus* is an indicator of erosion (Van Geel et al. 1989) that had higher occurrence between 1700 to 1000 cal yr BP. Also, a sharp shift in sedimentation rates occurred through 1700-1000 cal yr BP (subzones PNL-IIa and IIb). Probably less vegetation cover led to an increase in the accumulation of aeolian inputs (Fig. 2.5). Lowest accumulation rate for the last 1000 years may suggest vegetation recovery as the result of the wetter period.

Vegetation and other environmental changes in the study area

According to the pollen record (Fig. 2.3), the studied site was above the forest line at least over the past 4300 cal yr BP. The dominant diverse herbaceous vegetation covered the study area, and the most frequent species were Poaceae, Cichorioideae (Asteraceae), Amaranthaceae, *Artemisia,* and Apiaceae. In some distance from the coring site, *Quercus* (cf. *macranthera*), *Fagus orientalis*, *Carpinus,* and *Juniperus* spp. were the most probable frequent trees. However, less frequent trees consisted of *Zelkova*, *Ulmus*, *Acer,* and *Corylus*. The occurrence of *Pterocarya* and *Alnus* pollen in our record suggests their relatively long-distance pollen dispersal, as they grow in lower elevations. Winds which fellow from the CS lowlands might transport their pollen to the upper mountain area. As *Pinus* was not introduced to Iran before the last century (Ramezani et al. 2016), their pollen occurrence in the studied core is due to the long-distant transport, from the Caucasus or Turkey.

Period of 4300 to 1700 cal yr BP (zone PNL-I):

The record started with a wide variety of herbaceous plants with the dominance of Poaceae. Stable vegetational and environmental features obtained from high values of pollen concentration, low sedimentation rate, and the steady presence of the mineral elements (Fig. 2.4 & 2.5). Arboreal plants increased slightly (from 16% in PNL-Ia to 22% in PNL-Ib), and suggest occupation larger areas in comparison to the beginning of the record. Growing of Cyperaceae, along with the highest values of MI (Fig. 2.5) suggest wet conditions. Also, Ryabogina et al. (2019) indicated moisture increasing for the eastern part of the Caucasus between 2400 to 1700 cal yr BP.

Period of 1700 cal yr BP to present (zone PNL-II):

The results detected more substantial changes in vegetation for this period. Poaceae decreased while Cichorioideae, Amaranthaceae, and Brassicaceae increased until 1000 cal yr BP. Cichorioideae reached its highest values between 1700 to 1000 cal yr BP. It can be an indicator of drier conditions, an open landscape (Leroy et al. 2013a), and/or grazing activity (Florenzano et al. 2015). The high sedimentation rate, an increasing trend of the K and Ti, marked increase

in Cichorioideae and Brassicaceae, as well as *Glomus*, indicate that the area was sparsely vegetated (especially between 1700 to 1000 cal yr BP). Although the forest showed an increasing trend between 4300-1700 cal yr BP, it decreased from 1700 to 1000 cal yr BP (PNL-IIa and IIb). *Quercus* and *Fagus* were markedly less frequent ca. 1580 to 1000 cal yr BP. Ferns were present since the beginning of the record, but they increased in this period. It seems that, with the reduction of the arboreal plants, Ferns increased. Kooch et al. (2011) verified that ferns like *Dryopteris filix-mas* and *Pteridium aquilinum* grew more in disturbed forests, especially in the disturbed *Fagus* forests.

After 1000 cal yr BP (PNL-IIc), species of Poaceae became more frequent while Cichorioideae decreased in the mire vegetation of Pounel. Furthermore, forest re-expanded, and trees like *Quercus*, *Fagus,* and *Carpinus betulus* became more frequent in the forest. Ferns were still abundant during the last 1000 years, but they decreased whenever the forest recovered.

According to the calculated MI and the vegetational changes, it seems that since ca. 1700 until 1000cal yr BP, drier condition prevailed. While, In the last 1000 cal yr BP, increasing MI as well as recovered forest indicates the change to the wetter state. Other studies also support the transition from drier to wetter conditions for the last 1700 cal yr BP. Ryabogina et al. (2019) suggested dry and warm period during 1700-550 cal yr BP in the eastern part of the Caucasus. Sharifi et al. (2015) indicated that during 1800-1500 cal yr BP, dry condition prevailed in the whole country of Iran and led to the occurrence of famine. Hoogendooren et al. (2005) showed the Caspian Sea level began to decrease before 1500 cal yr BP and reached its minimum depth (- 42) until 1500 cal yr BP. Naderi Beni et al. (2013) indicated that the CS level increased up to – 21 m during the Little Ice Age.

Human impact

Besides climatic changes, the role of human activities in changing the vegetation since early times needs to be considered. Pastoralism and grazing occurred in the high elevation of the Talysh (Talesh) Mountain, ca. 40 km to the west of the PNL site, at least since 6500 cal yr BP (Ponel et al. 2013). The occurrence of Cichorioideae, Brassicaceae, *Plantago lanceolata* as well as coprophilous fungi and *Sordaria* spores suggested livestock grazing in the study area at least for the past 4300 years.

At the beginning of the Iron-age (around 4000-3500 BP (Ramezani et al. 2008)), the need for charcoal increased with the aim of metal smelting. Therefore, one possible reason for frequent charcoal before 2330 cal yr BP (PNL-Ia) may refer to an increase in metal usage in human life.

The iron mine of Masoule, along with Vaske village, is the good evidence of human practices with metals. Archaeologists suggested that the Iron mine of Masoule (ca. 50 km distance to PNL) discovered during the fourth millennium BP (Ghorbani 2013). Also, Vaske village is famous due to its found graves with handicrafts that referred to the Iron-Age (Fallahian 2013). (Fig. 2.1-III)

Setting fires for hunting animals is another probable reason for frequent fires. The marked decrease of frequent fires after 2330 cal yr BP may indicate changes in land use due to the growing human population. Alizadeh (2014) published a study that showed people during the Sasanian Empire (between 224-651 AD) constructed fantastic irrigation systems, known as Qanat, and that system let them be more farmers rather than hunters. Also, high occurrence of Cichorioideae between 1700 to 1000 cal yr BP, may reflect, increase in livestock grazing activity (Florenzano et al. 2015).

Woods has long been the primary source for different human needs, especially those like *Fagus, Quercus, Carpinus,* and *Pterocarya*. Therefore, besides the dry condition that could lead to reducing the number of arboreal plants, anthropogenic activities can also cause a reduction in trees, mainly *Fagus* and *Quercus*, around 1580 to 1000 cal yr BP.

More substantial increase of *Sordaria* spores as well as *Plantago lanceolata*, suggest an increase of grazing for the last 1000 years (PNL-IIc). Also, Ca (an indicator for $CaCO_3$ and presenting more livestock around the area (cf. Shahack-Gross et al. 2003)) showed a marked increase for the last 1000 years.

Summary and conclusions

The multi-proxy study of the PNL sediment core at 2284 m elevation reflects dominant steppe vegetation above the Hyrcanian forest, at least for the last 4300 years. Vegetation composition in the study area was relatively stable, but several changes could be detected. Climate change, as well as anthropogenic activities, affected the Pounel area throughout the period. Results of the different proxies indicated changing from wetter (ca. 4300 to 1700 cal yr BP) to the drier period (ca. 1700 to 1000 cal yr BP) and then back to wetter conditions (ca. last 1000 years) in the Pounel mire.

Melting metals like Iron, or/and setting fire aiming to hunt animals are the most probable reasons for the high frequency of fire between 4300 to 2330 cal yr BP. However, changing in land use is the possible reason for the reduction of fire since 1700 cal yr BP.

Through the whole record, steppe vegetation was dominant in the Pounel area. *Quercus*, *Fagus,* and *Carpinus* were the most prevalent trees in the Hyrcanian upper mountain forest. *Fagus* and

Quercus trees reduction may be due to the results of both human activities and prevailing drier conditions between 1580 to 1000 cal yr BP.

The MI, as well as the marked increase in Cichorioideae, Amaranthaceae and Brassicaceae species and decreased Poaceae together with arboreal plants in one hand and the increased K and Ti values, on the other hand, reflects changes from wetter to drier conditions. However, intensified grazing, with the assumption of increasing human population remains valid between 1700 to 1000 cal yr BP.

Forest recovery since 1000 cal yr BP suggests a change to wetter conditions. However, increased in the presence of Poaceae, *Plantago lanceolata,* as well as *Sordaria* spores and Ca value, recommend continuously intensive pastoralism. For investigating the role of humans in changing the landscape of Gilan through time, more palaeoecological and archaeological research is needed.

Acknowledgments

We like to appreciate the reviewer for her critical reading and comments on the manuscript. The study was part of the Ph.D. project of the first author, which was supported by the German Science Foundation DFG (grant BE2116/31-1) carried out at Georg-August-Universität Göttingen, Germany.

References

Akhani H, Djamali M, Ghorbanalizadeh A, Ramezani E (2010) Plant biodiversity of Hyrcanian relict forests, N. Iran: an overview of the flora, vegetation, palaeoecology and conservation. Pakistan Journal of Botany 42: 231-258.

Alijani B, Harman JR (1985) Synoptic climatology of precipitation in Iran. Annals of the Association of American Geographers 75(3): 404-416.

Alizadeh K (2014) Borderland Projects of Sasanian Empire: Intersection of Domestic and Foreign Policies. Journal of Ancient History 2(2): 93-115.

Beug HJ (2004) Leitfaden der Pollenbestimmung für Mitteleuropa und angrenzende Gebiete. Munich: Verlag Dr. Friedrich Pfeil.

Blaauw M, Christen JA (2011) Flexible paleoclimate age-depth models using an autoregressive gamma process. Bayesian Analysis 6(3): 457–474.

Croudace IW, Rindby A, Rothwell RG (2006) ITRAX: description and evaluation of a new multi-function X-ray core scanner. Geological Society Special Publications 267: 51–63.

Croudace IW, Rothwell RG (2015) Micro-XRF studies of sediment cores: Application of a non-destructive tool for the environmental sciences. Developments in Paleoenvironmental Research 17. DOI: 10.1007/978-94-017-9849-5

Daryaee T (2011) The Oxford Handbook of Iranian History. Oxford University Press.

Dehshiri MM (2018) Biodiversity in Iran. Global Biodiversity Volume 1: Selected Countries in Asia, 6.

Djamali M, de Beaulieu JL, Campagne P et al (2009a) Modern pollen rain-vegetation relationships along a forest-steppe transect in the Golestan National Park, NE Iran. Review of Palaeobotany and Palynology 153(3-4): 272-281.

Djamali M, de Beaulieu JL, Miller NF et al (2009b) Vegetation history of the SE section of Zagros Mountains during the last five millennia; a pollen record from the Maharlou Lake, Fars Province, Iran. Vegetation History and Archaeobotany 18(2): 123-136.

Domoers M, Kaviani M, Schaefer D (1998) An analysis of regional and intra-annual precipitation variability over Iran using multivariate statistical methods. Theoretical and Applied Climatology 61(3-4): 151-159.

Faegri K, Iversen J (1989) Textbook of Pollen Analysis. John Wiley and Sons, 328.

Fallahian Y (2013) Investigation of burial patterns in Iron Age of Gilan, Iran. Ancient Asia, 4, Art. 5. DOI: http://doi.org/10.5334/aa.12311

Florenzano A, Marignani M, Rosati L et al (2015) Are Cichorieae an indicator of open habitats and pastoralism in current and past vegetation studies? Plant Biosystems 149(1): 154-165. DOI: http://dx.doi.org/10.1080/11263504.2014.998311

Forest Rangelands and Watersheds Management Organization (2003) Forestry plan of Lomir basin booklet. Forest Rangelands and Watersheds Management Organization, Tehran, p 250.

Ghorbani M (2013) The Economic Geology of Iran, Mineral Deposits and Natural Resources. Springer Dordrecht Heidelberg New York London. DOI 10.1007/978-94-007-5625-0

Grimm EC (1987) CONISS: A FORTRAN 77 program for stratigraphically constrained cluster analysis by the methods of incremental sum of squares. Computers & geosciences 13(1): 13–35.

Haghani S, Leroy SAG, Khdir S et al (2015) An early 'Little Ice Age' brackish water invasion along the south coast of the Caspian Sea (sediment of Langrud wetland) and its wider impacts on environment and people. The Holocene 26(1): 3-16. https://doi.org/10.1177/0959683615596835

Heshmati G (2012) Vegetation characteristics of four ecological zones of Iran. International Journal of Plant Production 1(2): 215-224. DOI: 10.22069/IJPP.2012.538

Hoogendoorn RM, Boels JF, Kroonenberg SB (2005) Development of the Kura delta, Azerbaijan; a record of Holocene Caspian Sea-level changes. Marine Geology 222: 359-380.

Kakroodi AA, Kroonenberg SB, Hoogendoorn RM et al (2012) Rapid Holocene sea-level changes along the Iranian Caspian coast. Quaternary International 263: 93–103.

Kendrew WG (1961) The Climates of the Continents. Oxford University Press. London

Khakpour Saeej M, Ramezani E, Siyab Ghodsy AA, Zare H, Joosten H (2013) Palynological reconstruction of 1500 years of vegetation history of Veisar (N Iran). Rostaniha 14(2): 135-148.

Khalili A (1973) Precipitation patterns of Central Elburz. Theoretical and Applied Climatology 21(2-3): 215–232. https://doi.org/10.1007/BF02243729

Kooch Y, Hosseini SM, Mohammadi J, Hojjati SM (2011) Windthrow effects on biodiversity of natural forest ecosystem in local scale. Human and Environment 9(3): 65-72.

Leroy SAG, Amini A, Gregg MW et al (2019) Human responses to environmental change on the southern coastal plain of the Caspian Sea during the Mesolithic and Neolithic periods. Quaternary Science Reviews 218: 343-364.

Leroy SAG, Arpe K (2007) Glacial refugia for summer-green trees in Europe and south-west Asia as proposed by ECHAM3 time-slice atmospheric model simulations. Journal of Biogeography 34(12): 2115–2128.

Leroy SAG, Kakroodi AA, Kroonenberg SB et al (2013a) Holocene vegetation history and sea level changes in the SE corner of the Caspian Sea: relevance to SW Asia climate. Quaternary Science Reviews 70: 28-47.

Leroy SAG, Lahijani HK, Djamali M et al (2011) Late Little Ice Age palaeoenvironmental records from the Anzali and Amirkola Lagoons (south Caspian Sea): Vegetation and sea level changes. Palaeogeography, Palaeoclimatology, Palaeoecology 302(3-4): 415–434.

Leroy SAG, Roiron P (1996) Latest Pliocene pollen and leaf floras from Bernasso palaeolake (Escandorgue Massif, Hérault, France). Review of Palaeobotany and Palynology 94(3-4): 295-328.

Leroy SAG, Tudryn A, Chalie' FL, Lo'pez-Merino L, Gasse F (2013b) From the Allerød to the mid-Holocene: palynological evidence from the south basin of the Caspian Sea. Quaternary Science Reviews 78: 77-97.

Moradi A, Afsharzadeh S, Hamzehee B, Mozaffarian V (2019) Study of plant diversity and floristics in the westernmost Hyrcanian forest. Journal of Forestry Research: 1-10. DOI: 10.1007/s11676-019-00949-2

Naderi Beni A, Lahijani H, Mousavi Harami R et al (2013) Caspian Sea level changes during the last millennium: historical and geological evidences from the South Caspian Sea. Climate of the Past 9: 1645-1665.

Ponel P, Andrieu-Ponel V, Djamali M et al (2013) Fossil beetles as possible evidence for transhumance during the middle and late-Holocene in the high mountains of Talysch (Talesh) in NW Iran. Journal of Environmental Archaeology 18(3): 201–210.

Ramezani E (2013a) Palynological reconstruction of late-Holocene vegetation, climate, and human impact in Kelardasht (Mazandaran province, N Iran). Iranian Journal of Forest and Poplar Research 21(1): 48-62.

Ramezani E, Marvie Mohadjer MR, Knapp HD, Ahmadi H, Joosten H (2008) The late-Holocene vegetation history of the Central Caspian (Hyrcanian) forests of northern Iran. The Holocene 18(2): 307-3.

Ramezani E, Marvie Mohadjer MR, Knapp HD, Theuerkauf M, Manthey M, Joosten H (2013b) Pollen-vegetation relationships in the central Caspian (Hyrcanian) forests of northern Iran. Review of Palaeobotany and Palynology 189: 38-49.

Ramezani E, Mrotzek A, Marvie Mohadjer MR et al (2016) Between the mountains and the sea: Late-Holocene Caspian Sea level fluctuations and vegetation history of the lowland forests of northern Iran. Quaternary International 408: 52-64. DOI: 10.1016/j.quaint.2015.12.041

Reimer PJ, Bard E, Bayliss A et al (2013) IntCal13 and Marine13 radiocarbon age calibration curves 0–50000 years cal BP. Radiocarbon 55(4): 1869–1887.

Ryabogina N, Borisov A, Idrisov I, Bakushev M (2019) Holocene environmental history and populating of mountainous Dagestan (Eastern Caucasus, Russia). Quaternary International 516: 111-126. http://doi.org/10.1016/j.quaint.2018.06.020

Sabeti H (1994) Forests, trees and shrubs of Iran. Yazd University Press (in Persian, with English summary).

Sagheb-Talebi K, Sajedi T, Pourhashemi M (2014) Forests of Iran: A Treasure from the Past, a Hope for the Future. Volume 10 Springer Science and Business Media.

Sharifi A, Pourmand A, Canuel EA et al (2015) Abrupt climate variability since the last deglaciation based on a high-resolution, multi-proxy peat record from NW Iran: The hand that rocked the Cradle of Civilisation. Quaternary Science Reviews 123: 215–230.

Shumilovskikh L, Hopper K, Djamali M et al (2016) Landscape evolution and agro-sylvo-pastoral activities on the Gorgan Plain (NE Iran) in the last 6000 years. The Holocene 26(10): 1676 - 1691.

Stevenson J, Haberle S (2005) Macro Charcoal Analysis: a modified technique used by the Department of Archaeology and Natural History. Palaeoworks Technical Papers 5. Australian National University, Canberra.

Van Geel B, Coope GR, van der Hammen T (1989) Palaeoecology and stratigraphy of the Late glacial type section at Usselo (the Netherlands). Review of Palaeobotany and Palynology 60(1-2): 25-129.

Van Zeist W, Bottema S (1977) Palynological investigations in Western Iran. Palaeohistoria 19: 19–85.

Van Zeist W, Wright HE (1963) Preliminary pollen studies at Lake Zeribar, Zagros Mountains, Southwestern Iran. Science 140(3562): 65–67.

Wasylikowa K (2005) Palaeoecology of Lake Zeribar, Iran, in the Pleniglacial, Lateglacial and Holocene, reconstructed from plant macrofossils. The Holocene 15(5): 720–35.

Zohary M (1973) Geobotanical Foundations of the Middle East. Stuttgart (Germany): Gustav Fischer-Verlag.

Chapter 3: Paper II

Late Holocene paleoenvironmental changes inferred from multi-proxy studies of the Kholasht-Kouh Lake sediments in the Gilan mountains, northern Iran

Leila Homami Totmaj[1*] · Kammaledin Alizadeh[1] · Hermann Behling[1]

[1] University of Göttingen, Department of Palynology and Climate Dynamics, Albrecht-Von-Haller Institute for Plant Sciences, Untere Karspüle 2, 37073 Göttingen, Germany

Published by "Journal of Paleolimnology"

Abstract

Past vegetation and environmental changes and the role of climate as well as human activities are of major interest. The Hyrcanian region with a high number of endemic species has a poorly known paleoenvironmental history, especially the western region of northern Iran. This study aims to investigate a radiocarbon-dated sediment core of the Kholasht-Kouh Lake (KHL) for the recorded between ca. 510-1180 cal yr BP. KHL is located at 2000 m elevation and surrounded with steppe vegetation above the present-day forest line. Multi-proxy analyses including pollen, non-pollen palynomorphs, charcoal, loss on ignition, and X-ray fluorescence were applied to reconstruct past environmental dynamics. The results indicate the dominance of herbaceous vegetation (mainly Poaceae, Artemisia, and Amaranthaceae) around the lake during the whole record, except for the period between 1010-740 cal yr BP. During this period of the Medieval Climatic Anomaly (1000-700 cal yr BP) mixed forest increased, consisting mainly of Quercus, Fagus, Carpinus, and Juniperus. The K, Ti and Si elements (as indicators for increased in detrital inputs) suggest relatively humid condition between 1180 to 1010 cal yr BP. Furthermore, higher lake levels may indicate from low values of the Mn/Ti, Ca/Ti and Sr/Ti ratios. After 1010 until 740 cal yr BP the highest value of the Si/Fe ratio, suggested warmest period of the record. While the lowest value of the Si/Fe ratio, in line with the reduction of other elements and ratios, between 740 till 510 cal yr BP represented cold and dry period. Humans were present around the study area at least since beginning of the record, but did not played an important role impacting the vegetation.

Introduction

In northern Iran along the coastal and mountain region of the southern Caspian Sea occur temperate forests, known as Hyrcanian forests. These forests, are designated as a biodiversity hotspot and consist of last relicts of the deciduous broadleaved species from the Arcto-Tertiary era (Zohary 1973; Leroy and Roiron 1996) like *Gleditsia caspica, Parrotia persica, Pterocarya fraxinifolia* and *Zelkova carpinifolia*. These relict species were growing extensively in the temperate regions of the Northern Hemisphere during the Pliocene. Though, they became extinct in Europe and northern Asia through the Quaternary (Zohary 1973).

The distribution of the Hyrcanian forest prior to the Last Glacial Maximum is not well known (Leroy et al. 2013), though its current distribution is from the coast of the Caspian Sea up to the highlands of the Alborz and Talysh Mountains (Sabeti 1994). Despite the importance of understanding past interactions between the climate and human activities in this region, the

available studies are still insufficient and focused mainly on the coastal plains, especially the central and eastern plains (Beni et al. 2013; Khakpour Saeej et al. 2013; Leroy et al. 2013, 2019). The western region's (in Gilan province) have not been studied until last decade (Leroy et al. 2011; Haghani et al. 2015; Homami Totmaj et al. 2020; Gu et al. 2021). Although the mentioned studies did not cover the whole Holocene period, they shed some light on the vegetation of the western part of the Hyrcanian region.

Leroy et al. (2011) concluded that higher rainfall during the Little Ice Age (LIA) resulted in increase of the Caspian Sea level. They also indicated large-scale deforestation of the alder forest (*Alnus* sp.) between 300 to 220 cal yr BP (1700 to 1830 AD) due to more fire events, most probably related to the expansion of the rice paddies. (Haghani et al. 2015) published the LIA effect on the settlements and environments around the Langaroud wetland (coast of Gilan). For this period, they evidenced water incursion 10 km, which increased soil salinity, and as the result agricultural activities reduced, the alder forest damaged, and the grassland vegetation expanded. The first investigation from the highlands of the Gilan reconstructed the anthropogenic and environmental changes for the entire late Holocene period on the Pounel mire at 2280 m a.s.l. (Homami Totmaj et al. 2020). The study showed that around the Pounel mire steppe was dominant at least for the past four millennia. Also, frequent fires during the Iron Age and later intensive grazing documented long-term human activities around the mire. Based on the newly published study (Homami Totmaj et al. 2021) at the mid-elevated Hyrcanian forest, humans influenced the area since the beginning of the record (ca. 1690 cal yr BP), though the strongest human impact dates back to ca. 65 cal yr BP by intensive deforestation. The study also documented changing from warm and humid conditions to cold and dry after 520 cal yr BP.

Documenting past environmental changes and the probable causes of the changes are crucial for the nature conservation and management as well as background information for the archeology. In the current study we want to reconstruct environmental dynamics for the late Holocene applying the multiproxy analysis and aim to answer the following questions: 1) How did vegetation and climate change during the recorded period in this high-elevated area? 2) How strongly was the vegetation affected by climate events such as the Medieval Climatic Anomaly (MCA) and LIA? 3) What were the human impacts, and how strong was the vegetation affected?

Study area

Geographical setting and climate

The Kholash-Kouh Lake (KHL), with the coordinates of 36°45'43.49"N, 49°53'42.79"E,

located at the top of the mountain at 2000 m elevation above the tree line in the southeastern part of the Gilan province (Fig. 3.1). The lake has an area of ca. 15 km^2, with a water depth of

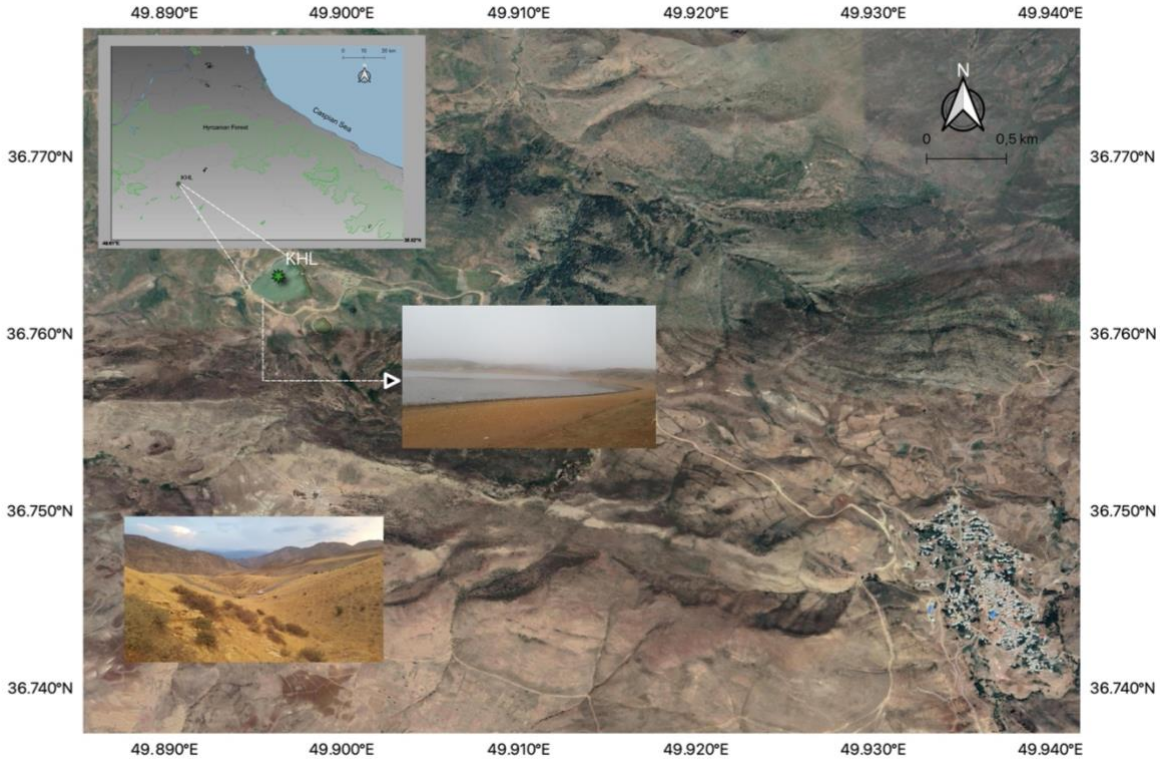

Fig. 3.1 Geographical location of the study area and the Kholasht-Kouh Lake (green asterisk). The defined light green color indicates forest distribution. The map was produced using natural earth data in a QGIS 3.14 environment.; C. Photo of the Kholasht-Kouh Lake (KHL) in September 2018.

3 m at the coring site. Klishom and Khoramkou or Kharehpu are the nearest villages located at 1900 and 1600 m a.s.l., respectively, with ca. 3.5 km distance to the Kholasht-Kouh Lake. Villagers live in the villages only during the summer, and cultivate mostly wheat, walnut and hazelnut.

The mid-latitude Westerlies and the Siberian Anticyclone are the two main climate systems that influence the whole Hyrcanian region in northern Iran (Djamali et al. 2010). Humidity gets blocked between the Caspian Sea (CS) and mountains, causing warm, humid summers with mild winters (Kendrew 1922). The precipitation decreases from the Caspian Sea's coastal plain to the Alborz mountain's highlands and from the western to the eastern region (Khalili 1973). The annual rainfall in Gilan, which is the highest through the whole country, is around 1400 mm per year (Rousta et al. 2017), but it decreases rapidly on the inland slopes of the coastal mountains. According to the nearest meteorological station (Jirandeh, at 11 km distance to the coring site at ca. 1500 m elevation) the average annual temperature and rainfall is 11.5 ^{o}C and 260 mm, respectively (Mohammadi Nia et al. 2015), representing semi-arid climate.

Vegetation

Based on the studies of (Ramezani et al. 2013) on the central part of the Hyrcanian region, the forests can divide into three main zones. Lowland forests (<550 m elevation) mainly consist of *Carpinus betulus*, *Parrotia persica* and *Buxus hyrcana*. Mid-elevated forests (1300-550 m) include the main taxa such as *Fagus orientalis*, *Alnus subcordata*, *Acer velutinum*, *C. betulus*, *Diospyros lotus* and *Pterocarya fraxinifolia*, and the high elevated forest (1300-2400 m) with the most dominant taxa of *F. orientalis*, *C. betulus* (lower than 1550 m), *C. orientalis*, *Sorbus torminalis*, *Pyrus*, *Acer campestre* and *Quercus macranthera*. However, the current site is located above the forest line (in subalpine and alpine meadows according to the (Akhani et al. 2010). The meadows consist mainly of grass species (*Poa*, *Festuca* and *Elymus*) together with hemicryptophytes and geophytes like *Rumex*, *Primula*, *Anemone*, *Thalictrum*, *Potentilla*, and *Scilla* (Akhani et al. 2010). The Euxino-Hyrcanian species, *Quercus macranthera* typically grows in the high-altitude forests (1800-2300 m) of the Alborz mountain (Akhani et al. 2010). However, related to the topographic structure and further intensive anthropogenic activities, the subalpine oak forest is disjointed and receives much sunshine (Akhani et al. 2010). Oak trees are small, and their open intervals are covered by different montane steppe vegetation types of the Irano-Turanian zone (Akhani et al. 2010), such as *Astragalus*, *Artemisia*, *Acantholimon*, *Cousinia*.

The area of open vegetation with montane steppe around the lake is mostly covered with species of Poaceae and Asteraceae (e.g. *Artemisia* and *Cousinia*), *Chamomile*, *Polygonatum* and *Echium*. At the lower elevation, most of the region is rangeland or agricultural land. There are scattered regions covered with arboreal taxa at lower elevations on adjacent slopes (the nearest is the small *Cypress* forest in 1 km distance to the lake), mainly consisting of *Cypress*, *Fagus*, *Carpinus*, *Quercus*, *Acer*, *Tilia*, *Juglans*, and *Crataegus*.

Materials and methods

Coring, radiocarbon dating and age-depth modeling

A sediment core of 135 cm length, called Kholash-Kouh (KHL), was collected in September 2018, with a modified Livingstone corer (Livingstone 1955). The recovered sediments were sealed and taken to the Department of Palynology and Climate Dynamics of the Göttingen University and stored under dark and cold conditions.

For the chronological framework, three organic sediment samples (1-2 cm^3 each) were collected and sent to the Poznan Radiocarbon Laboratory in Poland for the Accelerator Mass Spectrometry (AMS) radiocarbon dating. An age-depth model and the calibrated ages have

been done with the software R-Studio data platform, using CLAM package 2.4.0 (Blaauw 2010) (Fig. 3.2).

Palynological analysis

In total 34 pollen samples of 0.5 cm^3 were collected in intervals of 4 cm along the core. Prior to processing the sediment samples, one tablet with 9.666 ± 212 exotic *Lycopodium* spores was added to each sample to calculate pollen concentration (grains cm^{-3}) and pollen influx (grains cm^{-2} yr^{-1}). The samples were processed by pollen analytical treatment methods of (Faegri and Iversen 1989), using the chemical (10% HCl, 40% HF) and acetolysis.

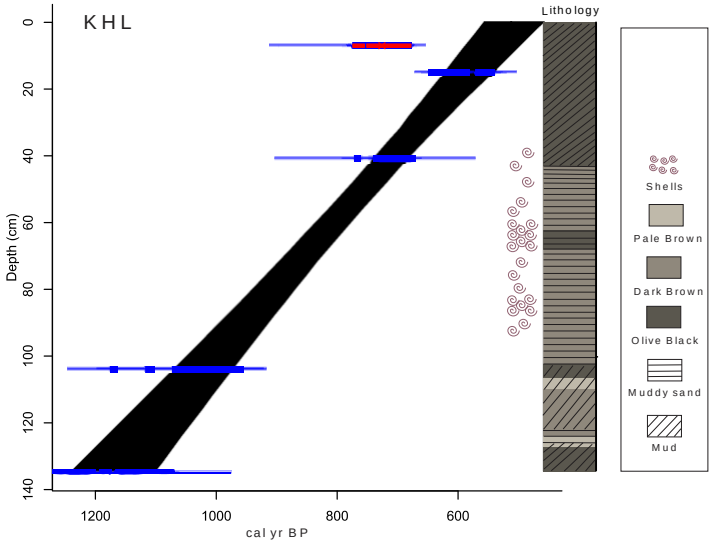

Fig. 3.2 Lithology and age-depth model for the KHL sediment core plotted in CLAM.

Samples were sieved with a 120 µm mesh size to separate palynomorphs. Pollen and spore identification followed the literature (Beug 2004) and the reference collections from the Department of Palynology and Climate Dynamics. A minimum count of 300 terrestrial pollen grains was counted for each sample. The percentages were calculated on the sum of arboreal (AP) (such as trees, shrubs, lianas) and non-arboreal pollen (NAP) (grasses and herbs) types, excluding pollen of aquatic plants and indeterminate taxa, spores, and non-pollen palynomorphs (NPPs).

ID	Depth	Age ^{14}C	Age cal yr BP	Material
Poz-128986	7	820 ± 30	545	Bulk organic sediment
Poz-140494	15	590 ± 30	585	Bulk organic sediment
Poz-122538	41	800 ± 30	715	Bulk organic sediment
Poz-122537	104	1125 ± 30	1024	Bulk organic sediment
Poz-107805	135	1245 ± 30	1176	Bulk organic sediment

Table 3.1 Results of radiocarbon dates calculations

Based on the pollen sum, the calculation and illustration of pollen, spores, and NPPs were made with TILIA and TILIAGRAPH program 2.1.1. (Grimm 1987). The pollen diagram zonation was done based on the cluster analysis of the percentages of the pollen included in the pollen sum, using CONISS (Grimm 1987).

Loss on ignition (LOI) analysis

For the determination of the organic and carbonate material, 34 samples were collected at 4 cm intervals along the core at the same depths as for pollen analysis. A P330 furnace was used at the Department of Palynology and Climate Dynamics of the Göttingen University for LOI (Heiri et al. 2001), while samples were dried for 24 h at 60 ^{o}C in advance. Then, 4 g of each dry sample were burnt at 550 ^{o}C for 4 h, to calculate the organic matter (LOI550) (Heiri et al. 2001). For calculation of the carbonate content, samples were burnt for a further 2 h at 950 ^{o}C.

Macro-charcoal analysis

In total 143 samples of 0.5 cm^3 were collected in intervals of 1 cm along the entire KHL core, to track the role of fire in the study area. All samples were processed according to the method of Stevenson and Haberle (2005). All the samples remained for 12 h in 10% KOH, and then for 24 h in 6% H_2O_2 and sieved using the 125 μm mesh size. Charcoal concentrations and influx were calculated in TILIA software.

Geochemical analysis

Non-destructive X-ray fluorescence (XRF) analysis with the purpose of analyzing the geochemical content of the sediment core has been carried out at GEOPOLAR, University of Bremen (Germany). The ITRAX XRF-core scanner prepared the COX analytical systems (Croudace et al. 2006) for each 2 mm step using a Cr tube. Among the 40 detected elements, only those that show meaningful variations were chosen. The main chosen elements were K, Ca, Ti, Si, Mn, Fe, Sr. For better sight through the precipitation rate, climate changes, and erosional events different ratios (K/Ti, Si/Ti, Mn/Ti, Ca/Ti, Sr/Ti, Si/Fe, and incoh./coh.) was calculated.

Results

Lithology, chronology, LOI and sedimentology

Sediments are mainly composed of mud and muddy sand with alternating colors (Fig. 3.2). From 95 to 41 cm core depth the sediments consist of shells. A probable reservoir effect must be considered due to the frequent occurrence of aquatic plants such as Potamogeton.

Table 1 shows the five AMS radiocarbon dates. The uppermost sample at 7 cm were excluded from the age-depth model due to the older age than the lower sample at 15 cm. The Bayesian age-depth model is based on the polynomial regressions for the KHL core (Fig. 3.2). Based on the core chronology, the deposits accumulated in the late Holocene. The core base at 135 cm has an age of 1180 cal yr BP and the core top at 0 cm would be extrapolated 510 cal yr BP. The sedimentation rate with an average of 0.2 cm/yr shows no significant changes through the whole core.

From the bottom at 135 up to 102 cm core depth, the organic content has the highest value (mean: 0.35%), and the carbonate content represents medium values (mean: 0.41%). Later, between 102 to 46 cm, organic and carbonate contents reach their lowest and the highest value (0.22%, 0.58%), respectively. Finally, from 46 cm up to the core top, the organic content increases slightly to 0.32%, while the carbonate content reaches its lowest value of 0.18%.

The pollen concentration and influx averages did not change markedly. Between 135 to 102 cm, the pollen concentration and influx are 15123 grains cm-3 and 3287 grains cm-2 yr-1, respectively, while the values increase slightly between 102 to 46 cm (pollen concentration and influx respectively are 17729 grains cm-3 and 3610 grains cm-2 yr-1). From 46 cm to the surface, the average value of the pollen concentration and influx increase to the highest value (19345 grains cm-3, 3938 grains cm-2 yr-1, respectively).

Description of the pollen, spores, NPPs, and macro-charcoal records

In total 63 pollen have been identified: 24 arboreal, 32 herb and 7 aquatic taxa. Also, two different types of fern spores and three NPPs (fungal spores and algae) have been recognized. The most frequent pollen taxa are illustrated in Figure 3.3 (for the whole pollen diagram see the supplementary material). Pollen of the *Juglans*, *Corylus*, *Prunus*, Cerealia-type, *Plantago lanceolata*-type, *P. major-media*-type, Fabaceae (Reticulate and Psilate), *Rumex*, and Brassicaceae are grouped as primary and secondary indicators of human activity.
Based on our floristic knowledge the CONISS cluster analysis dendrogram suggest two major zones KHL-A, which is divided in two subzones KHL-AI and KHL-AII, and KHL-B (Figs. 3.3 and 3.4).

Subzone KHL-AI (135-102 cm; 8 pollen samples; ca. 1180-1010 cal yr BP):

The AP (trees, shrubs and lianas) (51%) and NAP (herbs) (49%) are almost in balance with each other. Herbs are mainly represented by *Artemisia* (8-26%), Poaceae (7-14%), and Amaranthaceae (6-15%). Among AP *Quercus* (12-28%), *Fagus* (3-10%), *Carpinus*-type (5-14%), and *Juniperus* (4-13%) are the most frequent. Less frequent are *Alnus* (1-5%), *Pterocarya fraxinifolia* (1-4%) and *Juglans* (up to 2%), which show the highest value in this subzone. Aquatic pollen (except Cyperaceae (9-48%) and *Lemna* (2-55%)) have low frequencies. On the other hand, the human indicators pollen are well represented (5-12%), mainly by *Plantago lanceolata*-type (1-4%), Cerealia-type (1-4%), and *Juglans* (up to 2%) (Fig. 3). Fungal spores have the highest value (5-45%), mainly represented by the *Podospora*

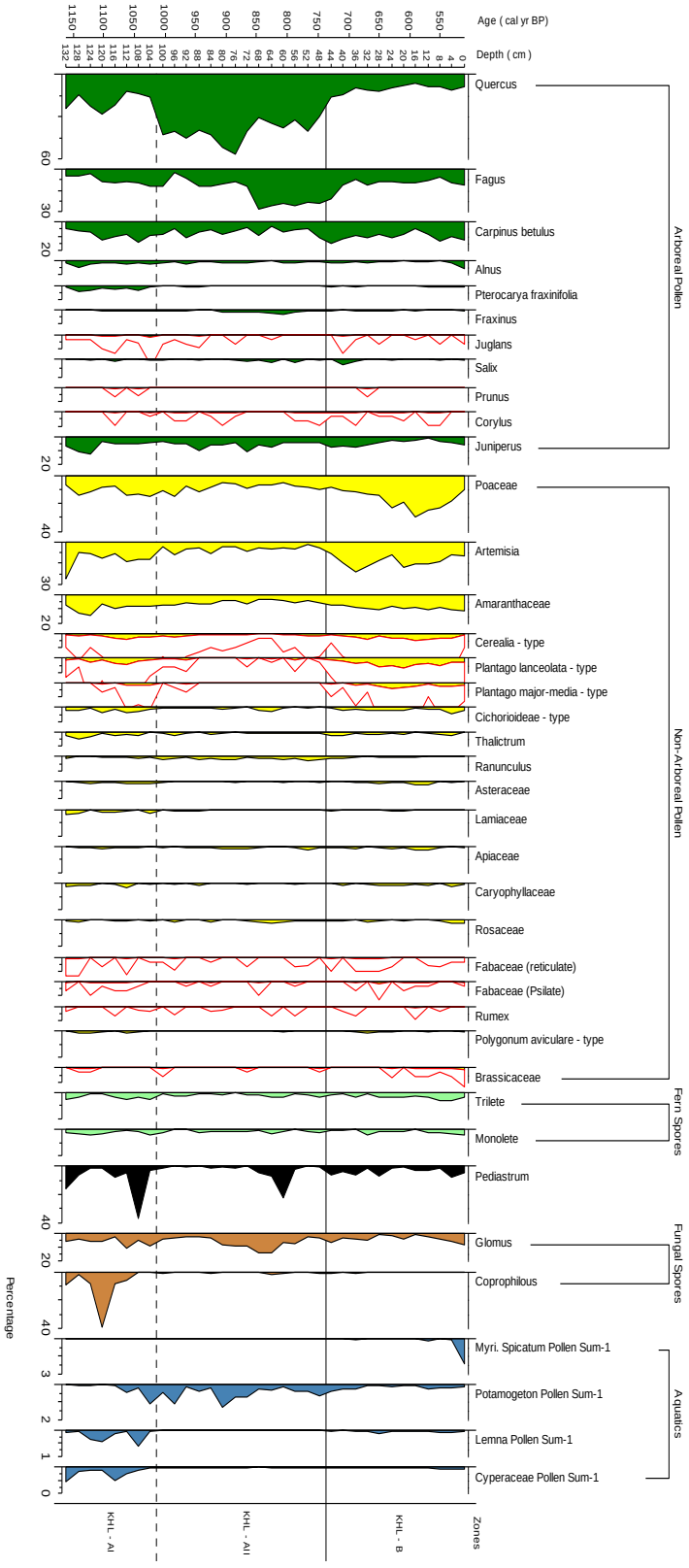

Fig. 3.3 Percentage diagram of the selected pollen taxa as well as fern spores and Non-arboreal pollen (NPPs) of the KHL core. Arboreal Pollen (AP) in green, Non-Arboreal Pollen (NAP) in yellow, Fern spores in pale green, *Pediastrum* (in black), NPPs in brown and ratios of aquatics to pollen sum in blue. The selected Human Indicators pollen is shown with a red outline with 10×, exaggeration.

(coprophilous spores) (0- 39%). The charcoal concentration and influx (with averages of 197 particles cm^{-3} and 46 particles cm^{-2} yr^{-1}, respectively) show their highest value only in the lowermost part of this subzone and then decrease continuously through the uppermost part of the core (Fig. 3.4).

Subzone KHL-AII (102-46 cm; 14 pollen samples; ca. 1010-740 cal yr BP):

This subzone is characterized by the high values of the AP and the low values of NAP. Arboreal pollen (50-81%) are represented mainly by *Quercus* (16-57%) and *Fagus* (3-28%). In comparison to other subzones, *Juglans* pollen decreases to the lowest value (0-1%), while *Salix* and *Fraxinus* increase (in particular in the uppermost part (0-2% and 0-3%, respectively). Herbaceous pollen representation is similar to the previous subzone by Poaceae (5-15%), *Artemisia* (1-12%), and Amaranthaceae (3-9%). The human indicator pollen decreases to the lowest values (1-9%). Aquatic pollen here is

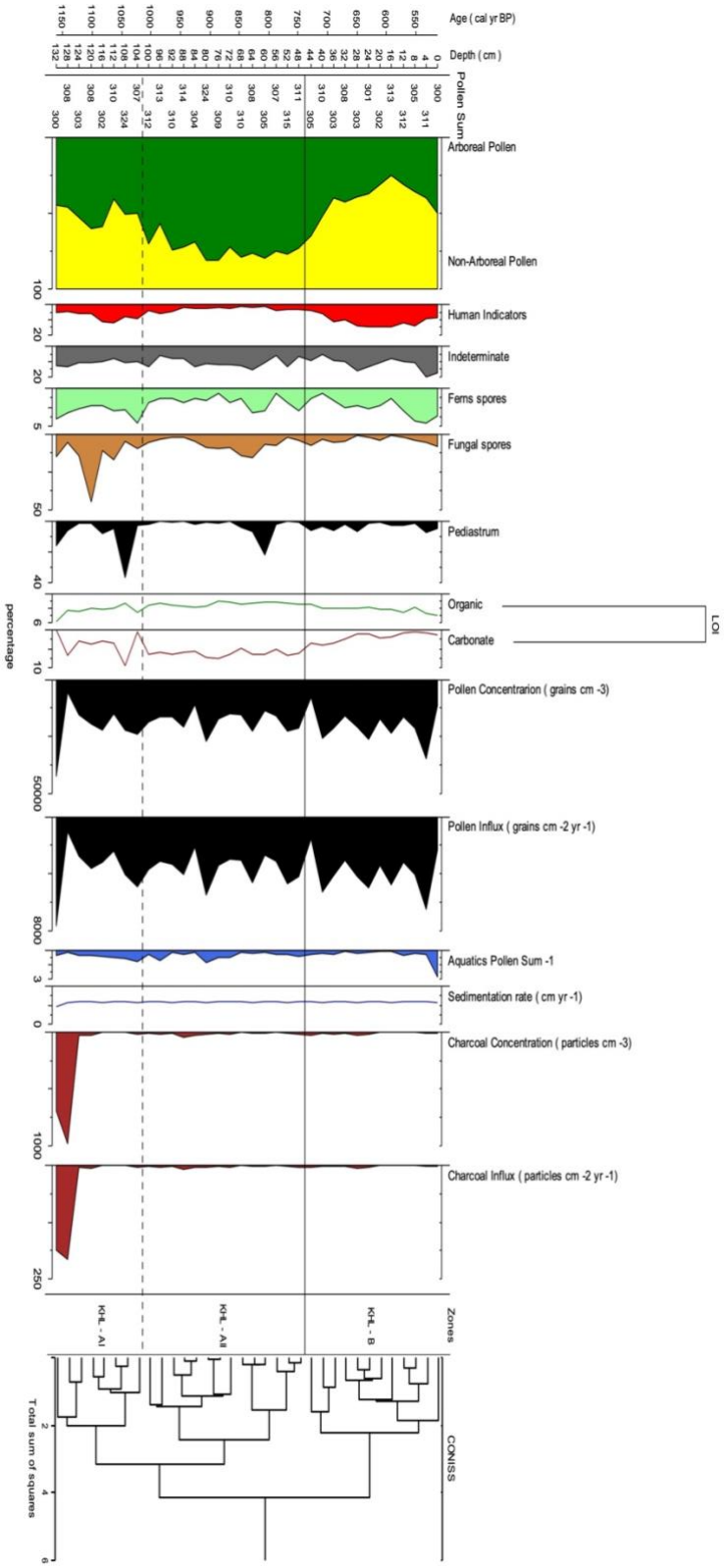

Fig. 3.4 Pollen summary diagram, the sum of AP (in green), NAP (in yellow), Aquatics (in blue), Human Indicators (in Red), Indeterminate pollen (in gray), Pollen concentration and influx (in black), Ferns spores (in pale green), Fungal spores (in brown), *Pediastrum* (in black), organic content (in green line), carbonate content (in brown line), sedimentation rate (in blue line), charcoal concentration and influx (in black dashes), CONISS of the pollen data (excluding Aquatics).

mainly represented by *Potamogeton* (average: 54%). *Pediastrum* has the lowest value (average: 3) among the other subzones only shows a single peak in the uppermost part of this subzone. The fungal spores are well represented (2-16%) and consist mainly of *Glomus* (2-14%) rather than coprophilous spores.

The charcoal concentration and influx decrease markedly (with the averages of 17 particles cm^{-3} and 4 particles cm^{-2} yr^{-1}, respectively).

Zone KHL-B (46-0 cm; 12 pollen samples; ca. 740-510 cal yr BP):

Herbaceous pollen (37-77%) prevailed to the AP (24-63%). *Quercus*, *Fagus*, and *Juniperus* values are markedly lower compared with the previous subzone. *Carpinus*-type is the most frequent AP (4-15%). *Juglans* (0-1%) and *Corylus* (0-1%) increase. According to the NAP, Poaceae (8-29%), *Artemisia* (8-21%), and Amaranthaceae (7-10%) are the most frequent taxa. Cerealia-type (1-5%), *Plantago lanceolata*-type (2-7%), and *P. major-media*-type (0-4%) represent their highest value among the profile. The human indicators pollen increases to the highest average value (11%) with the range of 4-15%. Aquatic pollen show a decreasing trend except for the record uppermost part of the record, which show a single maximum due to an increase in *Myriophyllum* pollen. *Pediastrum* algae is representing continuously with an average of 3.5%.

The charcoal concentration and influx have the lowest value in this subzone (with the averages of 13 particles cm^{-3} and 3 particles cm^{-2} yr^{-1}, respectively).

X-ray fluorescence analysis

From the elemental data set, the most reliable acquired elements were chosen. The elemental peak of K, Ca, Ti, Si, and ratios of K/Ti, Si/Ti, Mn/Ti, Ca/Ti, Sr/Ti, Si/Fe, and incoherent/coherent (inc./coh.) are shown in Fig.3.5. The zonation is based on the pollen cluster analysis (KHL-AI, AII, and B). In order to be able to quantify the strength of dependence between pairs of elements correlation matrices were constructed for each subzone Table 3.3. The strong correlations ($r \leq -0.70$ or ≥ 0.70) are detectable with asterisks. Although the constructed matrices represent coupling and decoupling between elements through the KHL profile, the Fe correlates with K and Ti in all the units strongly and hence detrital inputs (Kylander et al. 2011). Silicate for the first two subzones (KHL-AI and AII) correlates strongly with K, Ti, and Fe while in the last zone (KHL-B) it has a moderate relationship which represents it is controlled mainly by the silicate sources (Kylander et al. 2011). Calcium strongly correlates with Sr in KHL-AI and KHL-B and suggests the importance of the carbonate precipitation (Kylander et al. 2011), while the KHL-AII shows minimal correlation. The Ca

curve shows more distinct changes compared to other curves. At the base of the profile (KHL-AI), except for two peaks, it is not as high as the middle part (KHL-AII).

Depth (cm)		Si	K	Ca	Ti	Mn	Fe	Sr	Al
0 - 46	Si	1.00							
	K	0.66	1.00						
	Ca	0.19	0.17	1.00					
	Ti	0.62	0.89*	-0.12	1.00				
	Mn	0.30	0.31	0.26	0.25	1.00			
	Fe	0.64	0.86*	-0.16	0.94*	0.30	1.00		
	Sr	0.28	0.33	0.95*	0.06	0.32	0.02	1.00	
	Al	0.17	0.08	0.10	0.08	0.04	0.10	0.11	1.00
46 - 102	Si	1.00							
	K	0.81*	1.00						
	Ca	-0.32	-0.43	1.00					
	Ti	0.79*	0.97*	-0.48	1.00				
	Mn	0.20	0.28	0.20	0.25	1.00			
	Fe	0.75*	0.96*	-0.48	0.97*	0.31	1.00		
	Sr	0.05	0.08	0.20	0.07	0.12	0.04	1.00	
	Al	0.19	0.17	-0.05	0.15	0.06	0.16	-0.03	1.00
102 - 135	Si	1.00							
	K	0.96*	1.00						
	Ca	-0.05	-0.08	1.00					
	Ti	0.94*	0.96*	-0.27	1.00				
	Mn	0.53	0.52	0.53	0.42	1.00			
	Fe	0.91*	0.94*	-0.32	0.98*	0.37	1.00		
	Sr	0.18	0.15	0.95*	-0.04	0.68	-0.10	1.00	
	Al	0.28	0.25	0.16	0.20	0.20	0.20	0.20	1.00

Table 3.2 Correlations matrices (*r* values) for the Kholasht-Kouh sequence in each defined zones and subzones (* Strong correlations ($r \geq 0.7$ or $r \leq -0.7$))

The peak areas of Ca in the KHL-AII are high and more constant. The presence of the shells as the probable reason for this increment must be considered. From KHL-B the Ca profile shows a slightly decreasing trend. Potassium, Ti and Si show the same broad pattern for all the subzones. The elemental peaks at the base part (KHL-AI) are the highest. Except for the middle part of the KHL-AII that shows several manifest increasing peaks, the rest of the profile represents a long-term decreasing trend that continues up to the surface of the core. The depth profiles of all the ratios show almost the same pattern but different to the elemental profile. At the core base (KHL-AI), except for two small increases, they show a constant low amount. While during the middle part (KHL-AII) several increments and decreases are visible. The remaining portion of the core (KHL-B) is resumed the decreasing trend to the lowest amount.

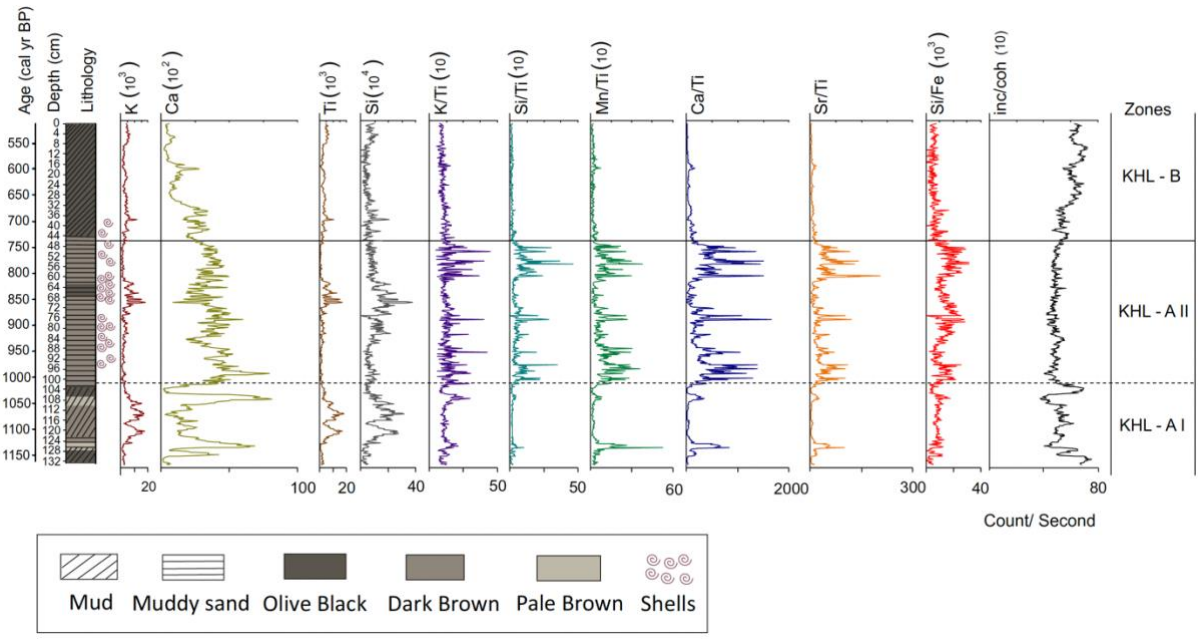

Fig. 3.5 Diagram with the lithology, and selected geochemical elements and ratios (based on counts per second).

The organic content profile (inc./coh. ratio) at the lowest subzone (KHL-AI) with several changes shows a decreasing trend during the KHL-AII. However, it is constant but reaches the lowest amount. From the beginning of the upper zone (KHL-B), there is a gradual increase.

Discussion

Chronological framework

The Kholash-Kouh lake is located near alluvial sediments. Possible inputs from the surrounding thin bedded limestone nummulite formation may influence the dating. The frequent occurrence of aquatic plants such as Potamogeton is likely to contribute to a reservoir effect in the dates that were obtained from bulk sediment samples (Marty and Myrbo 2014). Due to the lack of sufficient plant remains and charcoal particles, dating was done based on bulk organic matter. The chronology has uncertainties because of a potential reservoir effect and should be used with caution. Further studies may help for a better understanding of potential reservoir effects in the region.

Local environment of Kholash-Kouh Lake

Period 1180-1010 cal yr BP (778-940 AD, subzone KHL-AI)

The high occurrence of Cyperaceae, but rare aquatic plants such as *Potamogeton* and *Myriophyllum* and some algae of *Pediastrum* suggest shallow water at the initiation of the lake. Later during this period, *Lemna* and later *Potamogeton* as well as *Pediastrum* increased, while Cyperaceae decreased, except a short phase in the middle of the period, which suggests an

increasing and fluctuating lake levels, probably due to higher rainfall rates. The two phases with a high frequency of *Lemna* reflect a nutrient rich environment (Wolverton and Mcdonald 1981), which is in line with the highest amount of the organic content during this period.

During this period accumulated in the lake detritus mud and muddy sand. The selected XRF-data of elements such as K, Ti and Si indicate relatively humid condition. At around 1120-1040 cal yr BP (124-108 cm), the high amounts of K, Ti and Si show also high correlation in-between, and may indicate an increase in detrital inputs (Davies et al. 2015). High values of K/Ti ratio is an indicator for more physical weathering due to drier condition (Davies et al. 2015). In this case, the low value of K/Ti ratio (except the two peaks) may indicate humid condition for this period. Manganese as an insoluble oxide element can represent changes in the lake level or biological activity in the lake (Davison 1993; Kylander et al. 2011). Lower lake level and/or photosynthesis, both can increase the Mn/Ti ratio. The low Mn/Ti ratio, besides the Ca/Ti and Sr/Ti ratios (indicator for lower lake level (Haberzettl et al. 2009; Kylander et al. 2011, 2013)), and rare presence of *Potamogeton* which grows in shallow lakes (Xu et al. 2020), can point to the higher lake level. The Si/Fe ratio, which can be used as temperature indicator (Erbs-Hansen et al. 2013), showed an increasing trend.

At the end of this period Cyperaceae decreased markedly, and *Potamogeton* became abundant. At the same time, values of K, Ti, and Si together with the ratios of the K/Ti and Si/Fe decreased markedly, suggesting relatively cold temperatures with a short drought event.

Period 1010-740 cal yr BP (940-1214 AD, subzone KHL-AII)

The low occurrence of Cyperaceae at the lake shore vegetation and frequent *Potamogeton*, probably covering large parts of the lake surface, likely reduced strongly the occurrence of *Lemna*, suggesting a relatively low lake level. *Potamogeton* is common in water depths between 60 to 120 cm depth, and their distribution is limited to water depths higher than 200 cm (Zhou et al. 2017). *Pediastrum* is frequent in eutrophic lake conditions (Sá et al. 2019), therefore its low occurrence for most of the time in this period is in line with low amount of the organic matter.

During this period deposited in the lake mostly muddy sand material. The Mn/Ti, Ca/Ti, and Sr/Ti ratios are in line with the abundance of the *Potamogeton*, and verified the lower lake level for this period. Mn/Ti, Ca/Ti, and Sr/Ti ratios were high except for short periods between ca. 984 to 965 and ca. 807 to 748 cal yr BP (96-92 cm and 60-48 cm, respectively). In both mentioned periods the rainfall could be more frequent (due to the lowest K/Ti ratio). Besides reducing the temperature (referring to the reduction of the Si/Fe ratio) it may also reduce the

lake water evaporation and result in higher water levels. The increased K, Ti, and Si (indicators for detrital inputs) around 807 to 748 cal yr BP suggest that the deposit was fed mostly by the surface water. Potassium can confirm the dense vegetation covers (Davies et al. 2015) in close distance to the Kholash-Kouh lake, the denser vegetation increased the K leaching through chemical weathering and resulted in lower K values. Referring to the high Si/Fe ratio values, this period (ca. 1010 – 740 cal yr BP) was the warmest throughout the whole recorded late Holocene. This warm period occurred during the MCA, ca. 950-1250 AD or 1000-700 cal yr BP (Ruddiman 2008). Several records document this period as the warmest of the late Holocene (Ramezani 2013; Haghani et al. 2015; Homami Totmaj et al. 2021).

Period 740-510 cal yr BP (1214-1436 AD, zone KHL-B)

The lower occurrence of *Potamogeton*, the moderate occurrence of *Lemna* as well as the algae *Pediastrum* may indicate higher lake levels. All the elements remained low, specially the Si/Fe ratio which had the lowest value, and represented the coldest climate in the record during the LIA, ca. 1350-1850 AD or 600-100 cal yr BP (Mann et al. 2009). Also, the comprehensive study at Neor Lake (180 km northwest to the study site), documented the occurrence of the strongest Siberian High during the last 5000 years (Sharifi et al. 2015). Potassium, Ti, and Si also indicate lower detrital inputs for this period, which is verified with the lowest sedimentation rate. The ratios of Ca/Ti, Sr/Ti, and Mn/Ti represented the lowest values in the record. Carbonate and silicate weathering affected the amount of Ca and Sr elements in the catchment (Kylander et al. 2013). The lowest value of carbonate matter content verified low inputs of carbonate for this period. The possible reason for the Mn/Ti ratio reduction has been sedimentation during anoxic conditions in the lake. Ice cover and high organic matter content are the two important drivers for methanogenesis in lakes (Wetzel 2001; Kylander et al. 2013), which formed anoxic conditions. Also, the incoherent/coherent (inc/coh) ratio, commonly used as parameter for evaluating the organic content in the lake sediments (Burnett et al. 2011), verified the highest organic matter of the core during this period.

Vegetation changes (forest vs. open vegetation), and anthropogenic activities

Period 1180-1010 cal yr BP (778-940 AD, subzone KHL-AI)

The pollen record (Figs. 3.3 and 3.4) indicate that the study area was covered by relatively high proportion of non-arboreal vegetation. The open vegetation surrounding the lake was composed mainly of *Artemisia*, Amaranthaceae and Poaceae.

Forest areas at lower elevations, were mainly composed of *Quercus, Fagus, Carpinus* and *Juniperus*. After ca. 1100 cal yr BP (120 cm core depth) *Quercus* decreased, while *Fagus* and *Carpinus* species increased in the forest. This reduction of *Quercus* occurred with the increase of the human pollen indicator. The highest frequency of coprophilous spores and macro-charcoal particles at the beginning of this record indicate human settlements engaged in animal husbandry at lower elevations. A few Cerealia pollen, as well as *Plantago* and other indicators suggest anthropogenic activities in the region of the lake at lower elevations. The archaeological site of Ghale Kouti (16 km distance to Kholash-Kouh) at 1600 m a.s.l., consists of cemeteries from the Iron Age (Fallahian 2013) and verifies presence of humans at the lake's lower elevations since ancient times.

Period 1010-740 cal yr BP (940-1214 AD, subzone KHL-AII)

During this period, the dominant herbs decreased markedly, while trees increased in density and/or expanded from lower to upper elevations. The warm condition during this period, may provide favorable conditions for forest expansion. This forest expansion is also documented in our previous studies from Annal Lake (700 m elevation) and Pounel mire (2200 m elevation) for the same time period (Homami Totmaj et al. 2020, 2021), about 125 km and 145 km distance to the site, respectively. However, in the KHL record *Quercus* is the most abundant forest taxon, while in the Annal Lake *Carpinus betulus* and *Alnus* (characteristic tree for lower than 1000 m elevations) were the most abundant ones. After ca. 860 cal yr BP (72 cm core depth), *Fagus* trees became more frequent indicating more closed canopy compared to previous phase, *Fagus* sapling, as the shade tolerant taxa out compete the light-demanding *Quercus* sapling (Ligot et al. 2013). Alinezhad et al. (2021) showed also in their study on Neor Lake that over the last 1800 years, *Quercus* had the strongest occurrence at ca. 1000 cal yr BP, followed by a reduction after ca. 600 cal yr BP.

The human activities showed a reduction during this period, documented with the lowest frequency of Cerealia and other human indicator taxa, rarity of the coprophilous spores and macro-charcoal particles. Though, this reduction is opposite to our previous studies at Annal Lake and Pounel mire (Homami Totmaj et al. 2020, 2021), which showed increased anthropogenic activities. Based on the current settlements (there is a small summer use village in 3.5 km distance to the lake) we may argue that people were always present at several distances to the lake, nevertheless expansion of the forest, resulted in higher arboreal pollen deposition while reduced presence of the human pollen indicators specially the Cerealia.

Period 740-510 cal yr BP (1214-1436 AD, subzone KHL-B)

Since this period, herbs, specially Poaceae, *Artemisia*, and Amaranthaceae increased markedly probably due to deforestation. The strong reduction of arboreal plants, especially *Quercus* and *Fagus*, is the most characteristic of the last 740 to ca. 510 cal yr BP, most probably due to selective logging as the wood is better. However, *Carpinus* increased which may refer to the growth of the *Carpinus orientalis*, characteristic tree for the 2300 to 2400 elevation (Ramezani et al. 2013). A probable reason for the forest reduction may refers to the construction activities by humans and/or the need of wood for fire, as this period stay during the Little Ice Age with prevailed cold weather. However, fires were rare during this period, indicating that the possible practice of frequent burning of the steppe vegetation at the beginning of the record changed.
The highest values of Cerealia and *Plantago* is in line with reduction of the trees indicate intensified of anthropogenic activities lead to extensive deforestation and expansion of steppe vegetation.

Conclusions

Our multi-proxy analysis of the Kholash-Kouh lake core, located above the modern forest line, allowed to reconstruct the vegetation and climate changes, local fire history and anthropogenic activities since 1180 cal yr BP. Referring to the palynological reconstruction, three distinct periods have been identified. The surrounding of the lake was covered mainly by herbaceous vegetation with species of Poaceae, *Artemisia*, and Amaranthaceae, for the whole recorded period. The only exceptional period between 1010-740 cal yr BP, documented the dominance of the forest mainly with *Quercus*, *Fagus*, *Carpinus* and *Juniperus*, rather than steppe vegetation.

The geochemical elements such as K, Ti and Si represented relatively humid condition between 1180 to 1010 cal yr BP. Furthermore, low values of the Mn/Ti, Ca/Ti and Sr/Ti ratios suggested higher lake level. After 1010 up to 740 cal yr BP the highest value of the Si/Fe ratio, represented warmest period throughout the record. While its lowest value, in line with the reduction of other elements and ratios, after 740 cal yr BP represented cold and dry period. In conclusion, according to the XRF results, this study in line with the past surveys, verified the warmest and coldest conditions, due to the Medieval Climatic Anomaly (1000-700 cal yr BP) and Little Ice Age (600- 100 cal yr BP), respectively.

Finally, the human impacts on the lake and surroundings were investigated, indicating the strongest environmental disturbance obtained from the marked deforestation and expansion of steppe vegetation. The higher occurrence of Cerealia and *Plantago* reflect intensified agro-pastoral activities at lower elevation between ca.740 to 510 cal yr BP. As conclusion to

anthropogenic activities, it seems that humans were present only at several distances to the lake and seem to not play an important role in the lake's environmental changes.

Acknowledgments

We like to thank Dr. Arash Sharifi for his valuable time spending to help us regarding the age-depth model and geochemical data. We also are grateful the reviewers for their comments on the manuscript. We are so grateful to Dr. Giahchi and Mr. Amani from the Geology and Mineral Exploration of Gilan for their assistance during the field excursions. The study was part of the PhD project of the first author, which was supported by the German Science Foundation DFG (grant BE2116/31-1) carried out at Georg-August-Universität Göttingen, Germany. The data reported in this paper will be archived in www.neotoma.de.

References

Akhani H, Djamali M, Ghorbanalizadeh A, Ramezani E (2010) Plant biodiversity of Hyrcanian relict forests, N Iran: an overview of the flora, vegetation, palaeoecology and conservation. Pakistan Journal of Botany 42: 231-258

Alinezhad K, Ramezani E, Djamali M, Sharifi A, Naqinezhad A, Aubert C, Gandouin E, Pourmand A (2021) Lake Neor reveals how mountain vegetation responded to 7000 years of hydroclimate variability in northwestern Iran. Journ Quate Scien 36(4): 598-610 https://doi.org/10.1002/jqs.3310

Beni AN, Lahijani H, Harami RM, et al (2013) Caspian Sea-level changes during the last millennium: Historical and geological evidence from the south Caspian Sea. Climate of the Past 9:1645–1665. https://doi.org/10.5194/cp-9-1645-2013

Beug HJ (2004) Leitfaden der Pollenbestimmung für Mitteleuropa und angrenzende Gebiete. Verlag Friedrich Pfeil, Munich

Blaauw M (2010) Methods and code for 'classical'age-modelling of radiocarbon sequences. Quaternary Geochronology 5:512–518. https:// doi. org/ 10. 1016/j. quageo. 2010. 01. 002

Burnett AP, Soreghan MJ, Scholz CA, Brown ET (2011) Tropical East African climate change and its relation to global climate: a record from Lake Tanganyika, Tropical East Africa, over the past 90+ kyr. Palaeogeo, Palaeoclima, Palaeoeco 303(1–4):155–167. https:// doi. org/ 10. 1016/j. palaeo. 2010. 02. 011

Croudace IW, Rindby A, Rothwell RG (2006) ITRAX: description and evaluation of a new multi-function X-ray core scanner. Geology Society London Special Publications 267(1): 51–63

Davies SJ, Lamb HF, Roberts SJ (2015) Micro-XRF Core Scanning in Palaeolimnology: Recent Developments. Micro-XRF studies of sediment cores 189–226

Davison W (1993) Iron and manganese in lakes. Earth-Science Reviews 34:119–163

Djamali M, Akhani H, Andrieu-Ponel V, et al (2010) Indian summer Monsoon variations could have affected the early-Holocene woodland expansion in the Near East. Holocene 20:813–820. https://doi.org/10.1177/0959683610362813

Erbs-Hansen DR, Knudsen KL, Olsen J, et al (2013) Paleoceanographical development off Sisimiut, West Greenland, during the mid- and late Holocene: A multiproxy study. Marine Micropaleontology 102:79–97. https://doi.org/https://doi.org/10.1016/j.marmicro.2013.06.003

Faegri K, Iversen J (1989) Textbook of Pollen Analysis. John Wiley and Sons.

Fallahian Y (2013) Investigation of burial patterns in Iron Age of Gilan, Iran. Ancient Asia 4. https://doi.org/10.5334/aa.12311

Grimm EC (1987) CONISS: A FORTRAN 77 program for stratigraphically constrained cluster analysis by the method of incremental sum of squares*. Computers & Geosciences 13:13–35

Gu F, Ramezani E, Alizadeh K, Behling H (2021) Vegetation Dynamics, Environmental Changes, and Anthropogenic Impacts on the Coastal Hyrcanian Forests in Northern Iran. Journal of Coastal Research 37:611–619. https://doi.org/10.2112/JCOASTRES-D-20-00033.1

Haberzettl T, Anselmetti FS, Bowen SW, et al (2009) Late Pleistocene dust deposition in the Patagonian steppe - extending and refining the paleoenvironmental and tephrochronological record from Laguna Potrok Aike back to 55 ka. Quaternary Science Reviews 28:2927–2939. https://doi.org/10.1016/j.quascirev.2009.07.021

Haghani S, Leroy SAG, Khdir S, et al (2015) An early 'Little Ice Age' brackish water invasion along the south coast of the Caspian Sea (sediment of Langarud wetland) and its wider impacts on environment and people. Holocene 26:3–16. https://doi.org/10.1177/0959683615596835

Heiri O, Lotter AF, Lemcke G (2001) Loss on ignition as a method for estimating organic and carbonate content in sediments: reproducibility and comparability of results. Journal of Paleolimnology 25:101-110.

Homami Totmaj L, Alizadeh K, Giahchi P, et al (2021) Late Holocene Hyrcanian forest and environmental dynamics in the mid-elevatedhighland of the Alborz Mountains, northern Iran. Review of Palaeobotany and Palynology 295:104507.

Homami Totmaj L, Ramezani E, Alizadeh K, Behling H (2020) Four millennia of vegetation and environmental history above the Hyrcanian forest, northern Iran. Vegetation History and Archaeobotany. https://doi.org/10.1007/s00334-020-00813-y

Kendrew WG (1922) The climates of the continents. Claredon Press

Khakpour Saeej M, Ramezani E, Siyab Ghodsy A, et al (2013) Palynological reconstruction of 1500 years of vegetation history of Veisar (N Iran). Rostaniha 14:135–148

Khalili A (1973) Precipitation patterns of central Elburz. Archiv für Meteorologie, Geophysik und Bioklimatologie, Serie B 21:215–232

Kylander ME, Ampel L, Wohlfarth B, Veres D (2011) High-resolution X-ray fluorescence core scanning analysis of Les Echets (France) sedimentary sequence: New insights from chemical proxies. Journal of Quaternary Science 26:109–117. https://doi.org/10.1002/jqs.1438

Kylander ME, Klaminder J, Wohlfarth B, Löwemark L (2013) Geochemical responses to paleoclimatic changes in southern Sweden since the late glacial: The Hässeldala Port lake sediment record. Journal of Paleolimnology 50:57–70. https://doi.org/10.1007/s10933-013-9704-z

Leroy SAG, Amini A, Gregg MW, et al (2019) Human responses to environmental change on the southern coastal plain of the Caspian Sea during the Mesolithic and Neolithic periods. Quaternary Science Reviews 218:343–364. https://doi.org/10.1016/j.quascirev.2019.06.038

Leroy SAG, Lahijani HAK, Djamali M, et al (2011) Late Little Ice Age palaeoenvironmental records from the Anzali and Amirkola Lagoons (south Caspian Sea): Vegetation and sea level changes. Palaeogeography, Palaeoclimatology, Palaeoecology 302:415–434. https://doi.org/10.1016/j.palaeo.2011.02.002

Leroy SAG, Roiron P (1996) Latest Pliocene pollen and leaf floras from Bernasso palaeolake (Escandorgue Massif, H6rault, France)

Leroy SAG, Tudryn A, Chalié F, et al (2013) From the Allerød to the mid-Holocene: Palynological evidence from the south basin of the Caspian Sea. Quaternary Science Reviews 78:77–97. https://doi.org/10.1016/j.quascirev.2013.07.032

Ligot G, Balandier P, Fayolle A, et al (2013) Height competition between Quercus petraea and Fagus sylvatica natural regeneration in mixed and uneven-aged stands. Forest Ecology and Management 304:391–398. https://doi.org/10.1016/j.foreco.2013.05.050

Livingstone DA (1955) A Lightweight Piston Sampler for Lake Deposits. Ecology 36: 137-139

Mann ME, Zhang Z, Rutherford S, et al (2009) Global signatures and dynamical origins of the Little Ice Age and Medieval Climate Anomaly. Science 326:1256–1260

Marty J, Myrbo A (2014) Radiocarbon dating suitability of aquatic plant macrofossils. JPOL 52 (4): 435-443

Mohammadi Nia A, Alimohammadi A, Habibi R, Shirzadi MR (2015) Spatial and statistical analysis of leptospirosis in guilan province, Iran. In: International Archives of the Photogrammetry, Remote Sensing and Spatial Information Sciences - ISPRS Archives. International Society for Photogrammetry and Remote Sensing 497–502

Ramezani E (2013) Palynological reconstruction of late-Holocene vegetation, climate, and human impact in Kelardasht (Mazandaran province, N Iran). Iranian Journal of Forest and Poplar Research 21:48–62. https://doi.org/10.22092/ijfpr.2013.3338

Ramezani E, Marvie Mohadjer MR, Knapp HD, et al (2013) Pollen-vegetation relationships in the central Caspian (Hyrcanian) forests of northern Iran. Review of Palaeobotany and Palynology 189:38–49. https://doi.org/10.1016/j.revpalbo.2012.10.004

Rousta I, Doostkamian M, Haghighi E, et al (2017) Analysis of spatial autocorrelation patterns of heavy and super-heavy rainfall in Iran. Advances in Atmospheric Sciences 34:1069–1081

Ruddiman WF (2008) Earth's Climate:past and future. Second Edition Chapter 2 Climate Archives, Data, and Models.

Sá N de P, Carvalho M de A, Correia G da C (2019) Miocene paleoenvironmental changes in the Solimões Basin, western Amazon, Brazil: A reconstruction based on palynofacies analysis. Palaeogeography, Palaeoclimatology, Palaeoecology. https://doi.org/10.1016/j.palaeo.2019.109450

Sabeti H (1994) Forest, trees and bushes of Iran. Yazd University Press (in Persian, with English summary)

Sharifi A, Pourmand A, Canuel E.A, Ferer-Tyler E, Peterson L.C, Aichner B, Feakins, Touraj DaryaeeS.J, Djamali M, Naderi Beni A, Lahijani H.A.K, Swart P.K (2015) Abrupt climate variability since the last deglaciation based on a high-resolution, multi-proxy peat record from NW Iran: The hand that rocked the Cradle of Civilization? Quate Scie Revie 123: 215-230 http://dx.doi.org/10.1016/j.quascirev.2015.07.006

Stevenson J, Haberle S (2005) Palaeoworks Technical Papers 5. Macro Charcoal Analysis: A modified technique used by the department of Archaeology and Natural History. Department of Archaeology & Natural History, Palaeoworks Technical Papers 5 Australian National University, Canberra

Wetzel RG (2001) The nitrogen cycle. Limnology: Lake and river ecosystems 205–237

Wolverton BC, Mcdonald RC (1981) Energy from vascular plant wastewater treatment systems. Economic Botany 35:224. https://doi.org/10.1007/BF02858689

Xu J, Wang T, García Molinos J, et al (2020) Effects of warming, climate extremes and phosphorus enrichment on the growth, sexual reproduction and propagule carbon and nitrogen stoichiometry of Potamogeton crispus L. Environment International 137:105502. https://doi.org/10.1016/j.envint.2020.105502

Zhou N, Hu W, Deng J, et al (2017) The effects of water depth on the growth and reproduction of Potamogeton crispus in an in situ experiment. Journal of Plant Ecology 10:546–558. https://doi.org/10.1093/jpe/rtw048

Zohary M (1973) Geobotanical foundations of the Middle East, Volume 2. Fischer, Stuttgart

Chapter 4: Paper III

Late Holocene Hyrcanian forest and environmental dynamics in the mid-elevated highland of the Alborz Mountains, northern Iran

Leila Homami Totmaj[1]*, Kammaledin Alizadeh[1], Panthea Giahchi[2], Javad Darvishi Khatooni[3], Hermann Behling[1]

[1]University of Goettingen, Department of Palynology and Climate Dynamics, Albrecht-von-Haller Institute for Plant Sciences, Untere Karspüle 2, 37073 Goettingen, Germany

[2]General Directorate of Geology and Mineral Exploration of Gilan

[3]Marine Geology Department, Geological Survey of Iran

Published (2021) in "Review of Palaeobotany and Palynology 295, 104507"
doi.org/10.1016/j.revpalbo.2021.104507

Abstract

We present a high-resolution multi-proxy study including pollen, spores, non-pollen palynomorphs, charcoal, loss on ignition, and geochemical analysis from the radiocarbon dated sediment core of Annal Lake. The lake is located at 700 m elevation in the Hyrcanian forest of the Gilan province, northern Iran. Between ca. 1690-1450 cal yr BP, a mixed forest with *Alnus*, *Carpinus*, *Quercus*, and *Fagus* were present, as well as patches of grassland areas around the lake. At ca. 1450 cal yr BP, the forest expanded and reduced the open grassland areas until 65 cal yr BP. Different proxies indicate that humans were present in the studied area since the beginning of the recorded period. However, since 65 cal yr BP, human impact increased markedly by deforestation and cattle grazing, and settlers probably changed from pastoralism to more farmers. Ratios of geochemical elements such as V/Cr, K/Al, Rb/Al, Si/Fe, and Ca/K suggested the warmest period with the higher amount of rainfall and detrital inputs forming a shallow lake between ca. 1690 – 580 cal yr BP. In contrast, a colder and drier period occurred between ca. 580 to 250 cal yr BP, mostly corresponding to the Little Ice Age period. Based on the geochemical element ratios, the highest detrital inputs (Ti), the highest lake level (V/Cr, Rb/Al, K/Al), and the wettest climatic conditions (Ca/Ti) with high rainfall and a relatively stable climatic conditions occurred for the last ca. 250 cal yr BP since the recorded period.

Introduction

The southern coast of the Caspian Sea, the largest lake of the world, and the northern slopes of the Alborz and Talysh Mountains host the last relicts of the deciduous broadleaved forest species from the Arcto-Tertiary era (e.g., Leroy and Roiron, 1996; Ramezani et al. 2008; Zohary, 1973). These species (e.g., *Parrotia persica*, *Zelkova carpinifolia*, *Gleditsia caspica*, and *Pterocarya fraxinifolia*) were widespread in temperate regions of the Northern Hemisphere throughout the Pliocene. However, during the Quaternary, they extinct in Europe and northern Asia (Zohary, 1973). The expansion of the Hyrcanian forest prior to the Last Glacial Maximum (LGM) is not known (Leroy et al. 2013), but together with the Colchic forest of Georgia (Knapp, 2005), they can represent a framework for the European Pliocene and Early Pleistocene vegetation period (Leroy and Roiron, 1996).

So far, most palaeoecologists have focused on the central and eastern plains of the Caspian Sea (e.g., Ramezani et al. 2008; Djamali et al. 2009; Khakpour Saeej et al. 2013; Leroy et al. 2013, 2019), while the western part has been little considered.

In studies of the western lowland region, Leroy et al. (2011) investigated the lagoons of Anzali and Amirkola. They interpreted the sea level increase due to higher rainfall during the Little Ice

Age (LIA). Between 300 to 220 cal yr BP, dense Alnus forests were reduced by human activities like burning and expansion of paddies fields. Haghani et al. (2015) studied the LIA effect on the Langarud wetland and its impacts on the environment and people. The study site is located 10 km inland of water incursion due to LIA, which increased soil salinity, reduced agricultural activities, damaged the Alnus swamp, and expanded the grassland vegetation. Gu et al. (2021) reconstructed the Zarbijar wetland (12 km distance to the Langarud wetland) for the last 600 years. They indicated that the southwestern coastal ecosystems were influenced mainly by anthropogenic activities, which intensified for the last century.

Our previous study was the first study from the Gilan highlands (Pounel mire at 2280 m elevation) and covered the entire late Holocene period (Homami Totmaj et al. 2020). The record suggested wet conditions between 4300-1700 cal yr BP, which altered by a dry period between ca. 1700-1000 cal yr BP. However, more humid condition state prevailed in the area over the last millennium. Besides the climate changes, long-term human activities were confirmed, with frequent fires during the Iron Age and then by intense grazing.

This study investigates a lake archive for the first time inside the mid-elevated Hyrcanian forest area at 700 m of the Gilan province. For this unstudied region, we aim to investigate past vegetation and climate changes as well as anthropogenic activities applying multi-proxy analysis on the collected sediment core from Lake Anal.

The main research questions are: 1) How did vegetation and climate change during the recorded period in mid-elevated highland areas? 2) What were the impacts of the Medieval Climatic Anomaly (MCA) and LIA on the vegetation? 3) What were the human impacts, and how strong the vegetation was affected by humans? 4) How natural is the current Hyrcanian forest?

Study area

Geographical location

The Hyrcanian forest occupies a small ca. 800 km long belt between coast and mountains up to 2500 m elevation of northern Iran (Sagheb-Talebi et al. 2014) and located in three provinces: Gilan, Mazandaran, and Golestan (from west to east). The study area is located in the Gilan province, inside the mid-elevated Hyrcanian forest. This small lake, called Annal (ANL), with the coordinates of 37°31'44.83"N, 48°53'13.99"E, is located at 700 m a.s.l. (Fig. 4.1), in the small Annal village. The round isolated lake has an area of 160 m^2, with a diameter of 60 m and a maximum water depth of 2 m.

Climate

Three different climate systems influence the study region: the mid-latitude Westerlies, the Siberian Anticyclone (Djamali et al. 2010). Between the Caspian Sea (CS) and mountains, humidity gets blocked and causes a temperate climate with warm, humid summers and mild winters (Kendrew, 1961). In general, precipitation decreases from the west to the east and from the CS coastal plain to the Alborz mountain highlands (Khalili, 1973). Gilan has the highest rainfall in Iran, with in general ca. 1400 mm per year (Rousta et al. 2017). Based on the nearest meteorological station (Asbe Vooni, 13 km distant from the coring site at 1500 m elevation, Fig. 4.1A), the average annual precipitation for the last 20 years is 792 mm. The average yearly maximum and minimum temperatures are 21 and -3 °C, respectively.

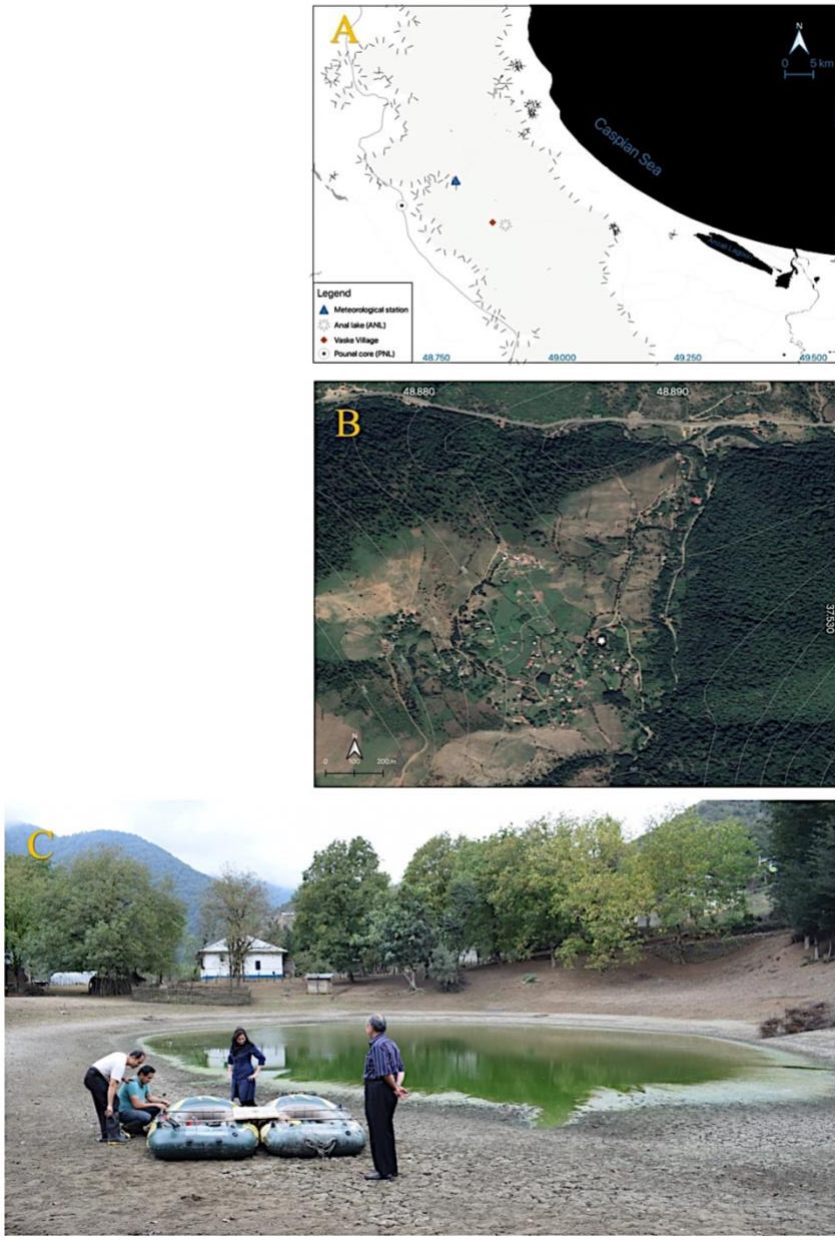

Fig. 4.1. A. Geographical location of the study area along with some other places discussed in this study; B. Geographical location of the Annal Lake (white asterisk), the defined light green color indicates forest distribution. The map was produced using natural earth data in a QGIS 3.14 environment; C. Photo of the Annal Lake coring site (ANL) in September 2018. (For interpretation of the references to color in this figure legend, the reader is referred to the web version of this article.)

Vegetation and human impact

In the surroundings of Lake Annal, soils are moist, black, and highly organic. The study area at 700 m elevation, is located in the Hyrcanian sub-montane deciduous forest zone between ca. 700 and 1400 m elevation (Akhani et al. 2010). The dominant observed arboreal vegetation

includes *Carpinus betulus*, *Carpinus orientalis*, *Quercus castaneifolia*, *Juglans regia*, *Cydonia oblonga*, *Zelkova carpinifolia and Crataegus pentagyna*. Important forbs around the village include species like *Chenopodium album*, *Eryngium caeruleum*, *Stellaria media*, *Artemisia annua*, *Convolvulus cantabrica*, *Erodium cicutarium*, *Geranium rotundifolium*, *Lycopus europaeus*, *Mentha longifolia*, *Salvia* sp., *Stachys byzantina*, *Teucrium hircanicum*, *Trifolium repens*, *Oxalis acetosella*, *Plantago lagopus*, *P. major*, *Polygonum aviculare*, *Rumex conglomeratus*, *R. pulcher*, *Parietaria judaica*, *Verbena officinalis*. The most abundant grasses are *Carex divulsa*, *Poa annua*, *P. nemoralis*, *P. trivialis*.

According to the archaeological site of the Vaske village (5 km distance to the Annal Lake, Fig. 4.1A), the region was occupied by the human probably at least since the Iron-Age era (Fallahian, 2013). Nowadays, the small Annal village consists of about 30 houses (Fig. 4.1B) and used the lower elevated farmlands mostly for the cultivation of cereals.

Materials and methods

In September 2018, we took a 272 cm-long sediment core from the center of the Annal Lake (ANL) with a modified Livingstone corer (Livingstone, 1955). After returning from the field, the sediment core was stored in the cold room (+4°C) of the Department of Palynology and Climate Dynamics, Göttingen University.

For the chronological framework, three 1-2 cm^3 bulk sediment samples, due to insufficient plant remains, were sent to the Poznan Radiocarbon Laboratory in Poland to be dated by accelerator mass spectrometry (AMS). The surface was assigned to the year of coring, 2018 (-68 cal yr BP). The samples were calibrated with linear interpolation, using the IntCal20-curve (Table 4.2) (Reimer et al. 2013). An age-depth model was constructed using RBacon package 2.4.3 (Blaauw and Christen, 2011) in the R-Studio data platform (Fig. 4.2).

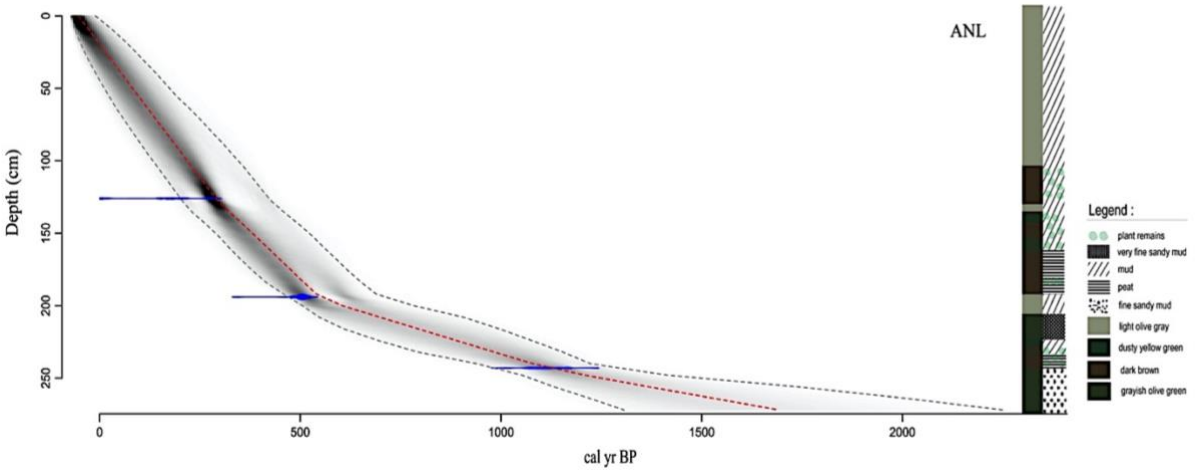

Fig. 4.2. Age-depth model for the ANL sediment core plotted by linear interpolation in BACON, as well as lithology.

For the loss on ignition (LOI) analyses, 35 samples were collected at 8 cm intervals along the core. According to this analysis, the content of the sediment's organic material and carbonate can be estimated. All samples were prepared following the procedure used by Heiri et al. (2001). For palynological analysis, 35 samples of 0.5 cm^3 were taken at 8 cm intervals along the sediment core. One tablet with 9.666 +/- 212 Lycopodium spores was added as a marker to each sample for calculating pollen concentration and influx. The samples were treated with 10% cold HCl, and 40% cold HF then sieved with a 120 µm mesh size before acetolysis, based on the pollen analytical methods (Faegri and Iversen, 1989). Each sample (except four samples) was counted until a minimum of 300 terrestrial pollen grains. Pollen and spores were identified based on the literature (Beug, 2004) and the reference collection of the Department of Palynology and Climate Dynamics. The pollen sum includes arboreal pollen (AP) (such as trees, shrubs, lianas), non-arboreal pollen (NAP) (grasses and herbs), and unknown pollen types. Indeterminate taxa consist of damaged and unrecognizable pollen. Pollen types attributable to indeterminate taxa, aquatic plants, spores, and non-pollen palynomorphs (NPPs) were excluded from the pollen sum. According to the total pollen sum, percentages of all pollen, spores, and NPPs data were illustrated with TILIA and TILIAGRAPH program 2.1.1. and CONISS cluster analysis was applied to the percentages of the terrestrial pollen data (Grimm, 1987).

For macro-charcoal analysis, 136 samples were taken continuously along the 272 cm-long Annal Lake core at every 2 cm intervals of 1 cm^3. All samples were placed into the 10% KOH for 12 hours and then in 6% H_2O_2 for 24 hours, following Stevenson and Haberle (2005) method. Afterward, samples were sieved using a mesh size of 125 µm. The charcoal particles were counted with a Zeiss stereomicroscope.

Depth	Material	Color	others
0 - 44	mud	light olive gray	-
44 - 105	mud	light olive gray	-
105 - 127	mud	dark brown	A few plant remains
127 - 139	mud	light olive gray	-
139 - 141	mud	dark brown	A few plant remains
141 - 145	mud	dusty yellow green	A few plant remains
145 - 154	mud	dark brown	A few plant remains
154 - 164	mud	grayish olive green	A few plant remains
164 - 196	peat	dark brown	A few plant remains (182-183 cm)
196 - 208	mud	light olive gray	-
208 - 224	very fine sandy mud	grayish olive green	-
224 - 228	mud	dusty yellow green	-
228 - 230	mud	dark brown	A few plant remains
230 - 233	mud	grayish olive green	A few plant remains
233 - 239	peat	dark brown	A few plant remains
239 - 272	fine sandy mud	grayish olive green	-

Table 4.1 Summary of the lithological changes in the materials and colors of the ANL core.

For analyzing the geochemical content of the sediment core, non-destructive X-ray fluorescence (XRF) analysis has been carried out at GEOPOLAR, University of Bremen

(Germany). The results were prepared using an ITRAX XRF-core scanner, COX analytical systems (Croudace et al. 2006) for each 2 mm step using a Cr tube. The scanner detected 40 elements. Though only Al, Ca, Cr, Fe, K, Rb, Si, Ti, and V were chosen to calculate different ratios for investigating precipitation rate, climate changes, and erosion. Furthermore, CONISS cluster analysis is also done on the counts of selected ratios of the V/Cr, Rb/Al, K/Al, Si/Fe, and Ca/Ti and single element of Ti for providing zones.

Results

Lithology, chronology, and sedimentology

The lithostratigraphy of the ANL sediment core is illustrated in Figure 4.2. The core consists mainly of four different deposits with different colors (Table 4.1). Mud, peat, very fine sandy mud, and fine sandy mud are repeating several times at different intervals. The most bottom part of the core consists of only a few small sands, which could not affect the calculations ahead like sedimentation rate or influxes. Based on the three radiocarbon dates (Table 4.2), a linear extra- and interpolated age-depth model was prepared for the ANL core. The base of the core at 272 cm has a calibrated age of 1690 yr BP, while the uppermost part is calculated at -53 cal yr BP. The calculated age is almost the coring year's age (2018) at -68 cal yr BP. It might be possible that a small part of the top core has not been recovered.

Based on the linear extra- and interpolation, at depths between 272 to 200 cm, the sedimentation rate has the lowest average of 0.08 cm/yr and increases between 200 and 136 cm with an average of 0.24 cm/yr. Between 136 to 0 cm, the sedimentation rate has an average of 0.36 cm/yr.

Laboratory name	Core depth (cm)	Dated material	Age ^{14}C (BP)	Age cal BP	Mean probability
Poz-115843	126	Bulk	190 ± 30	202 - 422	291
Poz-115845	194	Bulk	445 ± 30	481 - 722	556
Poz-107806	243	Bulk	1190 ± 30	1003 - 1257	1128

Table 4.2. Results of radiocarbon dates calculations.

The average of organic content is around 0.3%. The carbonate content is mostly stable with about 0.15% and shows a maximum at 168 cm (2%) (Fig. 4.4). It cannot be completely excluded that the low carbonate content affected the radiocarbon ages. As the linear extrapolated age of the core top is almost the modern age, the reservoir affect should be very low.

Description of the pollen, spores, NPPs, and macro-charcoal records

Based on the 35 analyzed samples, 66 identified pollen taxa are illustrated in Figure 4.3. Pollen of the Juglans, Prunus, Cerealia-type, Plantago lanceolata-type, P. major-media-type, Fabaceae (Reticulate and Psilate), Rumex, and Brassicaceae are considered as primary and secondary indicators of human activity. Referring to the cluster analysis by CONISS and variations in the pollen spectra, the diagram was divided into two pollen zones (ANL-I and II) and three subzones (ANL-IA, IB, and IC).

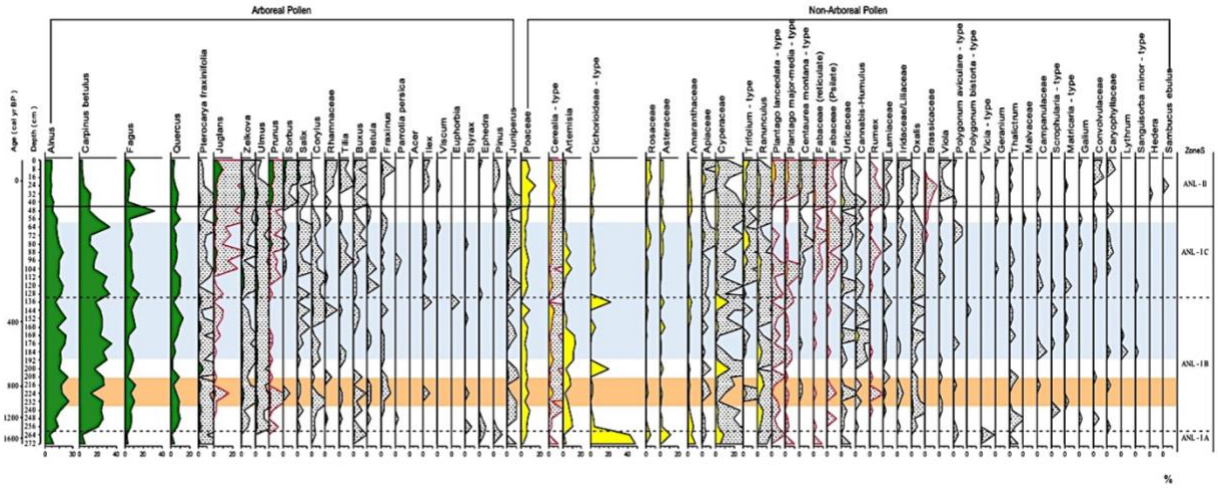

Fig. 4.3. The full percentage pollen diagram of the ANL core. Arboreal Pollen (AP) in green, and Non-Arboreal Pollen (NAP) in yellow. Stippled curves are exaggerated 10x, and selected Human Indicators pollen is shown with a red outline. Light orange and blue background color indicate Medieval Climatic Anomaly and the Little Ice Age, respectively.

Subzone ANL-IA (272-260 cm; 2 pollen samples)

The most characteristics of this subzone are the poor pollen preservation (Indeterminate taxa >35%) and the relatively low content of AP (an average <20%). *Alnus*, *Fagus*, and *Quercus* pollen have values of <10%. *Pinus* pollen is represented with a low amount. Among NAP, a few pollen of the Cerealia-type occur in the lowermost sample. Cerealia-type occurs in low values. Cichorioideae-type is the most abundant pollen (>45%) of this subzone. Also, Asteraceae and Amaranthaceae have their highest proportion. The pollen concentration and influx show the lowest values among the core (average of 2785 grains/cm^3 and 272 grains/cm^2/yr, respectively). Fern spores show the highest amount (Fig. 4.4). *Glomus*, with an average of 25%, is the most abundant Fungi in this subzone. Also, the Sordaria-type (ca. 10%) is the most dominant coprophilous spore. The average charcoal concentration is 14 particles/cm^3, and the charcoal influx is relatively low (average of 0.6 particles/cm^2/yr).

Subzone ANL-IB (260-132 cm; 16 pollen samples)

At the beginning of this subzone, AP decreased markedly while NAP decline. *Carpinus betulus*, *Alnus*, *Fagus*, and *Quercus* are the most abundant pollen in this subzone. *Juglans* is present, but with low values. *Parrotia persica* occurs at the beginning of the ANL-IB. Poaceae and *Artemisia* are the most frequent NAP. Cichorioideae-type in this subzone is rare and only shows some peaks. *Rumex* pollen occurs with low frequency. *Potamogeton* and Sparganium-type are the most frequent aquatic pollen grains. Human indicators increase slightly, including low values of the Cerealia-type. Pollen concentration and influx with several fluctuations are greater than the previous subzone (average of 33800 grains/cm^3 and 5600 grains/cm^2/yr, respectively). Furthermore, their values decrease twice, one at a depth of 200 cm and the other at 136 cm. Fern spore representations, with some exceptions, are reduced. *Glomus* shows several sharp increases. Sordaria-type, as well as other coprophilous, have low frequencies. Also, *Pediastrum* is represented with low percentages. The charcoal concentration and influx increase (average of 30 particles/cm^3 and 4.8 particles/cm^2/yr, respectively).

Subzone ANL-IC (132-44cm; 11 pollen samples)

The AP sum is higher than the NAP. *Carpinus betulus* (except for a single peak) decreases slightly. *Fagus* shows a single maximum at the end of this subzone. *Juglans* and *Prunus* have higher proportions compared to the previous subzones. *Parrotia persica* presents with a small amount at the middle of ANL-IC. Grass pollen are the most prevailing herbs. *Artemisia* increases slightly at the beginning of the subzone but then decreases. Fabaceae pollen shows an increasing trend. *Rumex* pollen with a low amount is represented continually. Among the occurrence of aquatic pollen of *Potamogeton* pollen decreases markedly. *Myriophyllum* and *Persicaria hydropiper* pollen have low percentages. Human indicator pollen is still increasing. Although pollen concentration is almost the same as the ANL-IB (average of 34700 grains/cm^3), the pollen influx rises to an average of 12000 grains/cm^2/yr. *Glomus* spores are not frequent, while the Sordaria-type increases constantly. Charcoal concentration decreases to an average of 19 particles/cm3, while the charcoal influx is almost constant (average of 5.3 particles/cm^2/yr).

Zone ANL-II (44-0cm; 6 pollen samples)

One of the most characteristics of this zone is the decrease of the AP and increase of the NAP. Another prominent feature is the highest proportion of the Human indicator pollen. *Carpinus betulus*, *Alnus*, *Fagus*, *Quercus*, and *Juniperus* decrease, while *Juglans* and *Prunus* increase.

Although pollen of *Sorbus*, *Salix*, Rhamnaceae, *Buxus*, *Fraxinus*, *Ilex*, and *Pinus* are still very low but compared to the previous zones, they increase. Among the NAP, Poaceae, Cerealia-type, Rosaceae, Plantago lanceolata-type, P. major-media-type, Centaurea montana-type, Fabaceae (Reticulate and Psilate), *Rumex*, and Brassicaceae increase. All the mentioned NAP except for the Fabaceae (Psilate) have their highest value throughout the whole core. Aquatics have the lowest proportion. *Utricularia* pollen occurs only during this zone. The pollen concentration and influx with fewer fluctuations decrease (average of 27000 grains/cm^3 and 9840 grains/cm^2/yr, respectively). *Glomus* and Sordaria-type are stable and increase compared to the subzone ANL-IC. The algae *Pediastrum* has the highest representation among the record. Both charcoal concentration (with the averages of 38 particles/cm^3) and influx (an average of 11.3 particles/cm^2/yr) reach the highest values.

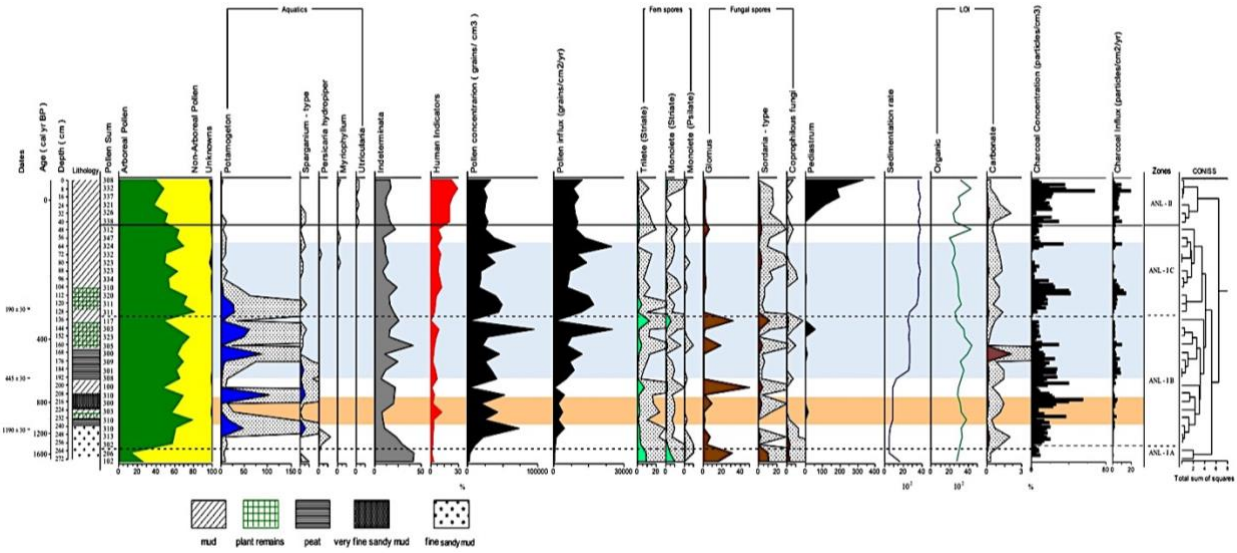

Fig. 4.4. Diagram with the lithology, pollen summary diagram with the sum of AP (in green), NAP (in yellow), and Unknowns (in black), Aquatics (in blue),Human Indicators (in Red), Pollen concentration and influx (hatched curves), Fern spores (in pale green), Fungal spores (in brown), Pediastrum (in black), sedimentation rate (in blue line), organic content (in green line), carbonate content (in black), charcoal concentration and influx (black bars), CONISS of the pollen data (excluding Aquatics). Stippled curves are exaggerated 10x. Light orange and blue background color indicate Medieval Climatic Anomaly and the Little Ice Age, respectively.

X-ray fluorescence analysis

From the XRF data set, nine important elements have been chosen. Five different ratios (V/Cr, K/Al, Rb/Al, Si/Fe, Ca/Ti) were calculated and together with the single element of Ti illustrated in Fig. 4.5. Based on Schroll (1975), the ratio of the V/Cr is used for investigating the moisture of lake deposits. It is also an indicator for the lake level changes (as the lower depth increases oxidation and higher depths increases reduction) (Calanchin et al. 1996; Riquier et al. 2006; Wang and Zhai, 2008). In warm and humid periods, the ratios of K/Al, Rb/Al, and Si/Fe increase (cf. Chen et al. 2013; Sun et al. 2008). More rainfall increases chemical weathering

and erosion, as a result, K/Al and Rb/Al increase (Gayantha et al. 2017). Increases in the Si/Fe ratio represent the warmer condition expressly, and it is used for determining the representative of glacial melting in the northern Atlantic (Erbs-Hansen et al. 2013). The Ca/Ti ratio can be used for investigating hydrological conditions (Haberzettl et al. 2009). The higher amount of Ca/Ti ratio may represent drought events. The geochemical element of Ti represents the changes in detrital inputs (Davies et al. 2015).

The average, maximum, minimum and differences between maximum and minimum values for each ratio and the Ti values are presented in Table 4.3. Based on the cluster analysis by CONISS and changes in the selected XRF ratios and Ti, the diagram is divided into two zones XRF Annal Zone I and II (XAZ-I and II) and two subzones (XAZ-Ia, Ib) (Fig. 4.5).

V/Cr	Rb/Al	K/Al	Si/Fe	Ca/Ti	Ti		Zones		Age (cal yr BP)
0.679	10.111	27.801	0.0038	2.733	0.017	Average	XAZ - II	wettest	ca. 250 – (-53)
2.254	64.5	159.5	0.0054	10.136	0.028	Maximum			
0	0	0	0.0017	0.733	0.005	Minimum			
2.254	64.5	159.5	0.0037	9.403	0.023	Max. – Min.			
0.669	7.691	21.337	0.0035	5.683	0.011	Average	XAZ – I b	Coldest and Driest	ca. 580 - 250
4.076	50.75	128	0.0067	31.951	0.032	Maximum			
0	0	0	0	0.710	0.0005	Minimum			
4.076	50.75	128	0.0067	31.240	0.032	Max. – Min.			
0.683	8.447	25.785	0.0049	3.350	0.024	Average	XAZ - I a	warmest	ca. 1690– 580
3.267	37.142	130.571	0.0078	15.199	0.040	Maximum			
0	0	0	0.0021	0.586	0.005	Minimum			
3.267	37.142	130.571	0.0057	14.613	0.035	Max. – Min.			

Table 4.3. Average, Maximum, Minimum, and differences between Maximum and minimum values of different geochemical ratios and Ti element for each geochemical zone.

Subzone XAZ-Ia (272-198 cm)

The V/Cr ratio has the highest mean (0.683). Rb/Al ratio has the lowest differences between maximum and minimum values (37.142). Si/Fe ratio and Ti values show their highest average values (0.0049 and 0.024 counts (C), respectively).

Subzone XAZ-Ib (198-112 cm)

Although the average of the V/Cr ratio does not show many differences, it shows the lowest value here (0.669). Rb/Al, K/Al, Si/Fe, and Ti ratios represent the lowest average throughout

the core (7.691, 21.337, 0.0035, and 0.011 (C), respectively). The differences between maximum and minimum values for the V/Cr, Si/Fe, and Ca/Ti ratios consider the highest amount in this subzone (4.076, 0.0067, and 31.24, respectively).

Zone XAZ-II (112-0 cm)

The Rb/Al, K/Al have the highest average throughout the whole core (10.111, 27.801, respectively). The Ca/Ti ratio has the lowest value (2.733). The differences between maximum and minimum values for the V/Cr, Si/Fe, Ca/Ti ratios, and Ti values are the lowest (2.254, 0.0037, 9.403, and 0.023 (C), respectively).

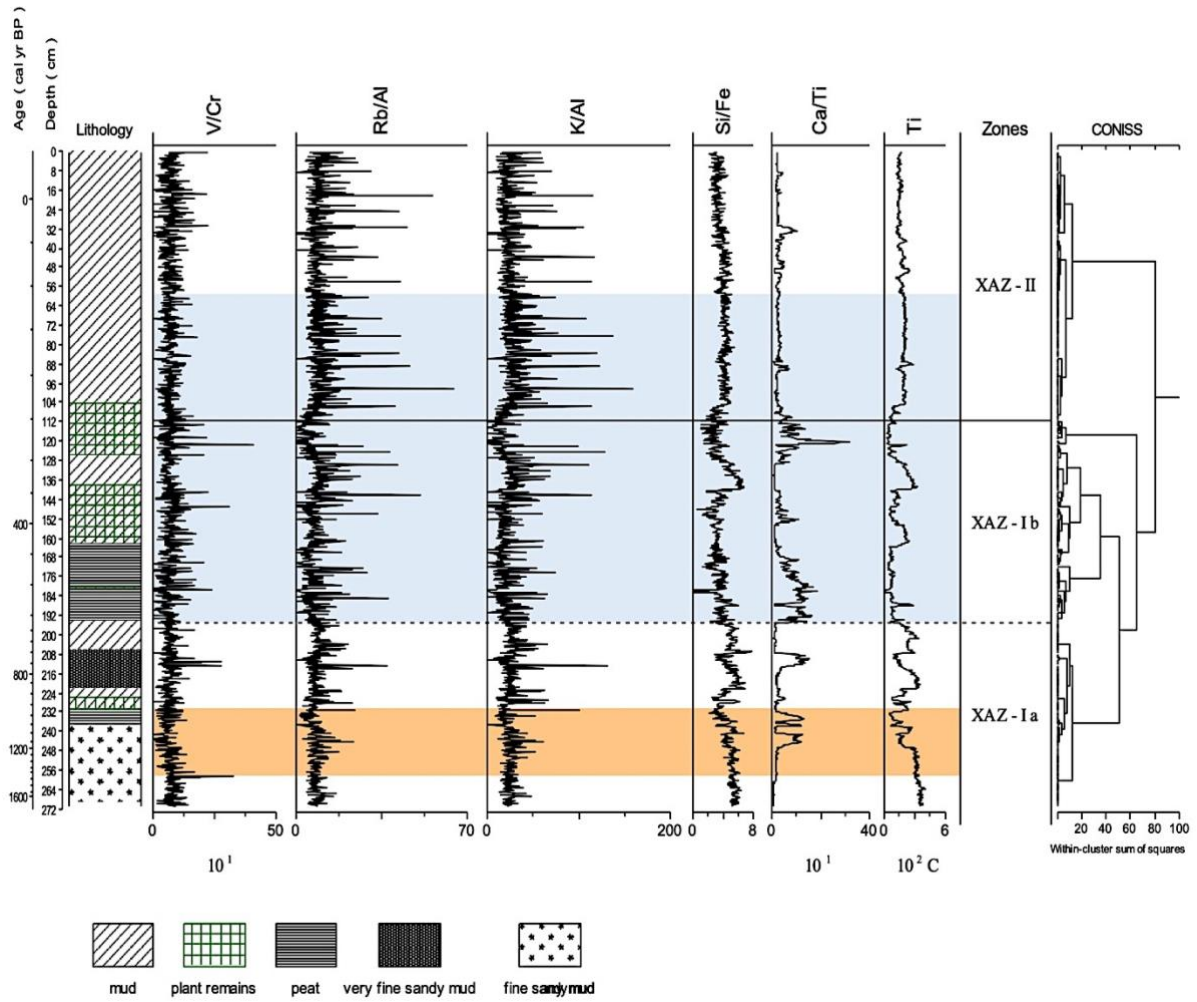

Fig. 4.5. Diagram with the lithology, selected geochemical ratios with the Ti element (based on counts per second), and CONISS of the selected ratios and single element of Ti. The Medieval Climatic Anomaly period is marked in light orange and the Little Ice Age in blue.

Interpretation and discussion

Annal Lake formation

According to the radiocarbon dating, the lake formation might start at 1690 cal yr BP. The sandy mud type of the sediment between 272 – 260 cm core depth, poor pollen preservation, and the high proportion of indeterminate may suggest first a non-permanent lake with partly oxic conditions. The high amount of Ti as an indicator for increased detrital inputs (Davies et al. 2015), besides the abundance of *Glomus* (as an erosion indicator (Van Geel et al. 1989)), suggests that the soil erosion was high at the beginning of the lake formation.
The much better pollen preservation (reduction in indeterminate pollen) in the sediment of ANL above the 260 cm core depth suggests the formation of a permanent lake after ca. 1450 cal yr BP. Furthermore, the almost absence of aquatic pollen below 260 cm and the occurrence of especially *Potamogeton* and Sparganium above that level suggest the formation of the permanent lake since that time.

Late Holocene vegetation and environmental dynamics

Vegetation dynamics and human impact

Period of ca. 1690 - 1450 cal yr BP (260 – 500 AD; subzone ANL-IA): Due to the relatively low pollen preservation during this period, the vegetation reconstruction has to be done with caution. However, the pollen analytical results suggest that the non-permanent lake was surrounded by more extensive areas of open herb vegetation frequent with Asteraceae subf. Cichorioideae as well as Poaceae, Amaranthaceae, and Cyperaceae. The high amount of the Cichorioideae at the beginning of the record could be an indicator for grazing (Florenzano et al. 2015) near the lake, which is in line with the highest occurrence of coprophilous (especially Sordaria) spores. In the forest of the study area, *Alnus*, *Carpinus*, *Fagus*, and *Quercus* are the most frequent trees. The occurrence of a few Pinus pollen suggest long-distance transportation as pine was introduced to Iran only during the last century (Ramezani et al. 2016).

Period of ca. 1450 - 310 cal yr BP (500 – 1640 AD; subzone ANL-IB): The pollen record indicates that the local open herb vegetation with frequent Artemisia and Poaceae around the previous non-permanent lake reduced markedly since the beginning of this period. The forest became much more abundant and prevailed in the study area. *Alnus*, *Carpinus*, *Fagus*, and *Quercus* were the most frequent trees in this mid-elevated Hyrcanian forest. Trees of *Juglans* and *Prunus* were cultivated in the study area. *Pterocarya fraxinifolia* was rare in the forest but

was expected to be more frequent as this species mostly grows below 1000 m elevation on wet soils (Ramezani et al. 2013). Drier climatic conditions and/or selective logging are possible reasons for its rare occurrence. Climatic fluctuations from Medieval Climatic Anomaly (MCA) to Little Ice Age (LIA) as well as the frequent use of timber for constructions of different dynasties, especially the Sasanian Empire, 224-651 AD, may have contributed to the low presence of this species (cf. Leroy et al. 2013; Ramezani et al. 2008, 2016).

The aquatic plants, especially *Potamogeton*, which grows in shallow lakes (Xu et al. 2020), had stronger fluctuations, indicating several changes in the lake level during this period. These can also be seen by changes in the ANL core sediments with altering deposition of fine sandy mud to very fine sandy mud, mud, and peat (Fig. 4.2). The human indicator pollen (like *Juglans*, *Prunus*, cereals) and relatively frequent fires suggest the presence of the humans around the lake.

Period of ca. 310 - 65 cal yr BP (1640 – 1885 AD; subzone ANL-IC): The pollen record indicates a slightly decreasing trend for most trees, which started during this period. *Alnus* and *Carpinus* decreased more than the other trees, while cultivated *Juglans* and *Prunus* increased, and may reflect the increasing use of the forest by settlers in the study area. Poaceae species were still the most frequent herbs, but *Artemisia* became rare. Instead, Cichorioideae, Rosaceae, Asteraceae, and Amaranthaceae were more frequent, probably due to the slight opening of the forest. Although cereals' presence did not increase markedly and consistently, it may suggest their cultivation in very small areas near the study site or pollen transport over short distance. The increase of the human indicators pollen together with some fires suggesting an expansion of the anthropogenic activities.

Period from ca. 65 cal yr BP – to present (1885 AD – to present; zone ANL-II): The pollen data indicate a marked decrease of the forest, especially by the most frequent trees like *Alnus*, *Carpinus*, and *Quercus*, indicating marked deforestation in the study area. However, the cultivated trees *Juglans* and *Prunus* increased. The increase of herbs, in particular Poaceae, and others like Rosaceae, Apiaceae, *Plantago lanceolata*, indicates larger non-forested areas around the Annal Lake since the beginning of this period. Also, Cerealia increased markedly, reflecting an amplification of agriculture activities during the last centuries.

Pediastrum (an indicator of the eutrophic freshwater) rarely existed before, but became abundant during this period. It is most probable that increased human activities around the lake caused the eutrophic condition. Even nowadays (Fig. 4.1C), the lake has low transparency and was impacted.

The clear indication of the increasing anthropogenic activities caused the reduction of the forests rather than climate. Also, it is in line with our previous investigation in the Gilan's highland (Homami Totmaj et al. 2020), 19 km far to the Annal Lake at 2280 m elevation (Fig. 4.1A,) that showed an increase in human activities over time, especially for the last thousand years. However, the intensification, starting at 65 cal yr BP at our new mid-elevated study area, occurred much later. Furthermore, the earlier human settlers were probably more pastoralists, and through time, along with animal husbandry, they have also increased agriculture activities.

Climatic changes in the study area

Period of ca. 1690 – 580 cal yr BP (260 – 1370 AD; subzone XAZ-Ia): The lake level indicator (V/Cr ratio), and indicators for rainfall, and chemical weathering (Rb/Al and K/Al ratios), as well as Ti values which is an indicator for detrital inputs, may suggest a change to wet condition, in line with the formation of the lake which was first non-permanent. Based on the temperature indicator (Si/Fe ratio), this period was the warmest, and Medieval Climatic Anomaly (MCA), which occurred in between (950 - 1250 AD (Ruddiman, 2008)), fit to our results. The highest organic content suggested the highest net primary productivity due to degradation and accumulation of the biomass (Richter et al. 2020). It is also inferred from the pollen assemblage that the open vegetation has replaced most trees during the subzone XAZ-Ia.

Period of ca. 580 – 250 cal yr BP (1370 – 1700 AD; subzone XAZ-Ib): Referring to the decrease in the ratios of V/Cr (lake level indicator), Rb/Al and K/Al (rainfall indicators), Si/Fe (temperature indicator) and Ti values (detrital inputs) and increase of the Ca/Ti ratio (drought indicator) this period with the lowest amount of rainfall and detrital inputs was the coldest and driest recorded period. Also, the newly published study of Foroozan et al. (2020), based on the tree-ring $\delta^{18}O$ variations of juniper trees on highlands of the Golestan province (SE of Caspian Sea), verified the dry condition of this period. Furthermore, based on the highest differences between maximum and minimum ratios in most of the XRF data (Fig. 4.5), this period had unstable climatic conditions.

The pollen record indicate that the forest did not change markedly during this colder period. However, other proxies verified unstable environmental conditions (e.g., several *Glomus* peaks as an erosion indicator, two samples with low pollen concentration, decreased organic content, and Potamogeton fluctuations). Comparing the changes in the XRF ratios, such as Rb/Al, Si/Fe, and Ca/Ti during this period, suggesting unstable colder and drier climatic conditions. However, the pollen assemblages showed almost stable percentages of *Alnus*, *Carpinus*, and

Fagus. It can be inferred that unstable climatic conditions had no and/or little effect on the forest vegetation. The lack of the forest changes may be due to standing altitudinally in the middle part of the Hyrcanian forest region, which covered the fluctuations in the lower and upper altitude.

The reduction of the organic content in the lake deposits to the lowest amount reflected the decline in the net primary productivity, probably due to the second part of the LIA.

Period of ca. 250 – (-53) cal yr BP (1700 AD to present zone XAZ-II): The geochemical ratios with the lowest differences between the maximum and minimum values represented the most stable climatic conditions in comparison to the past. Furthermore, based on the Rb/Al, K/Al, and Ca/Ti ratios, Annal Lake, during this period, experienced the wettest condition with the most rainfall throughout the recorded period that corresponds to the late LIA high-stand of the Caspian Sea (Beni et al. 2013; Leroy et al. 2011b). Furthermore, Foroozan et al. (2020) indicated that the wettest condition through the last 500 years occurred in the 18th century. Based on the Si/Fe ratio, this period was not as warm as the XAZ-Ia. The lithology of the ANL core also showed stable conditions for the lake sediments. However, the XRF ratios suggest stable climatic conditions, while the forest was significantly reduced.

Summary and conclusion

A high-resolution multi-proxy study from Annal Lake sediment core in the mid-elevated Hyrcanian forest region indicates several environmental changes in the recorded 1650 cal yr BP. Despite some taphonomical issues this period shows some open grassland areas, rich in subf. Cichorioideae around the non-permanent lake occurred during the first period. After 1450 cal yr BP, the lake became more permanent and the vegetation around the lake, was mostly replaced by forest and prevailed until 65 cal yr BP. The composition was relatively stable and rich in *Alnus*, *Carpinus*, *Fagus*, and *Quercus*.

The Si/Fe ratio suggested the warmest condition between ca. 1690 and 580 cal yr BP, known that MCA also occurred in between (1000 – 700 cal yr BP). Later around 580-250 cal yr BP, based on the XRF ratios (e.g. Si/Fe and Ca/Ti), the climatic condition changed to the coldest and driest recorded phase, most probably due to LIA (600 – 100 cal yr BP) effects. However, the forest composition seems to not affected due to locating the Annal Lake altitudinally in the middle of the Hyrcanian forest and the fluctuation at several distances to the lake not recorded exactly.

Humans have occupied this mid-elevated study area since the beginning of the recorded period, but the impact was not that detected. An increase in human indicator pollen, including *Juglans*, *Prunus*, cereals, ruderals, and grassland species accompanied by fires, indicate a slight expansion of the human settlements over time in the study area. The strongest human impact, here in the mid-elevated areas, occurred relatively late since 65 cal yr BP by deforestation including selective logging of Carpinus and Alnus, also changing the Hyrcanian composition forest.

In conclusion, the Hyrcanian mid-elevated forest that tolerated and prevailed during the recorded climate fluctuations, since 65 cal yr BP, lost large parts of its natural vegetation and have been replaced by grassland and agricultural areas due to recent expansions of anthropogenic activities.

Acknowledgments

We like to thank the reviewers for their critical reading and comments on the manuscript. We are so grateful to Mr. Amani and Mr. Jozi for their assistance during the field excursions. The study was part of the PhD project of the first author, which was supported by the German Science Foundation DFG (grant BE2116/31-1) carried out at Georg-August-Universität Göttingen, Germany. The data reported in this paper will be archived in www.neotoma.de

References

Akhani, H., Djamali, M., Ghorbanalizadeh, A., Ramezani, E., (2010) Plant biodiversity of Hyrcanian relict forests, N Iran: an overview of the flora, vegetation, palaeoecology and conservation. Pakistan Journal of Botany 42: 231–258.

Beni, A.N., Lahijani, H., Harami, R.M., et al (2013) Caspian Sea-level changes during the last millennium: Historical and geological evidence from the south Caspian Sea. Climate of the Past 9, 1645–1665. https://doi.org/10.5194/cp-9-1645-2013

Beug, H., (2004) Leitfaden der Pollenbestimmung für Mitteleuropa und angrenzende Gebiete. Munich: Verlag Dr. Friedrich Pfeil.

Blaauw, M., Christen, J.A., (2011) Flexible paleoclimate age-depth models using an autoregressive gamma process. Bayesian Analysis 6: 457–474.

Calanchi, N., Dinelli, E., Lucchini, F., Mordenti, A., (1996) Chemostratigraphy of late Quaternary sediments from Lake Albano and central Adriatic Sea cores (PALICLAS Project). Memorie-Istituto Italiano di Idrobiologia 55: 247–264.

Chen, F., Liu, J., Xu, Q., et al (2013) Environmental magnetic studies of sediment cores from Gonghai Lake: implications for monsoon evolution in North China during the late glacial and Holocene. Journal of Paleolimnology 49:447–464.

Croudace, I., Rindby, A., Rothwell, R., (2006) ITRAX: description and evaluation of a new multi-function X-ray core scanner. Geological Society Special Publications 267: 51–63.

Davies, S.J., Lamb, H.F., Roberts, S.J., (2015) Micro-XRF Core Scanning in Palaeolimnology: Recent Developments. https://doi.org/10.1007/978-94-017-9849-5_7

Djamali, M., Akhani, H., Andrieu-Ponel, V., et al (2010) Indian summer Monsoon variations could have affected the early-Holocene woodland expansion in the Near East. Holocene 20, 813–820. https://doi.org/10.1177/0959683610362813

Djamali, M., de Beaulieu, J.L., Campagne, P., et al (2009) Modern pollen rain-vegetation relationships along a forest-steppe transect in the Golestan National Park, NE Iran. Review of Palaeobotany and Palynology 153: 272–281. https://doi.org/10.1016/j.revpalbo.2008.08.005

Erbs-Hansen, D.R., Knudsen, K.L., Olsen, J., et al (2013) Paleoceanographycal development of Sisimiut, West Greenland, during the mid- and late Holocene: A multiproxy study. Marine Micropaleontology 1: 79–97.

Faegri, K., Iversen, J., (1989) Textbook of Pollen Analysis. John Wiley and Sons.

Fallahian, Y., (2013) Investigation of burial patterns in Iron Age of Gilan, Iran. Ancient Asia 4. https://doi.org/10.5334/aa.12311

Florenzano, A., Marignani, M., Rosati, L., Fascetti, S., Mercuri, A.M., (2015) Are Cichorieae an indicator of open habitats and pastoralism in current and past vegetation studies? Plant Biosystems 149: 154–165. https://doi.org/10.1080/11263504.2014.998311

Foroozan, Z., Grießinger, J., Pourtahmasi, K., Bräuning, A., (2020) 501 years of spring precipitation history for the semi-arid Northern Iran derived from tree-ring δ18O data. Atmosphere 11. https://doi.org/10.3390/ATMOS11090889

Gayantha, K., Routh, J., Chandrajith, R., (2017) A multi-proxy reconstruction of the late Holocene climate evolution in Lake Bolgoda, Sri Lanka. Palaeogeography, Palaeoclimatology, Palaeoecology 473: 16–25.

Grimm, E., (1987) CONISS: a FORTRAN 77 program for stratigraphically constrained cluster analysis by the method of incremental sum of squares. Computers & geosciences 13: 13–35.

Gu, F., Ramezani, E., Alizadeh, K., Behling, H., (2021) Vegetation Dynamics, Environmental Changes, and Anthropogenic Impacts on the Coastal Hyrcanian Forests in Northern Iran. Journal of Coastal Research 37: 611–619. https://doi.org/10.2112/JCOASTRES-D-20-00033.1

Haberzettl, T., Anselmetti, F.S., Bowen, S.W., et al (2009) Late Pleistocene dust deposition in the Patagonian steppe - extending and refining the paleoenvironmental and tephrochronological record from Laguna Potrok Aike back to 55 ka. Quaternary Science Reviews 28: 2927–2939. https://doi.org/10.1016/j.quascirev.2009.07.021

Haghani, S., Leroy, S.A.G., Khdir, S., et al (2015) An early 'Little Ice Age' brackish water invasion along the south coast of the Caspian Sea (sediment of Langarud wetland) and its wider impacts on environment and people. Holocene 26: 3–16. https://doi.org/10.1177/0959683615596835

Heiri, O., Lotter, A.F., Lemcke, G. (2001) Loss on ignition as a method for estimating organic and carbonate content in sediments: Reproducibility and comparability of results. Journal of Paleolimnology 25:101–110. https://doi.org/10.1023/A:1008119611481

Homami Totmaj, L., Ramezani, E., Alizadeh, K., Behling, H. (2020) Four millennia of vegetation and environmental history above the Hyrcanian forest, northern Iran. Vegetation History and Archaeobotany 30(5):611-621. https://doi.org/10.1007/s00334-020-00813-y

Hoyle, T.M., Leroy, S.A.G., López-Merino, L., Miggins, D.P., Koppers, A.A.P. (2020) Vegetation succession and climate change across the Plio-Pleistocene transition in eastern Azerbaijan, central Eurasia (2.77–2.45 Ma). Palaeogeography, Palaeoclimatology, Palaeoecology 538: 109386. https://doi.org/10.1016/j.palaeo.2019.109386

Kendrew, W., 1961. The Climates of the Continents. Oxford University Press.

Khakpour Saeej, M., Ramezani, E., Siyab Ghodsy, A.A., Zare, H., Joosten, H. (2013) Palynological reconstruction of 1500 years of vegetation history of Veisar (N Iran). Rostaniha 14: 135–148.

Khalili, A., (1973) Precipitation patterns of Central Elburz. Theoretical and Applied Climatology 21:215–231.

Knapp, H.D., (2005) Die globale Bedeutung der kaspischen Wälder. Nostrari K, Marvie Mohadjer R., Bode W. Und Knapp HD: Schutz der Biologischem Vielfalt und Intergtiertes Management der Kaspischen Walder (Nordiran)//Bundesamt fur Nsturschutz 45–70.

Leroy, S.A.G., Amini, A., Gregg, M.W. (2019) Human responses to environmental change on the southern coastal plain of the Caspian Sea during the Mesolithic and Neolithic periods. Quaternary Science Reviews 218:343–364. https://doi.org/10.1016/j.quascirev.2019.06.038

Leroy, S.A.G., Kakroodi, A.A., Kroonenberg, S. (2013) Holocene vegetation history and sea level changes in the SE corner of the caspian sea: Relevance to SW Asia climate. Quaternary Science Reviews 70:28–47. https://doi.org/10.1016/j.quascirev.2013.03.004

Leroy, S.A.G., Lahijani, H.A.K., Djamali, M. (2011a) Late Little Ice Age palaeoenvironmental records from the Anzali and Amirkola Lagoons (south Caspian Sea): Vegetation and sea level changes. Palaeogeography, Palaeoclimatology, Palaeoecology 302: 415–434. https://doi.org/10.1016/j.palaeo.2011.02.002

Leroy, S. A.G., Roiron, P. (1996) Latest Pliocene pollen and leaf floras from Bernasso palaeolake (Escandorgue Massif, Hérault, France). Review of Palaeobotany and Palynology 94:295–328.

Livingstone, D.A. (1955) A lightweight piston sampler for lake deposits. Ecology 36:137–139.

Ramezani, E., Marvie Mohadjer, M.R., Knapp, H.D., Ahmadi, H., Joosten, H. (2008a) The late-Holocene vegetation history of the Central Caspian (Hyrcanian) forests of northern Iran. Holocene 18: 307–321. https://doi.org/10.1177/0959683607086768

Ramezani, E., Marvie Mohadjer, M.R., Knapp, H.D. (2013) Pollen-vegetation relationships in the central Caspian (Hyrcanian) forests of northern Iran. Review of Palaeobotany and Palynology 189:38–49. https://doi.org/10.1016/j.revpalbo.2012.10.004

Ramezani, E., Mrotzek, A., Marvie Mohadjer, M.R. (2016) Between the mountains and the sea: Late Holocene Caspian Sea level fluctuations and vegetation history of the lowland forests of northern Iran. Quaternary International 408:52–64. https://doi.org/10.1016/j.quaint.2015.12.041

Reimer, P.J., Bard, E., Bayliss, A. (2013) IntCal13 and Marine13 radiocarbon age calibration curves 0–50,000 years cal BP. radiocarbon 55:1869–1887.

Richter, C., Wolf, D., Walther, F., Meng, S., Sahakyan, L., Hovakimyan, H., Wolpert, T., Fuchs, M., Faust, D. (2020) New insights into Southern Caucasian glacial–interglacial climate conditions inferred from Quaternary gastropod fauna. Journal of Quaternary Science 35: 634–649. https://doi.org/10.1002/jqs.3204

Riquier, L., Tribovillard, N., Averbuch, O., Devleeschouwer, X., Riboulleau, A. (2006) The Late Frasnian Kellwasser horizons of the Harz Mountains (Germany): two oxygen-deficient periods resulting from different mechanisms. Chemical Geology 233:137–155.

Rousta, I., Doostkamian, M., Haghighi, E., Ghafarian Malamiri, H.R., Yarahmadi, P. (2017) Analysis of spatial autocorrelation patterns of heavy and super-heavy rainfall in Iran. Advances in Atmospheric Sciences 34:1069–1081. https://doi.org/10.1007/s00376-017-6227y

Ruddiman, W.F. (2008) Climate changes during the last 1000 years. Earth's climate past and future, 2nd edn. WH Freeman and Company, New York 290–308.

Sagheb-Talebi, K., Pourhashemi, M., Sajedi, T. (2014) Forests of Iran: A Treasure from the Past, a Hope for the Future. Springer

Schroll, E. (1975) Analytsche Geochemie, Band I, Metodik. Ferdinand Enke Verlag Stattgard.

Stevenson, J., Haberle, S. (2005) "Palaeoworks Technical Papers 5. Macro Charcoal Analysis: A modified technique used by the department of Archaeology and Natural History."

Sun, Y., Wu, F., Clemens, S.C., Oppo, D.W. (2008) Processes controlling the geochemical composition of the South China Sea sediments during the last climatic cycle. Chemistry Geology 257:240–246. https://doi.org/10.1016/j.chemgeo.2008.10.002

Van Geel, B., Coope, G., van der Hammen, T. (1989) Palaeoecology and stratigraphy of the Late glacial type section at Usselo (the Netherlands). Review of Palaeobotany and Palynology 60:25–129.

Wang, G.P., Zhai, Z.L. (2008) Geochemical data as indicators of environmental change and human impact in sediments derived from downstream marshes of an ephemeral river, Northeast China. Environmental geology, 53: 1261–1270.

Xu, J., Wang, T., García Molinos, J., Li, C., Hu, B., Pan, M., Zhang, M. (2020) Effects of warming, climate extremes and phosphorus enrichment on the growth, sexual reproduction and propagule carbon and nitrogen stoichiometry of *Potamogeton crispus* L. Environment International 137. https://doi.org/10.1016/j.envint.2020.105502

Zohary, Michael (1973) Geobotanical foundations of the Middle East. Fischer.

Chapter 5: Paper IV

Representation of the Hyrcanian forest (northern Iran) in modern pollen rain revealed by palynological and DNA-metabarcoding data

Leila Homami Totmaj[1*] · Arash Rasi[2] · Katrin Neumann[3] · Sepideh Pirouzi[4] · Kammaledin Alizadeh[1,5] · Hermann Behling[1]

[1] University of Göttingen, Department of Palynology and Climate Dynamics, Albrecht-Von-Haller Institute for Plant Sciences, Untere Karspüle 2, 37073 Göttingen, Germany

[2] University of Tehran, Department of Agronomy and Plant Breeding, Agricultural and Natural Resources Collage, Division of plant Biotechnology, Alborz, Iran

[3] Lifeprint GmbH, Industriestrasse 12, 89257, Illertissen, Germany

[4] University of Tehran, Department of Plant Science, Center of Excellence in Phylogeny, School of Biology, College of Science, Tehran, Iran

[5] Quality Service International GmbH, Flughafendamm 9, 28199, Bremen, Germany

Submitted at Acta Palaeobotanica

Abstract

We studied the modern pollen rain in two different landscapes from Hyrcanian lowland forests up to the slopes of the Alborz Mountains in Gilan province for the first time. Pollen traps were installed for one year and moss samples were collected on two altitudinal transects from 100 to 1800 m and from 100 to 2300 m elevation. From 32 locations, the results of pollen counting and environmental DNA barcoding (metabarcoding) of the collected pollen traps and moss samples compared together. In total, 182 vascular plant species from 57 families were identified by metabarcoding, and 68 taxa belongs to 39 families identified by pollen counting. The pollen counting results reflect mainly wind-pollinated families such as Betulaceae and Fagaceae while results from metabarcoding of the rbcL and ITS2 loci were more in line with the vegetation around the collected pollen traps or moss samples. Furthermore, this study showed that the rbcL region is able to identify more taxa than the ITS2 region, while applying both markers provide a higher confidence. Also using both, metabarcoding and pollen data provide a better local and regional vegetation representation.

Introduction

Modern pollen rain studies are providing important data with different aims such as generating environmental and paleoenvironmental parameters or providing inside in the current plant diversity of the area. Furthermore, the modern pollen rain data can be used in studies related to paleogeographic studies, allergic diseases (hay fever), and occurrence of plant communities in a region (Gomes et al., 2021).

The first pollen-vegetation investigation of the Hyrcanian forest in the province of Golestan refers to Djamali et al. (2009). Their descriptive approaches were performed over the forest-steppe transect in Golestan National Park in the eastern Hyrcanian forest. Later, Ramezani et al. (2013) provided a study on the pollen-vegetation relationship along an altitudinal transect with a primary focus on trees distribution and their pollen grain dispersal ability in the central part of the Hyrcanian forest.

Different methods can be applied for pollen identification and classification, including image-based, spectroscopic, and DNA-based detection (Landsmeer et al., 2009; Rittenour et al., 2012; Longhi et al., 2009). The identification of pollen by morphological characteristics using a light microscope allows the identification to family and genus level, but rarely to species level (e.g. Halbritter et al., 2018). As an alternative to morphological pollen identification, DNA based technique can increase the taxonomic resolution (Polling et al., 2021). The DNA-based

technique relies on the fragments of the genome (known as barcode). DNA-Barcodes are detectable in a broad range of taxa (Coissac et al., 2012) on multi-copy plastid (plants) or mitochondrial genomes, containing similar sequences within taxa with enough variability to identify different species (Campbell et al., 2020). In plants, nuclear ribosomal region ITS and the chloroplast regions of the rbcL, matK, and trnH-psbA are used as DNA barcode, in a separate manner or combination (Fazekas et al., 2008; Fazekas et al., 2009; CBOL Plant Working Group 2009; Chen et al., 2010; Hollingsworth et al., 2011).

The recent application of the DNA barcode technique for pollen identification refers to two main problems. First, the standard barcoding loci are located mostly on the plastid genome, which can be found in several organelles, particularly in the chloroplast (Fujiwara et al., 2010). These plastids are inherited maternally (e.g., Sakamoto et al., 2008), and some studies have suggested the absence of the ptDNA (plastid DNA) in pollen grains (e.g., Willerslev et al., 2003). However, recent studies proved the presence of ptDNA in the pollen (Galimberti et al., 2014; Hawkins et al., 2015; Kraaijeveld et al., 2015; Richardson et al., 2015a), and the metabarcoding method on pollen became applied. The second issue referred to the samples containing mixture of multiple species, meaning that Sanger sequencing is not applicable for these samples (Matsuki et al., 2007; Aziz, Sauve, 2008). To overcome this problem, amplicon cloning technique can be used but is requiring intensive work (e.g., Galimberti et al., 2014). Recent developments in the high throughput sequencing led to a price reduction. This technique can address the mixed-taxa identification via the barcoding method (Hawkins et al., 2015; Keller et al., 2015; Kraaijeveld et al., 2015; Richardson et al., 2015b; Sickel et al., 2015), called environmental DNA metabarcoding.

Over the last few years, analysis of the environmental DNA (eDNA) for identifying plant taxa has become more applied in biodiversity research (Taberletet al., 2012a; Creer et al., 2016; Jarman et al., 2018). The eDNA metabarcoding study, based on the High Throughput Sequencing (HTS), is a valuable method, with lower cost, more accurate results, and the ability of the parallel multiple taxa identification, compared with Sanger sequencing (Taberlet et al., 2012b). However, many factors, including technical procedure, handling sample, and biological materials, can affect metabarcoding results. Therefore, every step should be done meticulously (Baksay et al., 2020).

Another application of the metabarcoding technique is estimating the frequency of pollen taxa. Studies show a correlation between pollen abundance and HTS read frequencies to detect pollen abundance (Hawkins et al., 2015; Richardson et al., 2015; Bell et al., 2017; Pornon et al., 2017;

Pinol et al., 2019). However, prior knowledge of pollen productivity is crucial for vegetation – pollen rain relationship using metabarcoding as well as pollen data.

For metabarcoding of pollen, four components are required (1) extraction protocol which yields high-quality DNA, (2) sets of genetic markers or barcodes to amplify (3) a database containing genetic markers, (4) high throughput bioinformatic method that allows identification simultaneously (Bell et al., 2016).

The main objectives of our study are (1) to study the finger print of modern vegetation as reflected in the pollen rain using DNA metabarcoding and conventional palynology, (2) to compare the capability of DNA metabarcoding method vs. pollen counting in biodiversity research, and (3) to investigate the pollen rain of different vegetation zones along the altitudinal transects.

Study area

The Hyrcanian forest belt, which is 20-70 km wide and 800 km long between the southern coast of the Caspian Sea and northern slopes of the Alborz Mountains, consists of broad-leaved deciduous trees in northern Iran and southern east Azerbaijan (Sabeti, 1994).

The study sites are located along two altitudinal transects in the Gilan province of northern Iran. The Asalem-Khalkhal (AS) transect (from 100 to 2300 m a.s.l.) and the Shanderman-Masal (SH) transect (from 100 to 1800 m a.s.l.) are located between the latitude 37°(N) and longitude 48 to 49° (E) (Fig. 5.1).

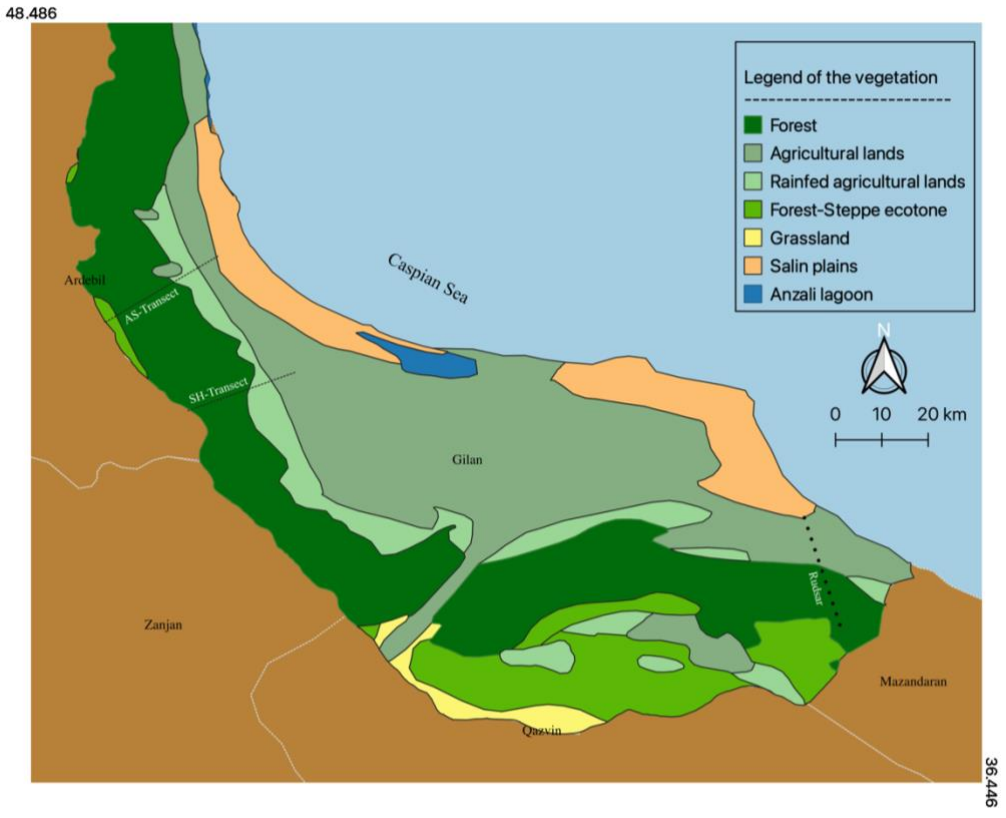

Fig. 5.1. Location of the two transects accompanied with Rudsar transect (Naghinezhad et al., 2015)

Gilan with a maximum annual precipitation of 1850 mm and mean annual temperature of 16ºC is known as the wettest province of Iran. However, the precipitation and temperature from west to east and from the coastal plain of Caspian Sea to the highlands of the Alborz Mountains decreases (Molavi-Arabshahi et al., 2016). Generally, from the coastal up to ca. 1500 m a.s.l. the area receives the highest precipitation, with warm and humid summer and moderate winter. Above 1500 m a.s.l. the summers are moderate but the winters are cold and with some snow. Based on the study done by Naghinezhad et al., (2015) on the altitudinal transect in the Rudsar area (Gilan province), the vegetation composition can be classified into three sectors: lowlands (up to 800 m a.s.l.), highlands (up to 1900 m a.s.l.) and ecotone from forest to steppe (upper than 1900 m a.s.l.).

1. The lowlands up to 800 m a.s.l. include species such as: *Parrotia persica, Diospyrus lotus, Alnus subcordata* var. *villosa*, *Acer velutinum* and *Ruscus hyrcanus*.
2. The highlands up to 1900 m a.s.l. include species such as: *Acer cappadocicum*, *Carpinus betulus*, *Quercus castaneifolia* subsp. *castaneifolia*, *Tilia platyphyllos* subsp. *caucasica* are dominant at highlands accompanied by herbal species like *Epipactis persica*, *Euphorbia amygdaloides*, *Festuca drymeia*, *Galium odoratumin*. The forest ranging from 1000 to 1900 m a.s.l. is occupied mostly by *Fagus orientalis* accompanied by *Acer velutinum*, *Laurocerasus officinalis* and *Vaccinum arctostaphylos*, *Aruncus vulgaris*, *Brachypodium sylvaticum*, *Cardamine impatiens* var. *pectinata*, *Carex pendula*.

The ecotone upper than 1900 m a.s.l. consist species such as: *Acer hyrcanum*, *Quercus macranthera* and *Viburnum lantana* which are dominant species mostly accompanied with *Geranium purpureum*, *Lapsana communis*, *Phuopsis stylosa*, *Stachys byzantine* and *Veronica rechingeri*.

Material and methods

Pollen rain sampling and modern vegetation estimation

In September 2019, 40 Falcon tubes (filled with small amount of synthetic cotton and glycerol and covered by a net to avoid trapping the insects) according to Behling-traps (Jantz et al., 2013) were placed for a year in two different altitudinal transects (from lowlands to highlands) in the Gilan province of Iran. However, only 18 traps could be collected in September 2020. For the replacement of the missing pollen traps, moss samples were collected (a total of 14 moss samples, approximately 25 cm^2) (Tab. 5.1). Regarding the vegetation along the two transects, list of the vascular plant species that growing within a 5 m radius of each sample prepared, during the sample collections (for more detail see supplementary). Also, percentage

of the vegetation cover according to the two categories of Arboreal and Herbaceous are estimated (Tab. 5.2).

A total of 32 collected samples were shipped to the Department of Palynology and Climate Dynamics at Göttingen University, Germany, and stored under dark conditions at 4 °C.

Later, samples were sieved with a 100 µm mesh size, washed with distilled water, and centrifuged at 3500 rpm for 5 min to isolate the pollen grains from other components as far as possible. This method yielded pollen pellets at the conical end of centrifuge tubes. The volume of each sample was increased with distilled water (Behling-traps increased to 20 ml and mosses to 10 ml). Later, 10 from Behling-traps and 5 ml from mosses was taken out for the palynological purpose, and the rest remained for DNA extraction.

Asalem-Khalkhal (AS)			Shanderman-Masal (SH)		
altitude	Prevailed Vegetation form	Kind of sample	altitude	Prevailed Vegetation form	Kind of sample
2300	Herbaceous	Trap (dry)			
2200	Herbaceous				
2100	Herbaceous				
2000	Herbaceous	Trap (moist)			
1900	Herbaceous				
1800	Herbaceous	Mosses			
1700	Herbaceous	Trap (liquid)	1700	Herbaceous	Mosses
1600	Arboreal	Trap (moist)	1600	Arboreal	
1500	Arboreal		1500	Herbaceous	Mosses
1400	Arb. & Herb	Trap (moist)	1400	Arboreal	Trap (moist)
1300	Arboreal	Mosses	1300	Arboreal	Trap (liquid)
1200	Arboreal	Mosses	1200	Herbaceous	Trap (dry)
1100	Arboreal	Mosses	1100	Arb. /Her.	Trap (liquid)
1000	Arboreal		1000	Arboreal	Trap (liquid)
900	Arboreal	Mosses	900	Arb. /Her.	Trap (liquid)
800	Arboreal		800	Arboreal	Trap (liquid)
700	Arboreal	Mosses	700	Arb. /Her.	Trap (liquid)
600	Arb. & Herb	Mosses	600	Herbaceous	Mosses
500	Arboreal	Mosses	500	Arboreal	
400	Arboreal	Mosses	400	Arb. /Her.	Trap (liquid)
300	Arboreal	Mosses	300	Herbaceous	Mosses
200	Herbaceous	Trap (liquid)	200	Arb. /Her.	Trap (liquid)
100	Herbaceous	Trap (moist)	100	Herbaceous	Trap (liquid)

Table 5.1. List of the complete pollen traps. Lost samples colored in gray. Note: Prevailed vegetation form is based on the vegetation surveys at the field.

Palynological analysis

Prior to the sample processing, one tablet of the exotic *Lycopodium* spores (9.666 +/- 212) was added to each Behling-trap sample for calculating concentration (grains/cm^3). Then the samples were processed by pollen analytical methods of Faegri and Iversen (1989), using the chemical

treatment (10% HCl, 40% HF and acetolysis). Pollen identification followed the literature (Beug, 2004) and the Department of Palynology and Climate Dynamics reference collections. A minimum of 300 terrestrial pollen grains was counted for each sample. Then, the percentages were calculated on the sum of arboreal (AP) (trees, shrubs, lianas) and non-arboreal pollen (NAP) (grasses and herbs). Based on the pollen sum, the percentage calculation and illustration of pollen were done with TILIA and TILIAGRAPH program 2.1.1. (Grimm, 1987).

	Shanderman-Masal (SH)		Asalem-Khalkhal (AS)	
Altitude m (a.s.l.)	Arboreal coverage	Herbaceous coverage	Arboreal coverage	Herbaceous coverage
100	40	50	20	55
200	60	55	20	50
300	35	67	75	58
400	50	40	78	37
500	75	36	73	32
600	40	75	62	65
700	70	57	85	20
800	78	35	70	35
900	65	60	74	62
1000	75	31	72	41
1100	56	48	70	45
1200	45	67	80	22
1300	70	34	85	18
1400	67	33	73	60
1500	30	76	84	17
1600	75	25	90	15
1700	0	95	38	70
1800	77	23	45	72
1900			0	73
2000			0	78
2100			0	70
2200			0	80
2300			0	68

Table 5.2. List of the estimated percent of the vascular plant coverage, within 5 m radius to each trap.

Metabarcoding

DNA extraction and amplification

The DNA extraction was done according to the manufacture instructions, using NucleoSpin Food Prep Kit from Macherey-Nagel (Düren, Germany). The libraries were prepared using a one-step PCR protocol according to dual indexes strategy described in Sickel et al., (2015), in short, amplification was performed for two target regions ITS2 and rbcL. The modified sequences of the standard primers for ITS2 (White et al., 1990; Chen et al., 2010) and rbcL (Erickson et al., 2017) were prepared to fit the dual-indexing metabarcoding strategy (Sickel et al., 2015). To reduce PCR bias, two separate reactions (25 µl in each) were performed. Also, negative and positive controls with the known species mixture were included in the run. The PCR mixture contained 12.5 µl AccuStart II PCR ToughMix (Quantabio), 1.25 µl 20x

EvaGreen (Biotium), 1.25 µl of each ITS2 primer (10µM, biomers), 0.75 µl of each rbcL primers (10 µM, biomers), 2.25 µl PCR grade water and 5 µl DNA (about 20 ng/µl). For the sample-specific labeling, the dual indexing primers with different forward/reverse index combinations were used for each sample. PCR under the following conditions was conducted with the Applied Biosystems 7300 Real-Time PCR System: initial denaturation at 95 °C for 10 min, 35 cycles of denaturation at 95 °C for 45 s, annealing at 52 °C for 60 s, and elongation at 72 °C for 60 s; followed by a final extension step at 72 °C for 10 min. Afterward, a dissociation curve was used as the control for amplification.

Sequencing

After PCR, the two amplifications product were pooled with equal volumes 40 µl AMPure beads were added to 50 µl of the mixed PCR product to combine and purify each duplicated sample with magnetic beads (AMPure XP, Beckmann Coulter).

Then samples were washed with 80% ethanol twice, and DNA was eluted in 30 µl of 10 µMTris (pH 8.5) then the concentration of the mixture was measured by applying a Qubit fluorometer. All samples were diluted to 4 nM (except for two with very little amplification which were used without dilution) and pooled in the 4 nM library. Lastly, the library was diluted to 7 pM, denatured, and spiked with 15% of the denature d PhiX Control (Illumina) as described in the 16S Metagenomic Sequencing Library Preparation workflow (Illumina). Finally, sequencing was performed on the Illumina MiSeq using 2 × 250 cycles v2 chemistry as described in Sickel et al. (2015). Since different forward/reverse index combinations were used for each sample, the MiSeq software can decomplex the reads into separated fastq files for forward and reverse reads of each sample.

Data analysis

The subsets of the ITS2 and rbcL markers were split up by applying the BLASTn, to estimate the first ten base pairs of each read, which are conserved for each marker and thus are a good discriminator. Then, forward and reverse reads of each marker were quality filtered, dereplicated, denoised, and finally merged to amplicon sequence variants (ASVs) using the DADA2 pipeline (Callahan et al. 2016a,b). The quality filtering parameters were set according to the ITS pipeline (Callahan et al. 2016 a,b) and pipeline for rbcL diatoms (Keck et al. 2019). The below parameters were set with the same values for both markers:

maxN = 0, maxEE = c (2, 2), truncQ = 2, rm.phix = TRUE

As reads belonging to ITS2 show natural length variation between 200-600 base pairs (bp), in order to obtain the maximum sequence diversity, the truncation was not applied to them. Instead, the minimum accepted length of sequences (minLen) was set to 50. Both forward and reverse reads from rbcL were truncated at 240. These numbers were gained from a quality profile plot. ASVs were classified taxonomically against the nr/nt databases of Genbank using the BLASTn (Benson et al. 2009). The order of criteria for selection was minimum E-value = 1e-50, maximum identity = 99%, and coverage = 99%. If more than one hit has the same quality metrics, the one with the taxon that has higher frequency among the hits for that sequence was selected and the other hits go to "other possible taxa" group. The possibility of occurrence of these taxa will be checked later using floristic literature and finally the taxa that is more probable from molecular and floristic point of view is selected.

Key species selection

All assigned taxa (including other possible taxa) were checked in reference books of the flora of Iran (Rechinger, 1963) and the recently reported paper Ghorbanalizade and Akhani (2021).

Statistical analysis

All the statistical analyses are done in R, version 4.1.1 (R core team, 2021). First, we calculated the percentage of each taxon per sample for each transect based on their total presence in the whole dataset for both metabarcoding and microscopy data. Then illustrated the abundant families (>5% across the entire dataset) as the pie chart for each sample. We also prepared a boxplot in order to compare the numbers of identified taxa between rbcL and ITS2.

Results

Asalem-Khalkhal (AS) transect

Of the 23 pollen traps so far, only seven Behling traps have been found after one year. Wherever were possible, as the replacement of the lost Behling traps, nine mosses samples collected. Six stations remained without any sample (Tab. 5.1).

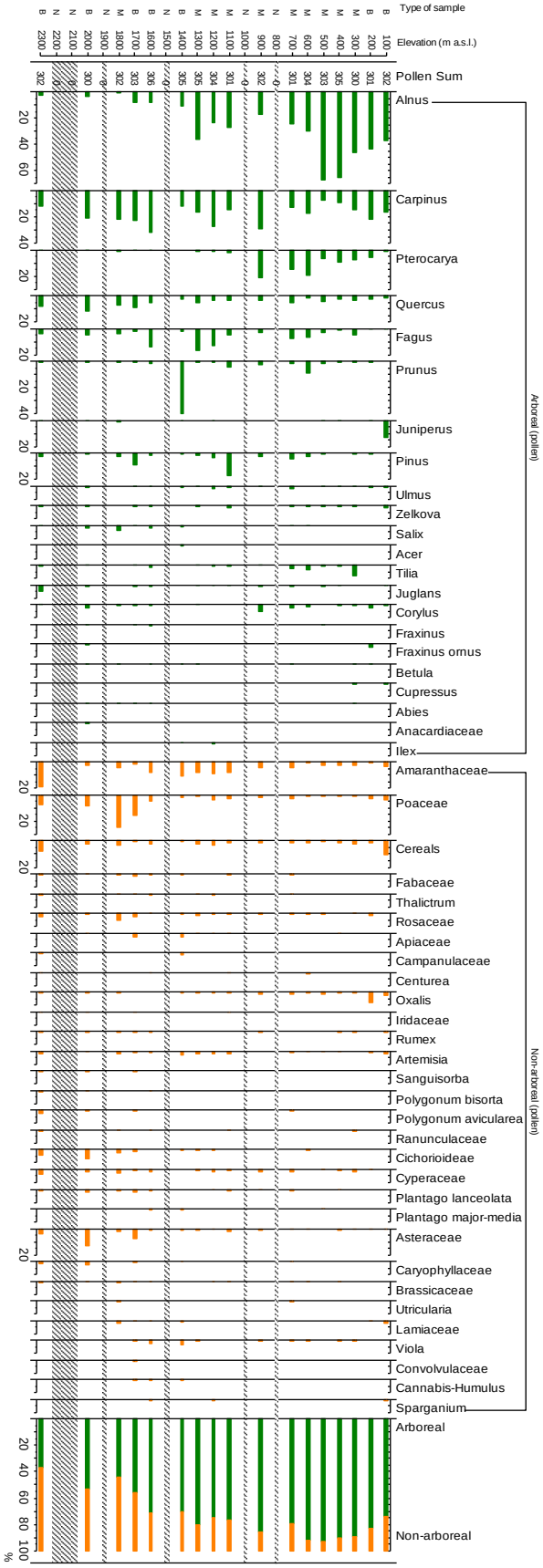

Fig. 5.2. Percentage of the most abundant taxa at AS-transect based on the pollen counting method. Type of the sample: Behling-trap (B), Mosses (M) and No-sample (N); the lost samples indicated with gray lines.

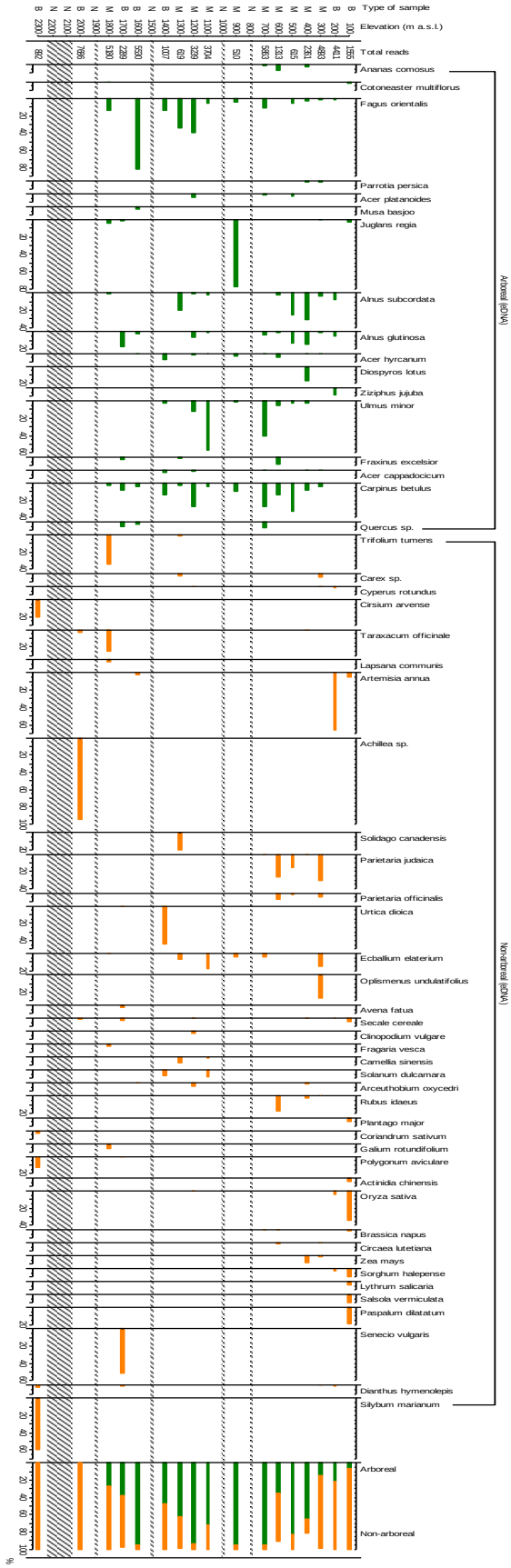

Fig. 5.3. Percentage of the most abundant taxa at AS-transect based on the metabarcoding (eDNA) method. Type of the sample: Behling-trap (B), Mosses (M) and No-sample (N); the lost samples indicated with gray lines.

Vegetation survey

Based on the vegetation description along the Asalem-Khalkhal (AS-transect) 150 vascular plant species (gymnosperms and angiosperms) have been identified. Between 300 to 1600 m the arboreal plants have higher percentage cover. Above and lower than that range the herbaceous plants are dominant (Tab. 5.2).

In more detail in the lowland of the AS-transect (up to 800 m a.s.l.) *Alnus subcordata, Acer velutinum, Carpinus betulus, Diospyros lotus* are dominant, together with grasses and herbs like *Brachypodium sylvaticum, Parietaria officinalis, Rubus hirsutus*.

The main vegetation around the samples in the mountain belt (up to 1800 m a.s.l.) consists of *Acer velutinum, Fagus orientalis, Alnus subcordata, Acer cappadocicum, Carpinus betulus* and grass and herbaceous taxa like *Festuca drymeja, Brachypodium sylvaticum, Galium odoratum,* and *Rubus hirsutus*.

Lastly, in the upper mountain area (above 1800 m a.s.l.) the grass and herbaceous taxa are the most frequent and consist mainly of *Trifolium repens*, *Bromus tectorum*, *Poa trivialis*, and *Deschampsia cespitosa* (for more detail see supplementary).

Pollen counting

A total of 54 pollen taxa at different ranks were identified which include 15 families, one subfamily (Cichorioideae), 32 genera and six species (consisting *Pterocarya fraxinifolia, Juglans regia, Polygonum bisorta, Polygonum aviculare, Plantago lanceolata* and *Plantago major-media*).

In the lowland (up to 800 m a.s.l., seven samples) *Alnus*, *Carpinus* and *Pterocarya* with 44.5%, 14% and 9.5%, respectively consist the most dominant pollen taxa. While, in the highland (up to 1800 m a.s.l., eight samples) *Carpinus* (22%) and *Alnus* (16%) remained the most abundant taxa accompanied by *Fagus* (7%), Poaceae (7%), Amaranthaceae (7%) and *Prunus* (6%). In the upper mountain area (above 1800 – 2300 m a.s.l., two samples) *Carpinus* (17%), Amaranthaceae (11%), *Quercus* (10%), Poaceae (8%) and Asteraceae (8%) are the main counted pollen (Fig. 5.2).

The most abundant families (>5% of the entire pollen count along the whole transect) are illustrated in Fig. 5.6 (A). Only seven families represent 85% of the total pollen and consist of Betulaceae 46%, Fagaceae 10%, Poaceae 8%, Rosaceae 5%, Juglandaceae 6%, Asteraceae 5% and Amaranthaceae 5%. The percentages of the pollen count show higher values for the arboreal taxa than non-arboreal between 100 to 1600 m, while between 1700 to 2000 m elevat-

Fig. 5.4. Percentage of the most abundant taxa at SH-transect based on the pollen counting method. Type of the sample: Behling-trap (B), Mosses (M) and No-sample (N); the lost samples indicated with gray lines.

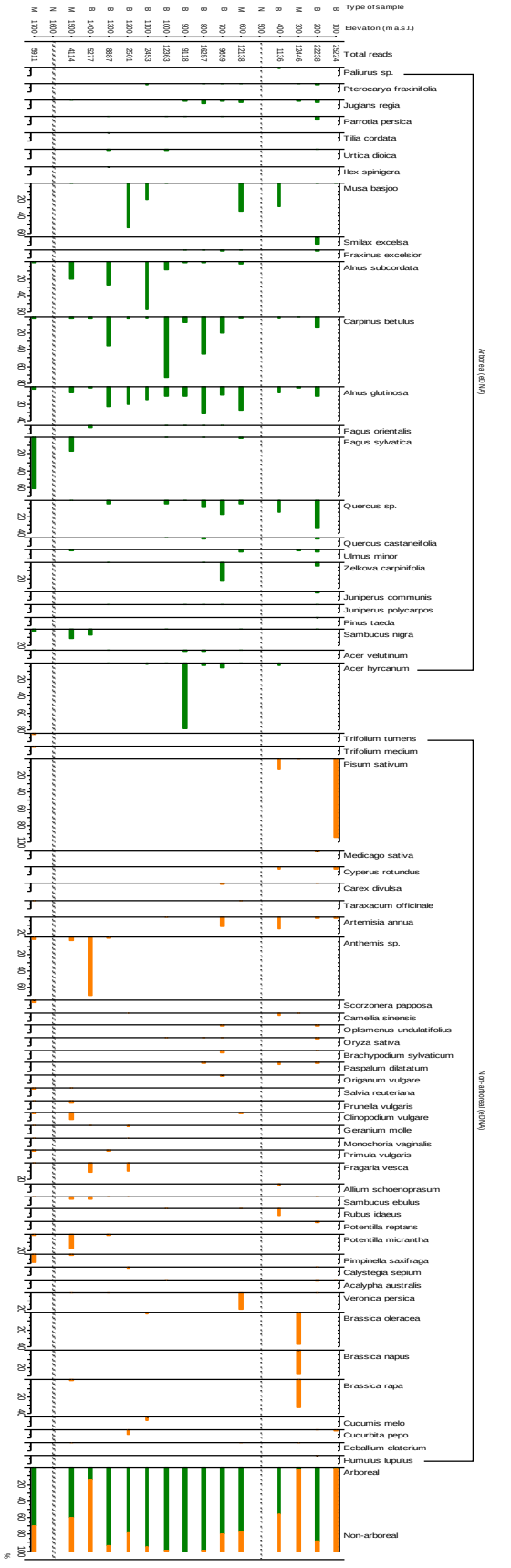

Fig. 5.5. Percentage of the most abundant taxa at SH-transect based on the metabarcoding (eDNA) method. Type of the sample: Behling-trap (B), Mosses (M) and No-sample (N); the lost samples indicated with gray lines.

ion, they have almost the same frequencies. However, at 2300 m elevation, the non-arboreal taxa overcome the arboreal ones (Fig. 5.9).

Metabarcoding

Overall, 99.77% of reads were classifiable to markers, with 67% rbcL and 33% ITS2. The separated reads entered the DADA2 pipeline to obtain unique sequences (ASVs) submitted to BLASTn for taxonomy assignment. According to available resources on the flora of Iran and Turkey, 107 species and four genera of the metabarcoding results have been recorded as being present in northern Iran, among which 59% of the species were identified by rbcL, 35% by ITS2, and 6% by both markers. These species belong to 89 genera and 47 families.

In the lowland (up to 800 m a.s.l., seven samples *Artemisia annua* (14%), *Carpinus betulus* (12%), *Ulmus minor* (12%), *Parietaria judaica* (9%), *Alnus subcordata* (7%) and *Oplismenus elaterium* (6%) represent the most abundant reads. At the mountainous area (up to 1800 m a.s.l., eight samples) *Fagus orientalis* (29%), *Ulmus minor* (12%), *Carpinus betulus* (8%), *Trifolium tumens* (8%) and *Taraxacum officinale* (6%) provide the highest reads. However, at the upper mountain areas (1900 – 2300 m a.s.l., two samples) the dominant reads belong to *Achillea* sp. with 85% and *Silybum marianum* with 6% (Fig. 5.3).

Along the whole transect six families consist of 80% of the total reads and Fig. 6B represents the contribution of each sample among those six families. These families include Asteraceae (28%), Fagaceae (16%), Betulaceae (15%), Ulmaceae (10%), Poaceae (6%), Urticaceae (5%). From 100 to 300 m and 1700 to 2300 m a.s.l., the majority of reads belong to non-arboreal formations, while between 400 to 1600 m, the reads belong mostly to arboreal taxa (Fig. 5.9).

Shanderman-Masal (SH) transect

Of the 17 pollen traps, 11 Behling traps have been found after one year. Four mosses samples, as the replacement of the lost Behling traps were used, while two stations remained without any sample (Tab. 5.1).

Vegetation survey

According to the vegetation survey along the Shanderman-Masal (SH-transect), 107 vascular plant species (gymnosperms and angiosperms) have been identified.

In the lowland of the SH-transect (up to 800 m a.s.l.) *Carpinus betulus*, *Alnus subcordata*, *Acer velutinum*, *Quercus castaneifolia*, *Oplismenus undulatifolius* have the highest frequencies.

While, the main vegetation around the samples in the mountain belt (up to 1700 m a.s.l.) consists of *Alnus subcordata*, *Fagus orientalis*, and *Carpinus betulus* are the dominant arboreal species. *Clinopodium umbrosum*, *Carex divulsa*, *Tanacetum parthenium*, *Brachypodium sylvaticum* and *Prunella vulgaris* are the most frequent grasses and herbs (for more detail see supplementary).

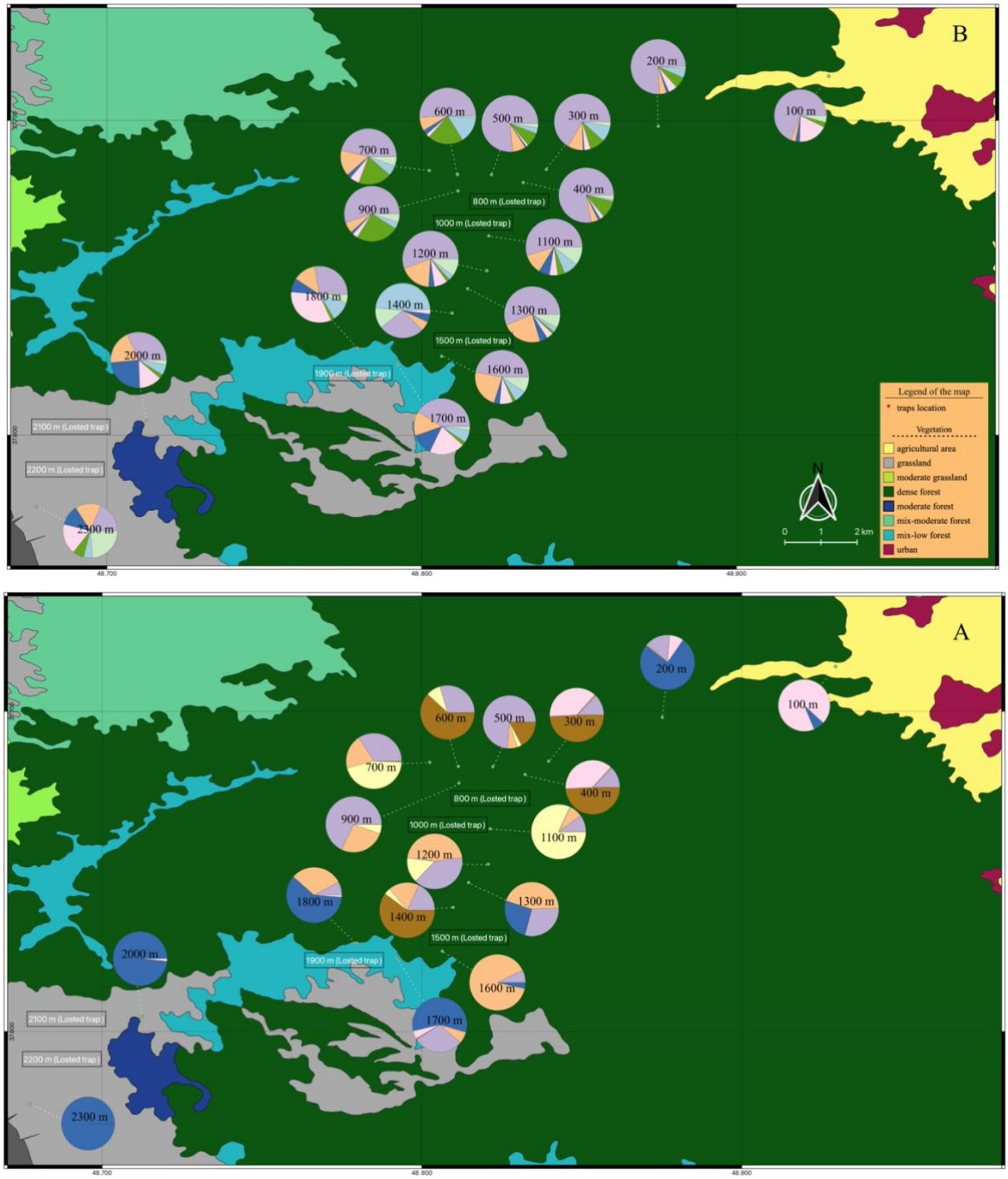

Fig. 5.6. The most abundant families at each elevation at the AS-transect. Pollen counting (A), metabarcoding (B)

Betulaceae Fagaceae Ulmaceae Juglandaceae
Asteraceae Poaceae Rosaceae Amaranthaceae Urticaceae

Pollen count data

A total of 58 taxa at different ranks were identified, which include 15 families, one subfamily (Cichorioideae), 35 genera and seven species (consisting *Pterocarya fraxinifolia*, *Juglans regia*, *Polygonum bisorta*, *Plantago lanceolata* and *Plantago major-media*, *Ephedra distachya*, *Fraxinus ornus*).

In the lowland (up to 800 m a.s.l., seven samples) *Alnus* (33%) *Carpinus* (22%) and *Pterocarya* (9%) provide the most abundant pollen (Fig. 5.4). However, in the highland (above 800 m a.s.l., eight samples) *Alnus* with 40% and *Carpinus* with 29% are the most dominant pollen.

The most dominant families (only those >5% of the entire pollen count) are shown in Fig. 5.7 (A), which represents 83% of the grains, including four families of Betulaceae 64%, Juglandaceae 8%, Fagaceae 7%, Asteraceae 4%. The remaining 32 families (each with less than 5%) provide 17% of the dataset.

Based on the percentage of the pollen counts (Fig. 5.10), the arboreal and non-arboreal taxa show differences. However, the arboreal pollen in all samples were dominant.

Metabarcoding

In total 99.85% of reads were classifiable to markers, with 60% rbcL and 40% ITS2. The taxonomic assignment followed the same as the AS-transect. Afterward, the probability of occurring was checked for each taxon with the flora of Iran and Turkey. As a result, 121 species and four genera have been approved as being present in northern Iran, in between 45% of the taxa belong to rbcL, 30% to ITS2, and 25% to both markers, which assigned to 101 genera and 48 families.

In the lowland (up to 800 m a.s.l., seven samples) the most abundant reads belong to *Pisum sativum* (24%), *Carpinus betulus* (12%), *Alnus glutinosa* (12%) and *Quercus* sp. (11%), while at highland (upper than 800 m a.s.l., eight samples) *Carpinus betulus* (27%), *Acer hyrcanum* (14%), *Alnus subcordata* (12%), *Alnus glutinosa* (11%) and *Anthemis* sp. (8%) represent the highest reads (Fig. 5.5).

The proportion of the most abundant families (>5% of the whole transepts' reads) is represented in Fig. 7B. Among the 48 families, only six families (including 80% total reads, Betulaceae 33%, Fabaceae 17%, Fagaceae 12%, Brassicaceae 8%, Sapindaceae 6%, Asteraceae 4%) account for 80% of the results and the rest 42 families provide the remaining 20%. At 200 m and 600 to 1300 m elevation, the arboreal taxa have greater values than non-arboreal ones, while at 100 and 300 m, the results are vice versa, and non-arboreal have higher value (Fig. 5.10).

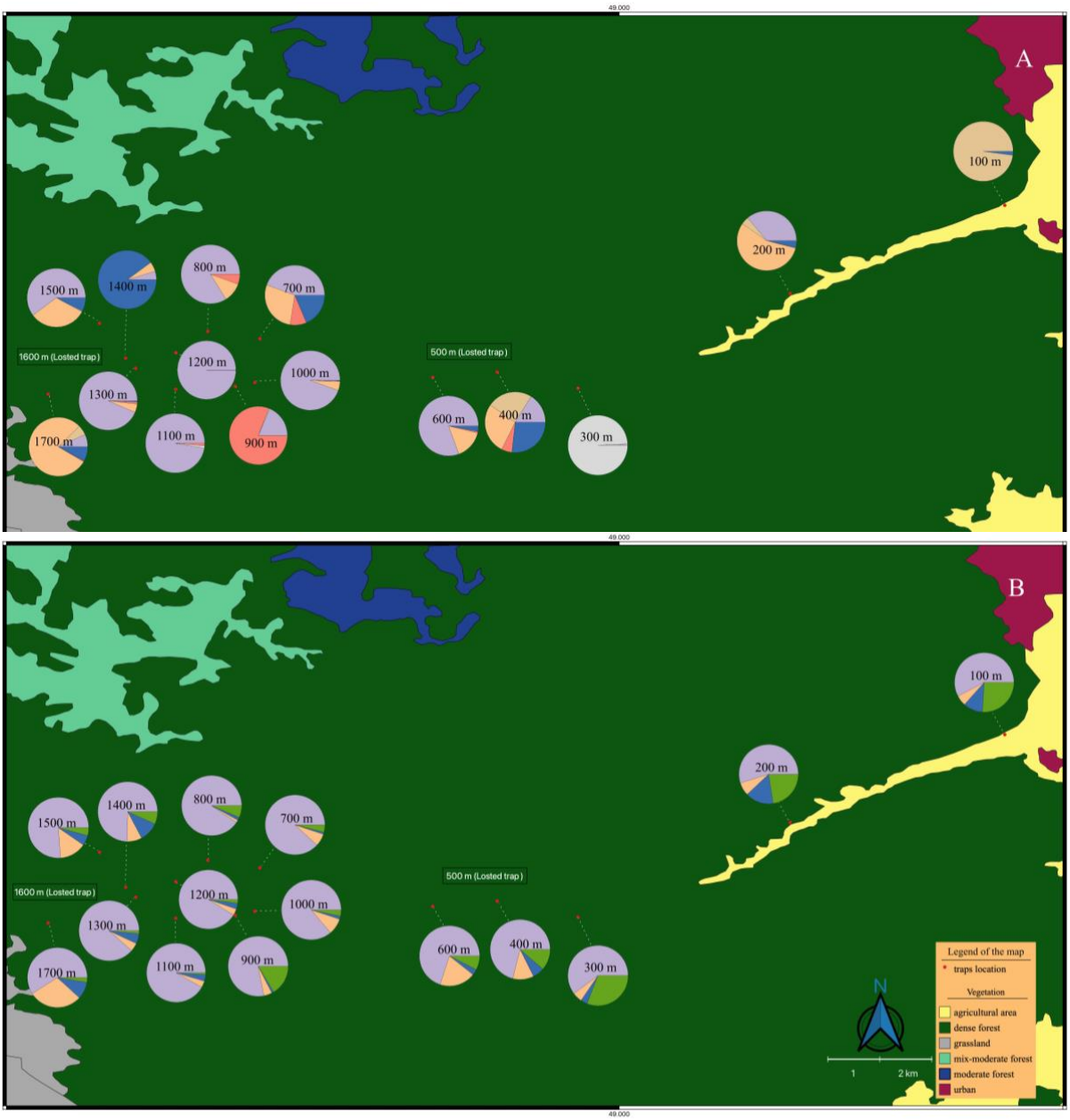

Fig. 5.7. The most abundant families at each elevation at the SH-transect. Pollen counting (A), metabarcoding (B)

Betulaceae Fagaceae Sapindaceae Juglandaceae
Asteraceae Fabaceae Brassicaceae

Discussion

Comparison of the two transects

Asalem-Khalkhal transect (AS) was up to 2300 m a.s.l., consists of different vegetation types, from lowland agricultural area to Hyrcanian forest and grasslands in the upper mountains. The

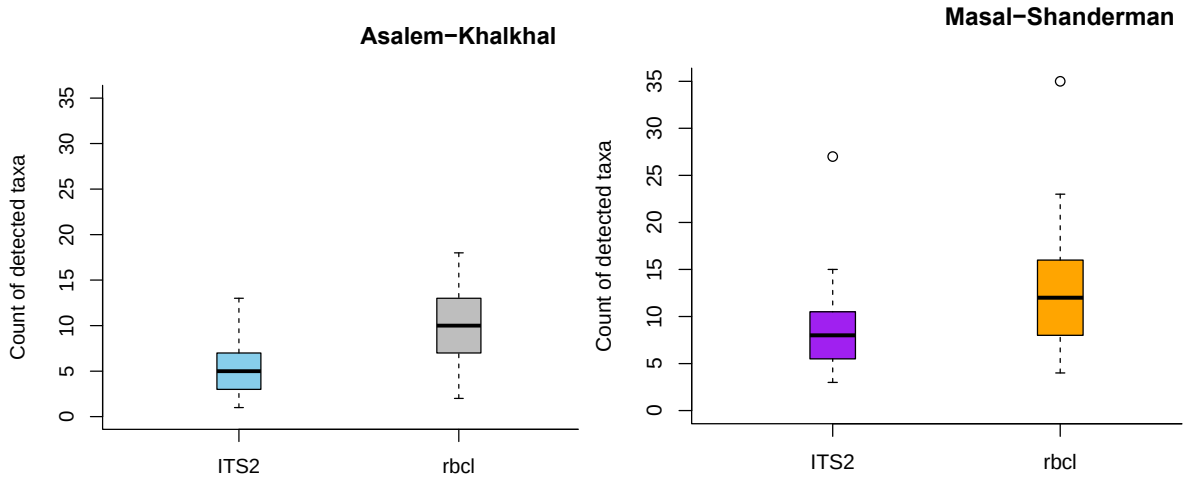

Fig. 5.8. Comparison of the detected species per sample between molecular markers of ITS2 and rbcL at both AS and SH- transects.

constructed road changed the natural composition of the area. The Shanderman-Masal transect (SH) has more forest areas which has notably lower human impact.

Comparing the metabarcoding with pollen counting results and both with vegetation survey, verified that the metabarcoding reflects more local vegetation while the pollen counting results reflects more regional vegetation. Also, comparing the two transects, indicate that the different zonal mountain vegetation at both transects is well reflected in the metabarcoding results of the pollen rain.

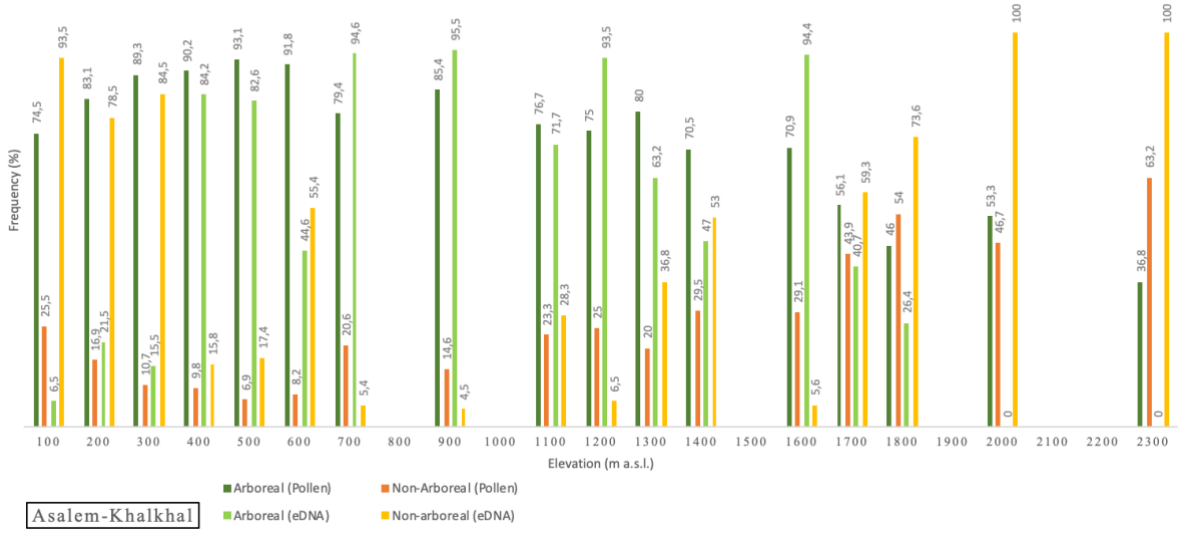

Fig.5.9. Showing the prevailed vegetation form, according to each method (eDNA and pollen counting) at different elevation of the AS-transect.

Metabarcoding:

At AS-transect the Behling-traps were mostly lost or dried out and didn't have the good condition. However, still 107 taxa belonging to 47 families were recognized. Taxa of the six

families were more abundant in the transect (Fig. 5.6B). From 100 to 600 m and upper than 1700 m, elevation, herbaceous plants from Poaceae, Asteraceae, and Urticaceae are dominant. Between 700 to 1600 m elevation, taxa of Betulaceae, Ulmaceae and Fagaceae are more abundant.

In the SH-transect 121 taxa belong to 48 families were identified. Six families are the most abundant ones. Majority of the reads belong to the rbcL region (Fig. 5.8). Up to 400 m elevation, taxa from Brassicaceae, Fabaceae and Asteraceae were abundant. Above 400 m, taxa of the Betulaceae, Fagaceae, Sapindaceae and Asteraceae are dominant (Fig. 5.7B).

Important taxa for the lowland zone (up to 800 m elevation) are *Carpinus betulus*, *Alnus glutinosa*, *Ulmus minor* and *Artemisia annua*, *Parietaria judaica* and *Pisum sativum*. For the mountainous zone (up to 1800 m elevation) the most frequent taxa are *Alnus glutinosa*, *Fagus orientalis*, *Carpinus betulus*, *Acer hyrcanum*.

The most important upper mountain taxa (up to 2300 m elevation) are only based on the AS-transect. These are *Achillea* sp., *Silybum marianum*, *Polygonum aviculare* and *Circium avense*.

Palynology:

A total of 54 pollen taxa (at different ranks) were identified in the As-transect. The identified taxa belong to 35 families from which seven families showed higher values along the transect (Fig. 5.6A). According to the pollen counting data from 100 to 1700 m elevation, arboreal mostly from Betulaceae, Juglandaceae and Fagaceae are prevailed, while above 1800 m non-arboreal (like Asteraceae, Poaceae and Rosaceae) are dominant (Fig. 5.9).

At SH-transect a total of 58 pollen taxa (at different ranks) were identified, which belong to 36 families. However, four families had more representatives along the transect. Taxa of the Betulaceae were the most abundant ones (Fig. 5.7A). Based on the percentage of the pollen counts (Fig. 5.10), the arboreal pollen taxa in all the samples were dominant.

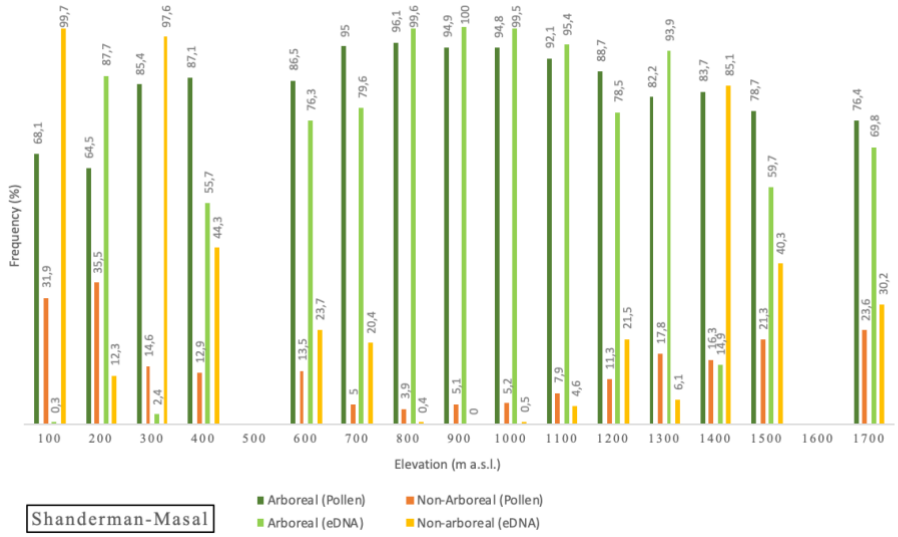

Fig.5.10. Showing the prevailed vegetation form, according to each method (eDNA and pollen counting) at different elevation of the SH-transect.

Highlights and challenges of the methods

The incomplete plant reference databases of the occurring plants in Iran and the missing pollen traps reduce partly the clarity of the results. Therefore, the interpretation of the results needed to be done with caution. However, the results of the pollen DNA metabarcoding, besides the pollen counting are valuable to identify the main plant taxa along the two transects. Some of the advantages and disadvantages of these approaches are also discussed below:

1. Although, the number of records from the Iranian plants on GenBank was relatively low, and made the taxonomic assignment section challenging, the DNA metabarcoding identified in total 182 species from 57 families.
2. At metabarcoding, except for a few taxa that were present in most of samples, the rest of the taxa were rarely detected in more than three samples, which can represent the efficiency of the method for investigating the vegetation composition.
3. In this study two different markers ITS2 and rbcL used, which the identified taxa with the rbcL were slightly higher in both transects (Fig. 5.8). While, applying both markers provided more evidence of the vegetation cover of the area.
4. Failure of collecting the samples, indicate duration of a year for traps is too long. We suggested for the future studies the traps collected maximum within six months.
5. By the pollen counting method, the identified taxa faced with limitations like rarely goes down to species level, while in metabarcoding, except for the rare cases, the identified taxa mainly were at the species level.

6. The pollen counting approach defined arboreal taxa as the most abundant plants in both transects (Fig. 5.9, 5.10), which is not supported by DNA results and our vegetation survey.
7. Counting pollen slides to a high number of pollen grains, such as more than 300 pollen per sample is time consuming and time for the pollen analysis was somehow limited (e.g. within this project). In general, anemophilous taxa like *Carpinus*, *Alnus*, and *Quercus* generally were more frequent than the taxa with lower pollen production. Those mentioned genera, were present in almost all the counted samples consistently, even in the samples of the non-forested area.
8. The last relicts of the deciduous broadleaved species from the Arcto-Tertiary era such as *Pterocarya fraxinifolia* and *Zelkova carpinifolia* (Leroy and Roiron, 1996), with low frequency were present in several samples of both transects at both methods.

Conclusion

We provided the first metabarcoding insight into the vegetation composition through the two altitudinal transects at the western part of the Hyrcanian forest, Iran. DNA metabarcoding of pollen grains can be a robust method which represents vegetation finger print in the pollen rain. Thus, our results can be a first step forward in the nature conservation of the Hyrcanian forest. However, for vegetation reconstruction, it still requires more studies to obtain a better estimation. Also, more studies need to be done to increase and improve the number of species at the dataset's library. Despite the missing pollen trap samples, we were still able to identify 182 different vascular plant species from 57 families, demonstrating that the technique's ability to identify species and its application in biodiversity studies.

Lastly, rbcL showed more superiority in species identification than ITS2. However, applying both markers provides more robust evidence of the vegetation cover of the area.

Acknowledgments

We are so grateful to Mr. Amani and Mr. Jozi for their assistance during the field excursions. The study was part of the PhD project of the first author, which was supported by the German Science Foundation DFG (grant BE2116/31-1) carried out at Georg-August-Universität Göttingen, Germany.

References

Aziz, AN., Sauve, RJ., 2008. Genetic mapping of Echinacea purpurea via individual pollen DNA fingerprinting. Molecular Breeding 21, 227–232. https://doi.org/10.1007/s11032-007-9123-9

Baksay, S., Pornon, A., Burrus, M., Mariette, J., Andalo, C., Escaravage, N., 2020. Experimental quantification of pollen with DNA metabarcoding using ITS1 and trnL. Scientific Reports 10, 4202. https://doi.org/10.1038/s41598-020-61198-6

Bell, KL., de Vere, N., Keller, A., Richardson, RT., Gous, A., Burgess, KS., Brosi, BJ., 2016. Pollen DNA barcoding: Current applications and future prospects. In: Genome. Canadian Science Publishing 629–640.

Bell, KL., Fowler, J., Burgess, KS., Dobbs, EK., Gruenewald, D., Lawley, B., Connor, M., Brosi, BJ., 2017. Applying Pollen DNA Metabarcoding to the Study of Plant–Pollinator Interactions. Applications in Plant Sciences 5, 1600124. https://doi.org/10.3732/apps.1600124

Benson, DA., Karsch-Mizrachi, I., Lipman, DJ., Ostell, J., Sayers, EW., 2009. GenBank. Nucleic acids research 37, 26–31.

Callahan, BJ., Sankaran, K., Fukuyama, JA., McMurdie, PJ., Holmes, SP., 2016. Bioconductor workflow for microbiome data analysis: from raw reads to community analyses. F1000Research 5.

Campbell, BC., al Kouba, J., Timbrell, V., Noor, MJ., Massel, K., Gilding, EK., Angel, N., Kemish, B., Hugenholtz, P., Godwin, ID., Davies, JM., 2020. Tracking seasonal changes in diversity of pollen allergen exposure: Targeted metabarcoding of a subtropical aerobiome. Science of the Total Environment 747, 141189. https://doi.org/10.1016/j.scitotenv.2020.141189

CBOL Plant Working Group 2009 A DNA barcode for land plants. Proceedings of the National Academy of Sciences of the United States of America. 4, 12794-7.

Chen, S., Vargas, YN., 2010. Improving the performance of particle swarms through dimension reductions—A case study with locust swarms. In: IEEE Congress on Evolutionary Computation. IEEE, 1–8.

Coissac, E., Riaz, T., Puillandre, N., 2012. Bioinformatic challenges for DNA metabarcoding of plants and animals. Molecular Ecology 21, 1834–1847.

Creer, S., Deiner, K., Frey, S., Porazinska, D., Taberlet, P., Thomas, WK., Potter, C., Bik, HM., 2016. The ecologist's field guide to sequence-based identification of biodiversity. Methods in Ecology and Evolution 7, 1008–1018.

Djamali, M., de Beaulieu, JL., Campagne, P., Andrieu-Ponel, V., Ponel, P., Leroy, SAG., Akhani, H., 2009. Modern pollen rain-vegetation relationships along a forest-steppe transect in the Golestan National Park, NE Iran. Review of Palaeobotany and Palynology 153, 272–281. https://doi.org/10.1016/j.revpalbo.2008.08.005

Erickson, DL., Reed, E., Ramachandran, P., Bourg, NA., McShea, WJ., Ottesen, A., 2017. Reconstructing a herbivore's diet using a novel rbc L DNA mini-barcode for plants. AoB Plants 9(3), plx015. https://doi.org/10.1093/aobpla/plx015

Faegri, K., Iversen, J., 1989. Textbook of Pollen Analysis. John Wiley and Sons.

Fazekas, AJ., Burgess, KS., Kesanakurti, PR., Graham, SW., Newmaster, SG., Husband, BC., Percy, DM., Hajibabaei, M., Barrett, SC., 2008. Multiple multilocus DNA barcodes from the plastid genome discriminate plant species equally well. PLoS One 3(7), 2802. https://doi.org/10.1371/journal.pone.0002802

Fazekas, AJ., Kesanakurti, PR., Burgess, KS., Percy, DM., Graham, SW., Barrett, SC., Newmaster, SG., Hajibabaei, M., Husband, BC., 2009. Are plant species inherently harder to discriminate than animal species using DNA barcoding markers? Molecular Ecology Resources 9, 130–139. https://doi.org/10.1111/j.1755-0998.2009.02652.x

Fujiwara, MT., Hashimoto, H., Kazama, Y., Hirano, T., Yoshioka, Y., Aoki, S., Sato, N., Itoh, RD., Abe, T., 2010. Dynamic morphologies of pollen plastids visualised by vegetative-specific FtsZ1-GFP in Arabidopsis thaliana. Protoplasma 242, 19–33. https://doi.org/10.1007/s00709-010-0119-7

Galimberti, A., de Mattia, F., Bruni, I., Scaccabarozzi, D., Sandionigi, A., Barbuto, M., Casiraghi, M., Labra, M., 2014. A DNA barcoding approach to characterize pollen collected by honeybees. PLoS One: 9(10):, 109363. https://doi.org/10.1371/journal.pone.0109363

Ghorbanalizadeh, A., Akhani, H., 2021. Plant diversity of Hyrcanian relict forests: An annotated checklist, chorology and threat categories of endemic and near endemic vascular plant species. Plant Diversity: 44(1), 39-69. https://doi.org/10.1016/j.pld.2021.07.005

Gomes, BT., Correa, A., Brunelli, ES., Bitencourt, AL., 2021. Modern pollen rain analysis from Itapuã State Park (Parque Estadual Itapuã), RS, Brazil. Anais da Academia Brasileira de Ciências: 93(1), e20200392. https://doi.org/10.1590/0001-3765202120200392

Hawkins, J., de Vere, N., Griffith, A., Ford, CR., Allainguillaume, J., Hegarty, MJ., Baillie, L., Adams-Groom, B., 2015. Using DNA metabarcoding to identify the floral composition of honey: A new tool for investigating honey bee foraging preferences. PLoS One 10(8), 0134735. https://doi.org/10.1371/journal.pone.0134735

Halbritter, H., Ulrich, S., Grímsson, F., Weber, M., Zetter, R., Hesse, M., Buchner, R., Svojtka, M., Frosch-Radivo, A., 2018. Illustrated pollen terminology. Springer.

Hollingsworth, PM., Graham, SW., Little, DP., 2011. Choosing and using a plant DNA barcode. PLoS One 6(5). https://doi.org/10.1371/journal.pone.0019254

Jantz, N., Homeier, J., León-Yánez, S., Moscoso, A., Behling, H., 2013. Trapping pollen in the tropics—Comparing modern pollen rain spectra of different pollen traps and surface samples across Andean vegetation zones. Review of Palaeobotany and Palynology 193, 57-69.

Jarman, SN., Berry, O., Bunce, M., 2018. The value of environmental DNA biobanking for long-term biomonitoring. Nature Ecology and Evolution 2, 1192–1193.

Keck, F., Rimet, F., Vasselon, V., Bouchez, A., 2019. GitHub - fkeck/DADA2_diatoms_pipeline: DADA2 Custom Pipeline for rbcL Diatoms. https://github.com/fkeck/DADA2_diatoms_pipeline

Keller, A., Danner, N., Grimmer, G., Ankenbrand, MVD., Von Der Ohe, K., Von Der Ohe, W., Rost, S., Härtel, S., Steffan-Dewenter, I., 2015. Evaluating multiplexed next-generation sequencing as a method in palynology for mixed pollen samples. Plant Biology 17, 558–566. https://doi.org/10.1111/plb.12251

Khalili, A., 1973. Precipitation patterns of central Elburz. Archiv für Meteorologie, Geophysik und Bioklimatologie, Serie B 2, 215–232.

Kraaijeveld, K., de Weger, LA., Ventayol García, M., Buermans, H., Frank, J., Hiemstra, PS., Den Dunnen, JT., 2015. Efficient and sensitive identification and quantification of airborne pollen using next-generation DNA sequencing. Molecular Ecology Resources 15, 8–16. https://doi.org/10.1111/1755-0998.12288

Landsmeer, SH., Hendriks, EA., de Weger, L., Reiber, JH., Stoel, BC., 2009. Detection of pollen grains in multifocal optical microscopy images of air samples. Microscopy Research and Technique 72, 424–430. https://doi.org/10.1002/jemt.20688

Leroy, SAG., Roiron, P., 1996. Latest Pliocene pollen and leaf floras from Bernasso palaeolake (Escandorgue Massif, H.rault, France). Review of Palaeobotany and Palynology 94, 295–328.

Longhi, S., Cristofori, A., Gatto, P., Cristofolini, F., Grando, MS., Gottardini, E., 2009. Biomolecular identification of allergenic pollen: A new perspective for aerobiological monitoring? Annals of Allergy, Asthma and Immunology 103, 508–514. https://doi.org/10.1016/S1081-1206(10)60268-2

Matsuki, Y., Isagi, Y., Suyama, Y., 2007. The determination of multiple microsatellite genotypes and DNA sequences from a single pollen grain: Technical article. Molecular Ecology Notes 7, 194–198. https://doi.org/10.1111/j.1471-8286.2006.01588.x

Molavi-Arabshahi, M., Arpe, K., Leroy, S.A.G., 2016. Precipitation and temperature of the Southwest Caspian Sea during the last 55 years, their trends and teleconnections with large-scale atmospheric phenomena. International Journal of Climatology 36, 2156–2172.

Naqinezhad, A., Zare-Maivan, H., Gholizadeh, H., 2015. A floristic survey of the Hyrcanian forests in Northern Iran, using two lowland-mountain transects. Journal of forestry research 26(1), 187-199. https://doi.org/10.1007/s11676-015-0019-y

Piñol, J., Senar, MA., Symondson, WOC., 2019. The choice of universal primers and the characteristics of the species mixture determine when DNA metabarcoding can be quantitative. Molecular Ecology 28, 407–419. https://doi.org/10.1111/mec.14776

Polling, M., Sin, M., de Weger, LA., Speksnijder, AG., Koenders, MJ., de Boer, H., Gravendeel, B., 2022. DNA metabarcoding using nrITS2 provides highly qualitative and quantitative results for airborne pollen monitoring. Science of the Total Environment 806, 150468. https://doi.org/10.1016/j.scitotenv.2021.150468

Pornon, A., Andalo, C., Burrus, M., Escaravage, N., 2017. DNA metabarcoding data unveils invisible pollination networks. Scientific Reports 7(1), 1-11.

Ramezani, E., Marvie Mohadjer, MR., Knapp, HD., Theuerkauf, M., Manthey, M., Joosten, H., 2013. Pollen-vegetation relationships in the central Caspian (Hyrcanian) forests of northern Iran. Review of Palaeobotany and Palynology 189, 38–49. https://doi.org/10.1016/j.revpalbo.2012.10.004

Rechinger, KH., 1963. Flora Iranica, Flora des iranischen Hochlandes und der umrahmenden Gebirge. Graz/Wien: Akademische Druck- u. Verlagsanstalt, und Naturhistorisches Museum Wien.

Richardson, RT., Lin, C., Quijia, JO., Riusech, NS., Goodell, K., Johnson, RM., 2015a. Rank-based characterization of pollen assemblages collected by honey bees using a multi-locus metabarcoding approach. Applications in Plant Sciences 3, 1500043. https://doi.org/10.3732/apps.1500043

Richardson, RT., Lin, C-H., Sponsler, DB., Quijia, JO., Goodell, K., Johnson, RM., 2015b. Application of ITS2 Metabarcoding to Determine the Provenance of Pollen Collected by Honey Bees in an Agroecosystem. Applications in Plant Sciences 3, 1400066. https://doi.org/10.3732/apps.1400066

Rittenour, WR., Hamilton, RG., Beezhold, DH., Green, BJ., 2012. Immunologic, spectrophotometric and nucleic acid based methods for the detection and quantification of airborne pollen. Journal of Immunological Methods 383, 47–53.

Sabeti, H., 1994. Forest, trees and bushes of Iran.

Sakamoto, W., Miyagishima, S., Jarvis, P., 2008. Chloroplast Biogenesis: Control of Plastid Development, Protein Import, Division and Inheritance. The Arabidopsis Book 6, 0110. https://doi.org/10.1199/tab.0110

Sickel, W., Ankenbrand, MJ., Grimmer, G., Holzschuh, A., Härtel, S., Lanzen, J., Steffan-Dewenter, I., Keller, A., 2015. Increased efficiency in identifying mixed pollen samples by meta-barcoding with a dual-indexing approach. BMC ecology 15, 1–9.

Sun, L., Luo, J., Qian, L., Deng, T., Sun, H., 2020. The relationship between elevation and seed-plant species richness in the Mt. Namjagbarwa region (Eastern Himalayas) and its underlying determinants. Global Ecology and Conservation 23, e01053. https://doi.org/10.1016/j.gecco.2020.e01053

Taberlet, P., Coissac, E., Hajibabaei, M., Rieseberg, LH., 2012a. Environmental DNA. Molecular Ecology 21, 1789–1793.

Taberlet, P., Coissac, E., Ois Pompanon, F., Brochmann, C., Willerslev, E.,2012b. Towards next-generation biodiversity assessment using DNA metabarcoding. Molecular Ecology 2045–2050.

White, TJ., Bruns, T., Lee, S., Taylor, J., 1990. Amplification and direct sequencing of fungal ribosomal RNA genes for phylogenetics. PCR protocols: a guide to methods and applications 18, 315–322.

Willerslev, E., Hansen, NJ., Binladen, J., Brand, TB., Gilbert, MTP., Shapiro, B., Bunce, M., Wiuf, C., Gilichinsky, DA., Cooper, A., 2003. Diverse Plant and Animal Genetic Records from Holocene and Pleistocene Sediments. Science 300, 791–795. https://doi.org/10.1126/science.1084114

Chapter 6: Synthesis

The outcomes of the current study, for the first time, contribute to improving our knowledge on palaeoecological changes during the late Holocene at high- to mid-elevated areas of the Gilan province (see Fig. 1.1 in chapter 1). Moreover, with the help of the multi-proxy palaeoecological approach, the resilience of the Hyrcanian forest to both anthropogenic and natural disturbances was also evaluated. Finally, as a pioneer study, the modern vegetation of the western Hyrcanian forest in two different altitudinal gradients was also assessed with the help of the DNA metabarcoding and pollen counting methods derived from the modern pollen rain.

The first record was the Pounel mire located at the highlands (ca. 2200 m a.s.l.) of the Gilan province, provided the oldest record from the province, dated back to 4300 cal yr BP (chapter 2). The second record was from the Kholasht-Kouh Lake, also located upper than the forest line (ca. 2000 m a.s.l.), dated back to the last 1200 years ago (chapter 3). Finally, the last report from the Annal Lake, located in the middle of the Hyrcanian forest (at 700 m a.s.l.), covered the past 1690 cal yr BP (chapter4).

Vegetation history from mid-elevated to High-elevated

With the help of the multi-proxy analysis, it has been shown that regional steppe vegetation at **Pounel mire** (PNL) remained stable at least since the last four millennia. During the covered time span, forest has never approached the mire surroundings. *Quercus*, *Fagus*, and *Carpinus* were the most prevalent trees of the downstream forests. Based on the study's outcomes, between 1700 to 1000 cal yr BP, Cichorioideae, Amaranthaceae, and Brassicaceae species increased while Poaceae and arboreal plants, especially *Fagus* and *Quercus* trees, decreased. After 1000 cal yr BP, forest recovered somehow. However, herbaceous plants, especially Poaceae and Cichorioideae, increased even more than before this period.

The **Kholasht-Kouh Lake** (KHL) results indicated that the study area was covered by a relatively high proportion of non-arboreal vegetation between 1200 and 1030 cal yr BP. The open vegetation surrounding the lake was composed mainly of *Artemisia*, Amaranthaceae, and Poaceae. Forest areas at lower elevations were mainly composed of *Quercus*, *Fagus*, *Carpinus*, and *Juniperus*. Between 1030 to 730 cal yr BP, the dominant herbs decreased markedly, while trees increased in density and/or expanded from lower to upper elevations. *Quercus* was the most abundant forest taxon, but after ca. 880 cal yr BP followed the decreasing trend while *Fagus* trees became more frequent. The replacement of *Quercus* with *Fagus* trees indicates a

more closed canopy compared to the previous phase, *Fagus* sapling, as the shade-tolerant taxa outcompete the light-demanding *Quercus* sapling (Ligot et al. 2013). Thus, the most characteristic of the last 700 years is the strong reduction of arboreal plants, especially *Quercus* and *Fagus*, while herbs, especially Poaceae, *Artemisia*, and Amaranthaceae, became abundant again. Opposite to *Quercus* and *Fagus*, *Carpinus* increased, which may refer to the growth of the *Carpinus orientalis*, characteristic tree for the 2300 to 2400 elevation (Ramezani et al. 2013).

The **Annal Lake** (ANL) results documented the mixed forest of *Alnus*, *Carpinus*, *Quercus*, and *Fagus*, as well as patches of grassland areas, frequent with Asteraceae subf. Cichorioideae, Poaceae, Amaranthaceae, and Cyperaceae around the lake between ca. 1690-1450 cal yr BP. After ca. 1450 cal yr BP, the local open herb vegetation with frequent *Artemisia* and Poaceae around the previous non-permanent lake reduced markedly. The forest became much more abundant and prevailed in the study area. *Alnus*, *Carpinus*, *Fagus*, and *Quercus* were the most frequent trees in this mid-elevated Hyrcanian forest. Trees of *Juglans* and *Prunus* were cultivated in the study area. By starting the 17th century, the arboreal plants decreased slightly, especially *Alnus* and *Carpinus*. However, cultivated trees of *Juglans* and *Prunus* increased. Poaceae species were still the most frequent herbs, but *Artemisia* became rare. Instead, Cichorioideae, Rosaceae, Asteraceae, and Amaranthaceae were more frequent, probably due to the slight opening of the forest. Since 65 years ago, reducing the most frequent trees like *Alnus*, *Carpinus*, and *Quercus* indicates marked deforestation in the study area. Nevertheless, *Juglans* and *Prunus* increased. The increase of herbs, in particular Poaceae, and others like Rosaceae, Apiaceae, *Plantago lanceolata*, as well as Cerealia, indicated larger non-forested areas around the Annal Lake during the last century.

Before this study, the three studies from the central Hyrcanian forests (Muzidarbon at 550 m a.s.l. (Ramezani et al. 2008), Tepe Kelar at 1080 m a.s.l. (Ramezani 2013), and Veisar at 1475 m a.s.l. (Khakpour Saeej et al. 2013)), were the only palaeoecological studies that provided altitudinal transect reports from the Hyrcanian region. The reports reconstructed the vegetation history, climatic condition, and anthropogenic influence of the central Hyrcanian region through the past 1500 years.

However, the results of the current study, together with the available reports from the lowlands of the Gilan (Leroy et al. 2011; Haghani et al. 2015, Gu et al. 2021a,b), make it able to reconstruct the vegetation history of the western Hyrcanian forest in an altitudinal gradient, at least for the past 1000 years.

The summary of the combined vegetation reconstructions is as follows:

I. During the last millennia, *Alnus*, *Carpinus*, *Fagus*, and *Quercus* have been present near the lowlands to mid-elevated areas, while at the highlands, below the steppe vegetation, *Fagus*, *Quercus*, and *Juniperus* were dominant.

II. The number of *Fagus*, *Quercus*, and some other forest trees through the whole slope gradually declined more likely due to human impact and also climatic factors.

III. Between 300 to 220 cal yr BP, dense *Alnus* forests at lowlands were reduced by human activities like burning and expanding paddies fields (Leroy et al. 2011; Haghani 2015).

IV. The pollen of the cultivated plants like *Juglans*, *Corylus*, *Prunus*, and Cereals, along with plants indicating open landscapes such as *Plantago*, Cichorioideae, *Polygonum*, Brassicaceae, increased especially during the last few centuries.

Past climate dynamics from mid-elevated to high-elevated areas

The data provided with X-ray fluorescence analysis (XRF) contribute to climatic changes reconstruction.

Medieval Climate Anomaly period and before (ca. 1600 to 700 cal yr BP): The high amounts of the V/Cr ratio (lake level indicator, Schroll (1975)), Rb/Al and K/Al ratios (indicators for rainfall, and chemical weathering, Gayantha et al. (2017)) as well as Ti values (indicator for detrital inputs, Davies et al. (2015)) between ca. 1600 to 700 cal yr BP suggested the wet condition around Annal Lake in mid-latitude.

Also, the selected geological elements such as K, Ti, and Si (with high correlation in-between) indicated an increase in detrital inputs (Davies et al. 2015) and validated the relatively humid condition around Kholasht-Kouh Lake at the highlands between ca. 1200 to 700 cal yr BP. Additionally, the low K/Ti ratio value from the KHL sediment core (an indicator for the physical weathering) validated the humid condition for the mentioned period.

Specifically, low values of Mn/Ti, Ca/Ti, and Sr/Ti ratios (lower lake level indicators (Haberzettl et al. 2009; Kylander et al. 2011, 2013)), besides the rare presence of *Potamogeton* (growing in shallow lakes (Xu et al. 2020)), pointed to the highest water level for the Kholasht-Kouh Lake between ca. 1200 to 1000 cal yr BP.

In both lakes, the Si/Fe ratio (temperature indicator, Erbs-Hansen et al. 2013) represented the highest value and pointed to the warmest period. Several records documented the ca. 1000 to 700 cal yr BP as the warmest period of the late Holocene (e.g., Ramezani 2013; Haghani et al. 2015), which is well known that the Medieval Climate Anomaly (MCA) occurred in between (Ruddiman, 2008).

Little Ice Age (ca. 600 to 250 cal yr BP): Referring to the decrease in the ratios of V/Cr, Rb/Al, K/Al, Si/Fe, and Ti values (detrital inputs) and the Ca/Ti ratio increase, the period between ca. 600 to 250 cal yr BP suggested the lowest rainfall and detrital inputs. Also, the fluctuations of the geochemical elements indicated unstable climate conditions during the coldest and driest period for the ANL record. Although the pollen record documented that the forest composition did not change markedly during this cold period, other proxies in line with XRF results verified unstable environmental conditions (e.g., several *Glomus* peaks as an erosion indicator, two samples with low pollen concentration, decreased organic content, and *Potamogeton* fluctuations). Therefore, the lack of forest changes may be interpreted as standing in the center of the Hyrcanian forest region, which can cover the fluctuations in the lower and upper altitudes. Meanwhile, during almost the same period at highlands, the lowest values of P, Ti, and Si, along with the lowest sedimentation rate, indicate lower detrital inputs for the KHL site, too. Furthermore, Si/ Fe ratio had the lowest value and represented the coldest climate in the KHL record during the LIA, ca. 600-100 cal yr BP (Mann et al. 2009).
Also, investigations by Foroozan et al. (2020) represented the dry condition for this period based on the tree-ring $\delta^{18}O$ variations of juniper trees located on highlands of the Golestan province (SE of Caspian Sea).

The last two centuries (ca. 250 to -56 cal yr BP): The lowest differences between the maximum and minimum values of the geochemical ratios may suggest the most stable climatic conditions for the last 200 years ago for the ANL site. According to the Rb/Al, K/Al, and Ca/Ti ratios, Annal Lake, during this period, experienced the wettest condition with the most rainfall throughout the recorded period that corresponds to the late LIA high-stand of the Caspian Sea (Beni et al. 2013; Leroy et al. 2011). Also, Foroozan et al. (2020) documented that the wettest condition through the last 500 years occurred in the 18th century. On the other hand, referring to the Si/Fe ratio, this period was not as warm as the 1600 to 700 cal yr BP.

Fire and humans

Besides climatic changes, the role of human activities in changing the vegetation since early times needs to be considered. Pastoralism and grazing occurred in the high elevation of the Talysh (Talesh) Mountain, ca. 40 km to the west of the **Pounel mire** (PNL), at least since 6500 cal yr BP (Ponel et al. 2013). According to the macro-charcoal results and vegetation dynamics around the investigated sites, we were also able to investigate the anthropogenic effects in the western part of the Hyrcanian region for the past four millennia.

Referring to the PNL results, at the beginning of the Iron-age (1500 BC (Fallahian 2013)), the need of charcoal for metal smelting increased. Therefore, one possible reason for frequent charcoal particles in the sediment core before 2330 cal yr BP may refer to increased metal usage in human life. The iron mine of Masoule, along with Vaske village, is a good evidence of human practices with metals. Archaeologists suggested that the iron mine of Masoule (ca. 50 km distance to PNL) was discovered during the fourth millennium BP (Ghorbani 2013). Also, Vaske village is famous due to its graves with handicrafts that referred to the Iron-Age (Fallahian 2013). (Fig. 2.1 III)

Setting fires for hunting animals is another probable reason for frequent fires. The marked decrease of frequent fires after 2330 cal yr BP may indicate changes in land use due to the growing human population. Alizadeh (2014) published a study showing that people during the Sasanian Empire (between 224-651 AD) constructed fantastic irrigation systems known as Qanat. That system allowed habitants to be more farmers than hunters. Also, the high occurrence of Cichorioideae between 1700 to 1000 cal yr BP may reflect an increase in livestock grazing activity (Florenzano et al. 2015). Wood has long been the primary source for different human needs, especially *Fagus*, *Quercus*, *Carpinus,* and *Pterocarya*. Therefore, besides the climatic condition that could reduce the number of arboreal plants, anthropogenic activities can also cause a reduction in trees, mainly *Fagus* and *Quercus,* around 1580 to 1000 cal yr BP.

A more substantial increase of *Sordaria* spores, as well as *Plantago lanceolata*, suggest an increase in grazing for the last 1000 years at Pounel mire. Also, Ca (an indicator for $CaCO_3$ and presenting more livestock around the area (cf. Shahack-Gross et al. 2003)) showed a marked increase for the last 1000 years.

Between 1700 to 1000 cal yr BP, a high proportion of Cichorioideae and Amaranthaceae and reducing portion of trees, particularly *Fagus* and *Quercus,* in lower elevations, indicate a strong proportion of human activities such as intense livestock grazing and deforestation. Soil erosion results from less vegetation due to dry conditions or/and human activities reconstructed from a marked increase of *Glomus* spores and high values of K and Ti. Since 1000 cal yr BP. The occurrence of still frequent Cichorioideae and *Plantago lanceolata* along with *Sordaria* reflect continued intense grazing of the human's livestock.

Different proxies indicate that humans were present around the **Annal Lake** (ANL), at least for the past ca. 1600 years, but their impact was not that strong detected. At the beginning of the record, the high amount of the Cichorioideae could indicate grazing (Florenzano et al. 2015) near the lake, which is in line with the highest occurrence of coprophilous (especially *Sordaria*)

spores. Therefore, it can be understood that the earlier human settlers were probably more pastoralists, and through time, along with animal husbandry, they improved their agriculture activities.

Here in the mid-elevated areas, the strongest human impact occurred relatively late by deforestation, including selective logging of *Carpinus* and *Alnus*, leading to changing the Hyrcanian forest composition. The increment of the human indicator pollen, including *Juglans*, *Prunus*, cereals, ruderals, and grassland species accompanied by fires, indicate intensified expansion of the human settlements since 65 cal yr BP.

Pediastrum (an indicator of the eutrophic freshwater) rarely existed before but became abundant during this period. Therefore, it is most probable that increased human activities around the lake caused the eutrophic condition. Even nowadays, the lake has low transparency and was impacted.

In conclusion, the Hyrcanian mid-elevated forest that tolerated and prevailed during the recorded climate fluctuations, since 65 cal yr BP, lost large parts of its natural or less disturbed vegetation and have been replaced by grassland and agricultural areas due to recent expansions of anthropogenic activities.

Based on the outcomes of the **Kholasht-Kouh Lake (KHL)** record, humans were present around the studied area at least since 1200 cal yr BP. However, they did not play an important role in impacting the vegetation.

The highest frequency of coprophilous spores and macro-charcoal particles at the beginning of the KHL record indicate human settlements engaged in animal husbandry at lower elevations. Furthermore, a few Cerealia pollen as well as *Plantago* and other indicators, suggest anthropogenic activities in the region of the lake at lower elevations. Worth mentioning that the archaeological site of Ghale Kouti (16 km distance to Kholash-Kouh) at 1600 m a.s.l., consists of cemeteries from the Iron Age (Fallahian 2013) and verifies the presence of humans at the lake's lower elevations since ancient times.

The human activities showed a reduction between ca. 1000 to 700 cal yr BP, documented with the lowest frequency of human indicator taxa like Cerealia, the rarity of the coprophilous spores and macro-charcoal particles. However, this reduction is opposite to our previous studies at Annal Lake and Pounel mire, which showed increased anthropogenic activities in that period. Based on the current settlements (there is a small summer use village within 3.5 km distance to the lake), we may argue that people were always present at several distances to the lake. Nevertheless, expansion of the forest resulted in higher arboreal pollen deposition and decreased the presence of the human pollen indicators, especially Cerealia. Another possible

explanation for the reduction of human activities could be that settlers were moved to other areas.

Between 700 to 50 cal yr BP, macro-charcoal particles were rare, indicating that the possible practice of frequent burning of the steppe vegetation at the beginning of the record changed. Meanwhile, the reduction of the forest may refer to the construction activities by humans and/or their requirements to the wood for the fire, as this period stayed during the LIA with prevailing cold weather. The highest values of Cerealia and *Plantago* are in line with the reduction of the forest, indicating intensified anthropogenic activities, which lead to extensive deforestation and expansion of steppe vegetation. The record from Arasbaran mire at 2470 m a.s.l. (Ramezani et al. 2021), in line with our finding, showed the increase in agro-pastoral activities for the last millennium.

In conclusion to anthropogenic activities and the role of humans in changing the landscape of Gilan through time, more palaeoecological and archaeological research is needed. From additional places of the Hyrcanian forest region in northern Iran.

Metabarcoding and palynological results

Although metabarcoding, as a new method, needs to be developed well to become standardized, it can still be applied for assessing biodiversity (Ruppert et al. 2019). Furthermore, the samples can be taken from any kind of environment, such as water or sediment. Therefore, we applied DNA metabarcoding and pollen counting, using pollen traps and surface samples in two altitudinal gradients for the first time to investigate the western Hyrcanian forest vegetation (Fig. 1.1).

In total, 32 samples (pollen traps and mosses samples) were collected for further analysis (Chapter 5). We compared the metabarcoding results with the pollen percentages and the vegetation abundances (cover area) around the collected samples. This study indicated that the DNA barcoding results were much more in line with the vegetation surveys around the samples, indicating a strong local input of the surrounding vegetation. While, several palynological results from both transects, did not followed the vegetation surrounding the samples. The mentioned samples were taken mainly from the wind-pollinated families such as Betulaceae and Fagaceae, which were not even present near the traps or mosses samples.

Furthermore, this study showed that rbcL is able to identify more species than ITS2, while applying both markers provide a higher confidence. Also, using both methods, metabarcoding and pollen data itself can provide a better local and regional vegetation representation.

Modern vegetation and past vegetation dynamics:

The results of the modern pollen rain are also comparable with the previous palaeoecological records of the Gilan province (Leroy et al. 2011; Haghani et al. 2015, 2018; Homami Totmaj et al. 2020,2021; Gu et al. 2021 a, b). Based on the studies, we can divide the results into three elevational zones:

1. Low elevation (0 to 400 m a.s.l.)
2. Mid elevation (500 to 1000 m a.s.l.)
3. High elevation (1100 to 2300 m a.s.l.)

1. Low elevation: Based on the pollen counting of the modern pollen rain results, the arboreal plants are the predominant vegetation. In both transects (**Asalem-Khalkhal** (AS) and **Shanderman- Masal** (SH)), *Alnus*, *Carpinus*, and *Pterocarya* had the most frequent pollen taxa. However, the Poaceae and Amaranthaceae in both transects represented the most abundant pollen among the NAP. Opposite to the pollen counting results, the metabarcoding results assessed the prevalence of the herbs to the trees. Fabaceae and Brassicaceae at SH transect and *Artemisia* and Poaceae at AS transect were the most abundant taxa. However, *Alnus* and *Carpinus* with low frequency were still the most common taxa among the arboreal plants. Based on the vegetational surveys we did around the collected samples, the trees have higher percentage cover at AS lowlands, while at SH, the herbs were slightly higher than trees (Table 5.2.).

As mentioned earlier, the previous paleoenvironmental studies of Gilan province were limited to the lowlands (Leroy et al. 2011; Haghani et al. 2015, 2018; Gu et al. 2021 a,b). Referring to those studies, arboreal plants were the dominant vegetation in the lowlands at least during the last 400 years ago. The most common abundant trees were *Alnus*, *Carpinus*, *Fagus*, *Quercus*, and *Pterocarya*, respectively. While the Poaceae, Cyperaceae, *Artemisia*, and Amaranthaceae were the most frequent taxa among the herbaceous plants.

As a conclusion for the lowlands of the western Hyrcanian forest, including palaeoecological data, at least since 400 cal yr BP *Alnus* and *Carpinus* were have been the most dominant taxa.

2. Mid elevation: The modern pollen rain study by both pollen analysis methods (pollen counting and metabarcoding on pollen) verified the arboreal plants as the most dominant vegetation form. It is noteworthy that *Alnus* and *Carpinus* in both transects were the most abundant taxa based on the pollen count results. *Pterocarya*, *Quercus*, *Fagus*, and *Ulmus* were

also frequent. In both transects, Poaceae, Amaranthaceae, and *Artemisia* had higher values among the non-arboreal plants. The metabarcoding results of SH transect represented the highest values for *Carpinus*, *Alnus*, and *Acer hyrcanum*, while at AS transect *Ulmus* and *Carpinus* were the most abundant taxa, respectively. Furthermore, the vegetation surveys verified the prevalence of the trees, with the highest frequencies for the *Carpinus*, *Alnus*, *Ulmus*, and *Quercus* for both transects.

The only palaeoecological study from mid-elevated area referrers to Annal Lake study (Chapter 4), which represented the abundance of the arboreal into herbs at least since 1600 cal yr BP. *Alnus* and *Carpinus* were the most frequent taxa, except *Fagus*, *Quercus*, *Juglans*, and *Zelkova* were present. Poaceae, *Artemisia*, Amaranthaceae, and Cyperaceae were also the most frequent non-arboreal plants.

As a conclusion for the mid-elevation of the western Hyrcanian forest, despite deforestation in the past centuries, *Alnus* and *Carpinus* were have been the most dominant taxa during the last 1600 years ago.

3. High elevation: To compare the previous palaeoecological studies with the modern vegetation, this zone is divided into two subzones: 1100 to 1700 m a.s.l. and 1800 m and above (only consisting AS transect).

For the second subzone (between 1100 - 1700 m a.s.l.), the pollen counting with almost the same results for both transects represented *Alnus* and *Carpinus* as the most identified taxa. Except for them, *Fagus* and *Quercus* were also frequent. Poaceae, Asteraceae, and Amaranthaceae were the most frequent herbs in those areas.
According to the metabarcoding results, *Fagus sylvatica* had the highest value at the AS transect, however, *Ulmus minor* and *Carpinus*, as well as Asteraceae, were also frequent. On the other hand, *Carpinus*, *Alnus subcordata*, *Fagus*, Musaceae, *Artemisia*, and Rosaceae were the most frequent taxa at the SH transect.

The AS pollen counting results represented Poaceae, *Carpinus*, Amaranthaceae, Asteraceae, *Quercus*, and *Fagus* as the most frequent taxa. While the DNA results in that subzone (between 1800 - 2300 m a.s.l.) showed Asteraceae and Fabaceae as the most dominant taxa. Also, based on our vegetation surveys, Poaceae was the most frequent taxa without any Betulaceae or Fagaceae trees in those areas.

The only reference from the highlands refer to our two studies from PNL and KHL. However, the documents from the highlands of the adjacent province are also helpful for our comparison.

The same to our studies results (Chapter 2 and 3), Ramezani et al. 2021, documented the dominant steppe vegetation for the highlands of the Talysh Mountains at 2400 m a.s.l. at least since 3000 cal yr BP. The notable point of the mentioned studies is the presence of Poaceae, Amaranthaceae, and Cyperaceae as the most dominant taxa in the pollen assemblage, while *Quercus*, *Carpinus*, *Juniperus*, and *Fagus* were identified as the most abundant trees.

Therefore, at least for the past 4000 years, higher than 1800 m elevation, the herbaceous taxa occupied the region, especially with Poaceae and Asteraceae.

Future perspective

The Hyrcanian region, as one of the biodiversity regions of the world, has not been studied well. Within this research, for the first time, the palaeoecological investigations at mid and high-elevated areas provide new insight on the past vegetation, climate, and human impact in the western part of the Hyrcanian region. Also, for the first time the vegetation investigated based on the modern pollen rain, in two altitudinal transects of the Gilan.

Based on the modern pollen rain results, the anemophilous plants (like *Carpinus*) with higher pollen production (Ramezani et al. 2013) have a greater chance to be deposited. In this case, the chance for identifying the entomophilous taxa such as *Acer*, *Parrotia persica*, etc., are markedly less frequent in pollen records. As the advantage for the metabarcoding method, most of the available taxa can be distinguished in species level. However, having sufficient samples for this method is crucial.

In conclusion, more palaeoecology studies are still needed from different elevations of the whole Hyrcanian region, going back still deeper into past, to provide better reconstructions. Also, more studies on modern pollen rain including metabarcoding are needed to improve the assessment of the pollen-vegetation relationship and biodiversity of the region.

References

Alizadeh K (2014) Borderland Projects of Sasanian Empire: Intersection of Domestic and Foreign Policies. Journal of Ancient History 0: https://doi.org/10.1515/jah-2014-0015

Davies SJ, Lamb HF, Roberts SJ (2015a) Micro-XRF Core Scanning in Palaeolimnology: Recent Developments

Davies SJ, Lamb HF, Roberts SJ (2015b) Micro-XRF Core Scanning in Palaeolimnology: Recent Developments. pp 189–226

Erbs-Hansen DR, Knudsen KL, Olsen J, et al (2013) Paleoceanographical development off Sisimiut, West Greenland, during the mid- and late Holocene: A multiproxy study. Marine Micropaleontology 102:79–97. https://doi.org/https://doi.org/10.1016/j.marmicro.2013.06.003

Fallahian Y (2013) Investigation of burial patterns in Iron Age of Gilan, Iran. Ancient Asia 4:5. https://doi.org/10.5334/aa.12311

Florenzano A, Marignani M, Rosati L, et al (2015) Are Cichorieae an indicator of open habitats and pastoralism in current and past vegetation studies? Plant Biosystems 149:154–165. https://doi.org/10.1080/11263504.2014.998311

Foroozan Z, Grießinger J, Pourtahmasi K, Bräuning A (2020) 501 years of spring precipitation history for the semi-arid Northern Iran derived from tree-ring δ18O data. Atmosphere 11:. https://doi.org/10.3390/ATMOS11090889

Gayantha K, Routh J, Chandrajith R (2017) A multi-proxy reconstruction of the late Holocene climate evolution in Lake Bolgoda, Sri Lanka. Palaeogeography, Palaeoclimatology, Palaeoecology 473:16–25

Gu F, Alizadeh K, Behling H (2021a) Late Holocene vegetation and environmental changes of coastal lowlands in northern Iran: possible role of climate, human impact and Caspian Sea level fluctuations. Wetlands

Gu F, Ramezani E, Alizadeh K, Behling H (2021b) Vegetation Dynamics, Environmental Changes, and Anthropogenic Impacts on the Coastal Hyrcanian Forests in Northern Iran. Journal of Coastal Research 37:611–619. https://doi.org/10.2112/JCOASTRES-D-20-00033.1

Haberzettl T, Anselmetti FS, Bowen SW, et al (2009) Late Pleistocene dust deposition in the Patagonian steppe - extending and refining the paleoenvironmental and tephrochronological record from Laguna Potrok Aike back to 55 ka. Quaternary Science Reviews 28:2927–2939. https://doi.org/10.1016/j.quascirev.2009.07.021

Haghani S, Leroy SAG, Khdir S, et al (2015a) An early 'Little Ice Age' brackish water invasion along the south coast of the Caspian Sea (sediment of Langarud wetland) and its wider impacts on environment and people. Holocene 26:3–16. https://doi.org/10.1177/0959683615596835

Haghani S, Leroy SAG, Khdir S, et al (2015b) An early 'Little Ice Age' brackish water invasion along the south coast of the Caspian Sea (sediment of Langarud wetland) and its wider impacts on environment and people. Holocene 26:3–16. https://doi.org/10.1177/0959683615596835

Homami Totmaj L, Alizadeh K, Giahchi P, et al (2021) Late Holocene Hyrcanian forest and environmental dynamics in the mid-elevatedhighland of the Alborz Mountains, northern Iran. Review of Palaeobotany and Palynology

Kylander ME, Ampel L, Wohlfarth B, Veres D (2011) High-resolution X-ray fluorescence core scanning analysis of Les Echets (France) sedimentary sequence: New insights from chemical proxies. Journal of Quaternary Science 26:109–117. https://doi.org/10.1002/jqs.1438

Kylander ME, Klaminder J, Wohlfarth B, Löwemark L (2013) Geochemical responses to paleoclimatic changes in southern Sweden since the late glacial: The Hässeldala Port lake sediment record. Journal of Paleolimnology 50:57–70. https://doi.org/10.1007/s10933-013-9704-z

Leroy SAG, Lahijani HAK, Djamali M, et al (2011) Late Little Ice Age palaeoenvironmental records from the Anzali and Amirkola Lagoons (south Caspian Sea): Vegetation and sea level changes. Palaeogeography, Palaeoclimatology, Palaeoecology 302:415–434. https://doi.org/10.1016/j.palaeo.2011.02.002

Mann ME, Zhang Z, Rutherford S, et al (2009) Global signatures and dynamical origins of the Little Ice Age and Medieval Climate Anomaly. Science 326:1256–1260

Naderi Beni A, Lahijani H, Moussavi Harami R, et al (2013) Development of spit-lagoon complexes in response to Little Ice Age rapid sea-level changes in the central Guilan coast, South Caspian Sea, Iran. Geomorphology 187:11–26. https://doi.org/10.1016/j.geomorph.2012.11.026

Ponel P, Andrieu-Ponel V, Djamali M et al (2013) Fossil beetles as possible evidence for transhumance during the middle and late-Holocene in the high mountains of Talysch (Talesh) in NW Iran. Journal of Environmental Archaeology 18(3): 201–210.

Ramezani E (2013) Palynological reconstruction of late-Holocene vegetation, climate, and human impact in Kelardasht (Mazandaran province, N Iran). Iranian Journal of Forest and Poplar Research 21:48–62. https://doi.org/10.22092/ijfpr.2013.3338

Ramezani E, Marvie Mohadjer MR, Knapp HD, et al (2008) The late-Holocene vegetation history of the Central Caspian (Hyrcanian) forests of northern Iran. Holocene 18:307–321. https://doi.org/10.1177/0959683607086768

Ramezani E, Talebi T, Alizadeh K, et al (2021) Long-term persistence of steppe vegetation in the highlands of Arasbaran protected area, northwestern Iran, as inferred from a pollen record. Palynology 45:15–26. https://doi.org/10.1080/01916122.2019.1702117

Ruddiman WF (2008) Climate changes during the last 1000 years. Earth's climate past and future, 2nd edn WH Freeman and Company, New York 290–308

Ruppert KM, Kline RJ, Rahman MS (2019) Past, present, and future perspectives of environmental DNA (eDNA) metabarcoding: A systematic review in methods, monitoring, and applications of global eDNA. Global Ecology and Conservation 17:e00547

Schroll E (1975) Analytsche Geochemie, Band I, Metodik. Ferdinand Enke Verlag Stattgard

Shahack-Gross R, Marshall F, Weiner S (2003) Geo-ethnoarchaeology of pastoral sites: The identification of livestock enclosures in abandoned Maasai settlements. Journal of Archaeological Science 30:439–459. https://doi.org/10.1006/jasc.2002.0853

Xu J, Wang T, García Molinos J, et al (2020) Effects of warming, climate extremes and phosphorus enrichment on the growth, sexual reproduction and propagule carbon and nitrogen stoichiometry of Potamogeton crispus L. Environment International 137:105502-undefined. https://doi.org/10.1016/j.envint.2020.105502

Appendix I:

Complete number of metabarcoding reads at the Shanderman-Masal transect

Family	Taxon	100 m	200 m	300 m	400 m	600 m	700 m	800 m	900 m	1000 m	1100 m	1200 m	1300 m	1400 m	1500 m	1700 m
	Trifolium tumens	0	0	0	0	0	0	0	0	0	0	0	0	0	0	52
	Trifolium resupinatum	0	75	0	0	0	0	0	0	0	0	0	0	0	0	0
	Trifolium repens	0	0	0	0	0	0	0	0	0	0	0	0	0	0	46
	Trifolium medium	0	0	0	0	0	0	0	0	0	0	0	0	0	0	92
	Trifolium hybridum	0	52	0	0	0	0	0	0	0	0	0	0	0	0	62
	Astragalus microcephalus	40	0	0	0	0	0	0	0	0	0	0	0	0	0	0
	Cicer arietinum	0	24	0	0	0	0	0	0	0	0	0	0	0	0	0
	Melilotus indicus	0	29	0	0	0	0	0	0	0	0	0	0	0	0	0
	Melilotus officinalis	0	27	0	0	0	0	0	0	0	0	0	0	0	0	0
	Vicia crocea	20	0	0	0	0	0	0	0	0	0	0	0	0	0	0
	Pisum sativum	23876	0	7	142	0	0	0	0	0	0	0	0	0	0	0
	Medicago sativa	0	385	0	0	0	0	0	0	0	0	0	0	0	0	0
Fabaceae		23936	592	7	142	0	0	0	0	0	0	0	0	0	0	252
	Carex sp.	0	97	0	0	0	0	0	0	0	0	0	0	0	0	0
	Carex humilis	0	0	0	0	0	0	0	0	0	0	0	0	0	0	36
	Carex divulsa	0	24	0	0	0	90	0	0	0	0	0	0	0	0	0
	Cyperus rotundus	529	0	0	23	0	0	0	0	0	0	0	0	0	0	0
Cyperaceae		529	121	0	23	0	90	0	0	0	0	0	0	0	0	36
	Taraxacum officinale	0	0	0	0	137	0	0	0	0	0	0	0	0	0	52
	Lapsana communis	0	0	0	0	0	0	0	0	0	0	0	0	0	16	0
	Artemisia annua	416	540	0	157	0	1152	0	0	36	0	0	0	0	0	0
	Artemisia vulgaris	0	0	0	0	0	0	0	0	0	0	0	0	0	0	7
	Anthemis sp.	0	0	0	0	0	0	0	0	0	0	0	40	3632	135	156
	Tanacetum parthenium	0	0	0	0	0	0	0	0	0	0	0	9	14	9	17

Appendix II

Continue ⟶

Family	Taxon	100 m	200 m	300 m	400 m	600 m	700 m	800 m	900 m	1000 m	1100 m	1200 m	1300 m	1400 m	1500 m	1700 m
	Conyza bonariensis	81	0	0	0	0	0	0	0	0	0	0	0	0	0	0
	Xanthium strumarium	14	0	0	0	0	0	0	0	0	0	0	0	0	0	0
	Scorzonera papposa	0	0	0	0	0	0	0	0	0	0	0	0	0	0	137
Asteraceae		511	540	0	157	137	1152	0	0	36	0	0	49	3646	160	369
	Carpinus betulus	0	2942	8	20	153	1854	7391	718	9066	50	86	3139	140	126	201
	Alnus glutinosa	0	2225	69	75	3288	900	5085	947	1391	347	523	2040	49	288	86
	Alnus subcordata	0	0	0	0	175	0	35	3	1131	1405	0	2421	0	850	30
Betulaceae		0	5167	77	95	3616	2754	12511	1668	11588	1802	609	7600	189	1264	317
	Fagus orientalis	0	0	0	0	0	36	49	39	27	0	0	0	219	0	0
	Fagus sylvatica	0	0	0	0	206	0	47	0	9	0	0	0	0	658	3645
	Quercus sp.	0	7711	0	160	495	1701	1329	9	570	0	0	377	0	10	0
	Quercus castaneifolia	0	245	0	0	0	0	163	0	7	0	0	0	0	0	0
Fagaceae		0	7956	0	160	701	1737	1588	48	613	0	0	377	219	668	3645
	Zelkova carpinifolia	0	764	0	0	0	2206	56	0	0	0	0	16	0	0	0
	Ulmus minor	0	581	13	0	231	0	0	0	0	0	0	0	0	17	0
Ulmaceae		0	1345	13	0	231	2206	56	0	0	0	0	16	0	17	0
	Oplismenus undulatifolius	0	69	0	0	0	146	0	0	0	0	0	0	0	0	0
	Poa bulbosa	0	9	0	0	0	0	0	0	0	0	0	0	0	0	0
	Digitaria sanguinalis	0	30	0	0	0	0	0	0	0	0	0	0	0	0	0
	Oryza sativa	0	234	0	0	0	22	20	0	4	0	0	0	0	0	0
	Brachypodium sylvaticum	0	27	0	0	0	365	0	0	0	0	0	0	0	0	0
	Zea mays	0	0	0	0	0	0	0	0	6	0	0	0	0	0	0
	Sorghum halepense	0	28	0	0	0	0	0	0	0	0	0	0	0	0	0
	Lolium multiflorum	0	0	0	0	0	0	0	0	0	16	0	0	0	0	0
	Echinochloa crus-galli	0	0	0	0	0	17	0	0	0	0	0	0	0	0	0
	Paspalum dilatatum	0	68	0	18	0	0	43	0	0	0	0	0	0	0	0

Appendix II

Continue ⟶

Family	Taxon	100 m	200 m	300 m	400 m	600 m	700 m	800 m	900 m	1000 m	1100 m	1200 m	1300 m	1400 m	1500 m	1700 m
	Poa trivialis	0	37	0	0	44	0	0	0	0	0	0	7	0	0	0
Poaceae		0	502	0	18	44	550	63	0	10	16	0	7	0	0	0
	Origanum vulgare	0	0	0	0	0	167	0	0	0	0	0	0	0	0	0
	Salvia reuteriana	0	0	0	0	0	0	0	0	0	0	0	0	0	2	122
	Prunella vulgaris	0	0	0	0	0	0	0	0	0	0	0	0	0	158	37
	Clinopodium vulgare	0	0	0	0	123	0	0	0	0	0	0	0	0	320	83
Lamiaceae		0	0	0	0	123	167	0	0	0	0	0	0	0	480	242
	Juniperus communis	0	292	0	0	0	0	0	0	0	0	0	0	0	0	0
	Juniperus polycarpos	0	185	0	0	0	27	140	5	0	0	0	81	0	0	0
Cupressaceae		0	477	0	0	0	27	140	5	0	0	0	81	0	0	0
	Primula vulgaris	0	0	0	0	0	0	0	0	0	0	0	129	0	0	56
	Primula veris	0	0	0	0	0	0	0	0	0	0	0	39	0	0	4
Primulaceae		0	0	0	0	0	0	0	0	0	0	0	168	0	0	60
	Fragaria vesca	0	0	0	0	0	0	0	0	0	0	262	0	606	0	14
	Prunus avium(cerasus avium)	0	0	0	0	0	0	12	0	0	0	0	0	0	0	0
	Rubus idaeus	0	0	0	97	9	0	0	0	5	0	0	0	0	0	0
	Cotoneaster multiflorus	0	28	0	0	8	0	0	0	0	0	0	0	0	0	26
	Geum urbanum	0	0	0	0	0	0	0	0	0	0	0	0	0	8	0
	Potentilla reptans	0	111	0	0	0	0	0	0	0	0	0	0	0	0	0
	Prunus cerasifera	0	0	0	0	66	0	0	0	0	0	0	0	0	0	0
	Potentila reptans	0	110	0	0	0	0	0	0	0	0	0	0	0	0	0
	Potentilla micrantha	0	0	0	0	0	0	0	0	0	0	0	159	0	736	121
Rosaceae		0	249	0	97	83	0	12	0	5	0	262	159	606	744	161
	Pimpinella saxifraga	0	0	0	0	0	0	0	0	0	0	0	0	0	15	568
	Daucus carota	0	0	0	11	0	0	0	0	0	0	0	0	0	0	0
	Turgenia latifolia	0	0	0	0	13	0	0	0	0	0	0	0	0	0	0

Appendix II

Continues ⟶

Family	Taxon	100 m	200 m	300 m	400 m	600 m	700 m	800 m	900 m	1000 m	1100 m	1200 m	1300 m	1400 m	1500 m	1700 m
Apiaceae		0	0	0	11	13	0	0	0	0	0	0	0	0	15	568
	Picea orientalis	0	32	0	0	0	0	97	0	0	0	0	0	0	0	0
	Pinus taeda	0	175	0	0	0	0	0	0	0	0	0	0	0	0	0
Pinaceae		0	207	0	0	0	0	97	0	0	0	0	0	0	0	0
	Sambucus ebulus	0	19	0	0	0	0	0	0	0	0	22	60	172	157	25
	Sambucus nigra	0	54	0	0	25	0	0	0	35	0	0	0	380	470	125
Adoxaceae		0	73	0	0	25	0	0	0	35	0	22	60	552	627	150
	Acer velutinum	0	0	0	0	16	0	246	76	0	0	0	36	0	0	12
	Acer platanoides	0	28	0	0	0	0	0	0	0	0	0	0	0	0	0
	Acer cappadocicum	0	0	0	0	0	0	7	0	0	0	0	0	0	0	0
	Acer hyrcanum	0	0	0	33	16	549	571	7181	27	27	0	56	0	0	0
Sapindaceae		0	28	0	33	32	549	824	7257	27	27	0	92	0	0	12
	Veronica persica	0	8	0	0	2398	0	0	0	0	0	0	8	0	11	0
	Plantago major	0	9	0	0	0	0	0	0	0	0	0	0	0	0	0
Plantaginaceae		0	17	0	0	2398	0	0	0	0	0	0	8	0	11	0
	Dianthus hymenolepis	0	0	0	4	0	2	0	0	0	0	0	22	0	0	9
	Stellaria pallida	0	0	0	0	19	0	0	0	0	0	0	13	0	0	0
Caryophyllaceae		0	0	0	4	19	2	0	0	0	0	0	35	0	0	9
	Chenopodium album	0	18	0	0	0	0	0	0	0	0	0	0	0	0	0
	Amaranthus hybridus	0	51	0	0	0	0	0	0	0	0	0	0	0	0	0
	Salsola dendroides	0	44	0	0	0	0	0	0	0	0	0	0	0	0	0
	Panderia pilosa	0	0	0	0	0	0	0	0	0	0	0	37	0	0	0
	Halocnemum strobilaceum	0	21	0	0	0	0	0	0	0	0	0	21	0	0	0
	Salsola vermiculata	0	32	0	0	0	0	0	0	0	0	0	0	0	0	0
	Phedimus spurius	0	0	0	0	0	0	0	0	0	0	0	0	0	19	0
Amaranthaceae		0	166	0	0	0	0	0	0	0	0	0	58	0	19	0

Appendix II

Continue ⟶

Family	Taxon	100 m	200 m	300 m	400 m	600 m	700 m	800 m	900 m	1000 m	1100 m	1200 m	1300 m	1400 m	1500 m	1700 m
	Sinapis arvensis	0	0	0	0	0	0	0	0	0	0	0	0	0	0	5
	Brassica oleracea	0	0	4682	0	0	0	0	0	0	23	0	0	0	0	0
	Brassica napus	0	0	3329	0	0	0	0	0	0	0	0	0	0	0	0
	Brassica rapa	0	0	4044	0	0	0	0	0	0	0	0	0	0	7	0
Brassicaceae		0	0	12055	0	0	0	0	0	0	23	0	0	0	7	5
	Cucumis melo	0	0	0	0	0	0	0	0	0	73	0	0	0	0	0
	Cucurbita pepo	138	45	0	0	0	0	0	0	0	0	129	0	0	0	0
	Ecballium elaterium	0	0	61	0	68	0	0	0	0	0	0	0	0	26	0
Cucurbitaceae		138	45	61	0	68	0	0	0	0	73	129	0	0	26	0
	Viola odorata	0	0	0	0	24	0	0	0	0	0	0	0	0	0	0
	Viola reichenbachiana	0	0	0	0	0	0	0	0	0	0	0	0	0	4	0
Violaceae		0	0	0	0	24	0	0	0	0	0	0	0	0	4	0
	Viscum album	0	16	0	0	0	0	66	0	0	0	0	0	0	0	0
	Arceuthobium oxycedri	0	48	0	0	0	0	0	0	6	0	0	0	0	0	11
Santalaceae		0	64	0	0	0	0	66	0	6	0	0	0	0	0	11
	Cannabis sativa	0	0	0	0	0	9	0	0	0	0	0	0	0	0	0
	Humulus lupulus	0	183	0	0	0	0	0	0	0	0	0	0	0	0	0
Cannabaceae		0	183	0	0	0	9	0	0	0	0	0	0	0	0	0
	Paliurus sp.	0	0	0	21	0	0	0	0	0	0	0	0	0	0	0
	Ziziphus jujuba	0	0	0	0	0	0	26	0	0	0	0	0	0	0	0
Rhamnaceae		0	0	0	21	0	0	26	0	0	0	0	0	0	0	0
	Pterocarya fraxinifolia	0	298	24	0	69	19	51	0	0	26	0	0	0	0	0
	Juglans regia	0	739	184	0	293	179	673	105	0	0	0	0	0	21	0
Juglandaceae		0	1037	208	0	362	198	724	105	0	26	0	0	0	21	0
Hamamelidaceae	*Parrotia persica*	0	922	0	0	0	28	0	11	9	0	0	29	0	0	0
Boraginaceae	*Cynoglossum officinale*	0	0	0	0	0	0	0	0	0	0	0	0	0	0	15

Appendix II

Continue ⟶

Family	Taxon	100 m	200 m	300 m	400 m	600 m	700 m	800 m	900 m	1000 m	1100 m	1200 m	1300 m	1400 m	1500 m	1700 m
Malvaceae	*Tilia cordata*	0	0	0	0	0	0	0	0	0	0	0	18	0	0	0
Rubiaceae	*Galium rotundifolium*	0	0	0	0	0	0	0	0	0	0	0	0	0	19	0
Convolvulaceae	*Calystegia sepium*	0	32	0	0	0	0	0	0	0	0	33	0	0	0	0
Euphorbiaceae	*Acalypha australis*	22	214	0	0	0	0	0	0	7	0	0	0	0	0	0
Urticaceae	*Urtica dioica*	0	5	0	0	0	0	0	0	15	0	0	72	0	0	0
Moraceae	*Morus alba*	0	14	0	0	0	0	0	0	0	0	0	0	0	0	0
Aquifoliaceae	*Ilex spinigera*	0	0	0	0	0	0	0	0	0	0	0	58	0	0	0
Pontederiaceae	*Monochoria vaginalis*	0	0	0	0	0	0	0	0	0	0	21	0	0	0	7
Salicaceae	*Populus deltoides*	0	12	0	0	0	0	0	0	0	0	0	0	0	0	0
Musaceae	*Musa basjoo*	88	33	0	324	4192	0	0	0	12	486	1354	0	0	7	0
Platanaceae	*Platanus orientalis*	0	83	0	0	0	0	0	0	0	0	0	0	0	8	0
Amaryllidaceae	*Allium schoenoprasum*	0	0	0	15	0	0	0	0	0	0	0	0	0	0	0
Geraniaceae	*Geranium molle*	0	0	0	0	0	0	0	0	0	0	34	0	7	0	12
Buxaceae	*Buxus sempervirens*	0	0	0	0	0	72	0	0	0	0	0	0	0	0	0
Hypericaceae	*Hypericum androsaemum*	0	0	0	0	0	0	0	0	0	0	0	0	58	17	0
Smilacaceae	*Smilax excelsa*	0	1755	0	0	0	0	0	0	0	0	0	0	0	0	0
Polygonaceae	*Rumex patientia*	0	0	0	0	0	0	0	0	0	0	0	0	0	0	23
Polygonaceae	*Rumex bucephalophorus*	0	0	0	0	0	0	0	0	0	0	6	0	0	0	0
Oxalidaceae	*Oxalis corniculata*	0	0	0	0	38	0	0	0	0	0	0	0	0	0	0
Oleaceae	*Fraxinus excelsior*	0	399	0	0	32	118	150	24	0	0	0	0	0	0	0
Theaceae	*Camellia sinensis*	0	0	25	36	0	0	0	0	0	0	27	0	0	0	0
Solanaceae	*Solanum tuberosum*	0	0	0	0	0	0	0	0	0	0	0	0	0	0	17
Gentianaceae	*Centaurium tenuiflorum*	0	0	0	0	0	0	0	0	0	0	4	0	0	0	0

Complete number of metabarcoding reads at the Asalem-Khalkhal transect

Family	Taxon	2300 m	2000 m	1800 m	1700 m	1600 m	1400 m	1300 m	1200 m	1100 m	900 m	700 m	600 m	500 m	400 m	300 m	200 m	100 m
	Trifolium tumens	0	0	1736	0	0	0	5	0	0	0	0	0	0	0	0	0	0
	Trifolium hybridum	0	0	54	0	0	0	0	0	9	0	0	0	0	0	0	0	0
	Trifolium repens	0	0	0	0	0	0	0	3	0	0	5	0	0	0	0	0	0
	Melilotus officinalis	0	0	0	0	0	0	0	0	0	0	0	0	0	8	0	0	0
	Onobrychis cornuta	0	0	0	9	0	0	0	0	0	0	0	0	0	0	0	0	0
	Vicia faba	0	0	0	0	0	0	0	0	0	0	0	4	0	0	0	0	0
Fabaceae		0	0	1790	9	0	0	5	3	9	0	5	4	0	8	0	0	0
	Carex sp.	0	0	0	0	0	0	13	0	0	0	0	0	0	0	167	0	0
	Cyperus rotundus	0	0	0	0	0	0	0	2	0	0	0	0	0	0	13	62	0
Cyperaceae		0	0	0	0	0	0	13	2	0	0	0	0	0	0	180	62	0
	Cirsium arvense	185	0	0	0	0	0	0	0	0	0	0	0	0	0	0	0	0
	Achillea millefolium	0	0	45	0	0	0	0	0	0	0	0	0	0	0	0	0	0
	Taraxacum officinale	0	245	1282	0	0	0	0	0	0	0	0	0	0	10	0	0	0
	Lapsana communis	0	0	86	0	0	0	0	0	0	0	0	0	0	0	0	0	0
	Artemisia annua	0	0	0	0	134	0	0	0	0	0	0	0	0	0	0	2890	73
	Achillea sp.	0	7283	0	0	0	0	0	0	0	0	0	0	0	0	0	0	0
	Cousinia kornhuberi	0	16	0	0	0	0	0	0	0	0	0	0	0	0	0	0	0
	Lactuca sativa	0	0	0	0	48	0	0	0	0	0	0	0	0	0	0	0	0
	Solidago canadensis	0	0	0	0	0	0	123	0	0	0	0	0	0	0	0	0	0
	Silybum marianum	536	0	0	0	0	0	0	0	0	0	0	0	0	0	0	0	0
	Sigesbeckia orientalis	0	0	0	0	0	0	0	0	0	0	0	0	0	20	0	0	0
	Senecio vulgaris	0	0	0	1172	0	0	0	0	0	0	0	0	0	0	0	0	0
	Helianthus annuus	0	0	0	0	0	0	0	0	0	0	0	0	0	0	11	0	0
	Erigeron canadensis	0	0	0	0	0	0	0	0	0	0	0	0	0	0	0	12	0
	Xanthium strumarium	0	0	0	0	0	0	0	0	0	0	0	0	0	0	0	33	0
Asteraceae		721	7544	1413	1172	182	0	123	0	0	0	0	0	0	30	11	2935	73
	Alnus subcordata	0	0	34	0	0	0	125	27	58	0	0	27	155	733	148	317	0
	Carpinus betulus	0	0	148	204	261	132	17	875	154	51	1643	172	205	210	223	0	0
	Alnus glutinosa	0	0	0	399	111	0	0	189	50	0	202	17	82	332	62	238	0
Betulaceae		0	0	182	603	372	132	142	1091	262	51	1845	216	442	1275	433	555	0
	Fagus sylvatica	0	0	723	0	4476	0	0	1262	0	0	669	0	0	0	0	0	0
	Fagus orientalis	0	0	0	0	0	130	212	0	200	20	0	0	35	54	27	34	0
	Quercus macranthera	0	0	0	0	0	0	0	0	0	0	9	0	0	0	0	0	0
	Quercus sp.	0	0	0	138	120	0	0	0	0	0	383	0	0	0	0	0	0
	Quercus suber	0	0	0	0	0	0	0	0	0	0	8	0	0	0	0	0	0

Appendix II

Continue →

Family	Taxon	2300 m	2000 m	1800 m	1700 m	1600 m	1400 m	1300 m	1200 m	1100 m	900 m	700 m	600 m	500 m	400 m	300 m	200 m	100 m
Fagaceae		0	0	723	138	4596	130	212	1262	200	20	1069	0	35	54	27	34	0
	Sambucus ebulus	0	0	33	0	51	0	0	0	0	0	10	0	0	0	0	0	0
	Sambucus nigra	0	0	214	0	45	0	0	0	0	0	10	0	0	0	0	0	0
Adoxaceae		0	0	247	0	96	0	0	0	0	0	20	0	0	0	0	0	0
	Acer velutinum	0	0	0	0	0	79	21	0	14	0	0	32	0	0	35	0	0
	Acer hyrcanum	0	0	0	0	27	77	0	58	37	13	21	61	0	23	21	0	0
	Acer platanoides	0	0	0	0	0	0	0	147	0	0	51	0	14	0	0	0	0
	Acer cappadocicum	0	0	0	0	0	27	0	63	0	0	23	0	0	7	17	0	0
Sapindaceae		0	0	0	0	27	183	21	268	51	13	95	93	14	30	73	0	0
	Parietaria judaica	0	0	0	0	0	0	0	0	0	0	31	346	95	21	1498	0	0
	Parietaria officinalis	0	0	0	0	0	0	0	0	0	0	0	105	8	0	243	0	0
	Urtica dioica	0	0	0	9	0	438	0	0	0	0	0	0	0	0	0	0	0
Urticaceae		0	0	0	9	0	438	0	0	0	0	31	451	103	21	1741	0	0
	Ecballium elaterium	0	0	16	0	0	0	46	0	667	23	230	0	0	0	761	0	0
	Cucurbita pepo	0	0	0	0	26	0	0	0	0	0	0	8	0	0	0	18	0
Cucurbitaceae		0	0	16	0	26	0	46	0	667	23	230	8	0	0	761	18	0
	Oplismenus undulatifolius	0	0	0	0	0	0	0	0	0	0	0	0	0	0	1288	0	0
	Agrostis gigantea	0	0	29	0	0	0	0	0	0	0	0	0	0	0	0	0	0
	Sorghum halepense	0	0	0	0	0	0	0	0	0	0	0	0	0	0	0	130	146
	Oryza sativa	0	0	0	0	0	0	0	3	0	0	0	0	0	0	0	187	521
	Thinopyrum intermedium	0	0	0	0	0	0	0	0	14	0	0	0	0	0	0	0	0
	Paspalum dilatatum	0	0	0	0	0	0	0	0	0	0	0	0	0	0	0	0	292
	Zea mays	0	0	0	0	0	0	0	0	0	0	0	0	0	201	44	0	0
	Avena fatua	0	0	0	50	0	0	0	0	0	0	0	0	0	0	0	0	0
	Secale cereale	0	123	0	47	0	0	0	11	0	0	0	0	0	9	0	13	57
Poaceae		0	123	29	97	0	0	0	14	14	0	0	0	0	210	1332	330	1016
	Juniperus communis	0	0	0	0	9	0	0	0	0	0	0	0	0	0	0	0	8
	Juniperus polycarpos	0	0	0	87	0	0	0	0	0	0	0	0	0	0	0	0	0
Cupressaceae		0	0	0	87	9	0	0	0	0	0	0	0	0	0	0	0	8
	Fragaria vesca	0	0	103	0	0	0	0	0	0	0	0	0	0	0	0	0	0
	Cotoneaster multiflorus	0	0	44	0	0	0	0	0	0	0	0	0	0	0	0	0	30
	Prunus avium	0	0	0	0	0	0	0	0	0	0	28	0	0	0	0	0	0
	Rubus idaeus	0	0	0	0	0	0	0	0	0	0	0	237	0	67	11	0	0
	Prunus armeniaca	0	0	44	0	0	0	0	0	0	0	0	0	0	0	0	0	0
	Alchemilla arvensis	0	0	0	0	0	4	0	0	0	0	0	0	0	0	0	0	0
	Malus domestica	0	0	0	0	0	0	0	0	0	0	0	0	0	3	0	0	0
	Geum urbanum	0	0	0	0	0	0	0	0	0	0	0	0	0	0	19	0	0

Appendix II

Continue →

Family	Taxon	2300 m	2000 m	1800 m	1700 m	1600 m	1400 m	1300 m	1200 m	1100 m	900 m	700 m	600 m	500 m	400 m	300 m	200 m	100 m
Rosaceae		0	0	191	0	0	4	0	0	0	0	28	237	0	70	30	0	30
	Solanum dulcamara	0	0	0	0	0	64	0	0	308	0	0	0	0	0	0	0	0
	Solanum tuberosum	0	0	0	0	0	0	0	0	0	0	0	0	4	0	0	0	0
Solanaceae		0	0	0	0	0	64	0	0	308	0	0	0	4	0	0	0	0
	Ulmus minor	0	0	0	0	0	28	0	403	2119	4	2414	63	17	55	0	0	0
	Zelkova carpinifolia	0	0	0	0	0	0	0	0	0	0	37	0	0	0	0	0	0
Ulmaceae		0	0	0	0	0	28	0	403	2119	4	2451	63	17	55	0	0	0
	Abies nordmanniana	0	0	0	0	0	0	7	0	0	0	0	0	0	0	0	0	0
	Picea abies	0	0	0	0	0	0	0	3	0	0	0	0	0	0	0	0	0
	Abies grandis	0	0	0	0	0	0	0	0	17	0	0	0	0	0	0	0	0
Pinaceae		0	0	0	0	0	0	7	3	17	0	0	0	0	0	0	0	0
	Plantago lanceolata	0	0	0	2	0	0	0	0	0	0	0	0	0	0	0	0	0
	Plantago major	0	0	0	0	0	0	0	0	0	0	0	0	0	0	0	0	72
Plantaginaceae		0	0	0	2	0	0	0	0	0	0	0	0	0	0	0	0	72
	Eryngium maritimum	0	0	0	19	0	0	0	0	0	0	0	0	0	0	0	0	0
	Coriandrum sativum	29	0	0	0	0	0	0	0	0	0	0	0	0	0	0	0	0
Apiaceae		29	0	0	19	0	0	0	0	0	0	0	0	0	0	0	0	0
	Galium tricornutum	0	19	0	0	0	0	0	0	0	0	0	0	0	0	0	0	0
	Galium rotundifolium	0	0	282	0	0	0	0	0	0	0	0	0	0	0	0	0	0
Rubiaceae		0	19	282	0	0	0	0	0	0	0	0	0	0	0	0	0	0
	Chenopodium album	0	0	0	5	0	0	0	0	0	0	0	0	0	0	0	0	0
	Salsola vermiculata	0	0	0	0	0	0	0	0	0	0	0	0	0	0	0	0	140
	Suaeda microphylla	0	0	0	0	0	0	0	0	0	0	0	0	0	0	0	15	0
	Amaranthus retroflexus	0	0	0	0	16	0	0	0	0	0	0	0	0	0	0	0	0
Amaranthaceae		0	0	0	5	16	0	0	0	0	0	0	0	0	0	0	15	140
	Brassica rapa	0	0	0	0	0	0	0	0	0	0	0	0	0	0	8	27	0
	Cardamine impatiens	0	0	0	0	12	19	0	0	0	0	14	0	0	0	0	0	0
	Brassica oleracea	0	0	0	0	0	0	0	4	0	0	0	0	0	0	9	0	0
	Brassica napus	0	0	0	0	0	0	0	0	0	0	15	3	0	0	0	0	32
	Cardamine bulbifera	0	0	0	0	0	9	0	0	0	0	0	0	0	0	0	0	0
Brassicaceae		0	0	0	0	12	28	0	4	0	0	29	3	0	0	17	27	32
	Rumex patientia	0	0	0	0	0	0	0	0	0	0	0	0	0	0	23	0	0
	Polygonum aviculare	120	0	0	8	0	0	0	0	0	0	0	0	0	0	0	0	0
Polygonaceae		120	0	0	8	0	0	0	0	0	0	0	0	0	0	23	0	0
	Hypericum perforatum	0	0	46	24	0	0	0	0	0	0	0	0	0	0	0	0	0
	Hypericum androsaemum	0	0	0	0	0	0	0	0	0	0	0	0	0	0	8	0	0
Hypericaceae		0	0	46	24	0	0	0	0	0	0	0	0	0	0	8	0	0

Appendix II

Continue →

Family	Taxon	2300 m	2000 m	1800 m	1700 m	1600 m	1400 m	1300 m	1200 m	1100 m	900 m	700 m	600 m	500 m	400 m	300 m	200 m	100 m
Caryophyllaceae	*Dianthus hymenolepis*	22	0	0	13	0	0	0	0	0	0	0	0	0	0	9	75	0
Euphorbiaceae	*Acalypha australis*	0	0	0	0	0	0	0	0	0	0	0	0	0	11	0	0	0
Ebenaceae	*Diospyros lotus*	0	0	0	0	0	0	0	0	0	0	0	0	0	403	0	0	0
Convolvulaceae	*Cuscuta sp.*	0	0	0	0	0	0	0	0	0	0	0	0	0	15	4	0	0
Rhamnaceae	*Ziziphus jujuba*	0	0	0	0	0	0	0	0	0	0	0	0	0	0	0	360	0
Campanulaceae	*Campanula rapunculus*	0	0	23	0	0	0	0	0	0	0	0	0	0	0	0	0	0
Linaceae	*Linum bienne*	0	0	0	0	0	0	0	0	0	0	11	0	0	0	0	0	0
Gentianaceae	*Centaurium tenuiflorum*	0	0	0	0	0	0	0	0	0	0	0	0	0	0	11	0	0
Actinidiaceae	*Actinidia chinensis*	0	0	0	0	0	0	0	0	0	0	0	0	0	0	0	0	60
Moraceae	*Ficus carica*	0	0	0	0	0	0	0	0	0	0	0	0	0	0	0	0	12
Musaceae	*Musa basjoo*	0	0	0	0	163	0	0	0	0	0	0	0	0	0	0	0	0
Juglandaceae	*Juglans regia*	0	0	205	46	0	0	0	0	0	399	0	0	0	0	37	0	51
Boraginaceae	*Myosotis propinqua*	0	0	23	0	0	0	0	0	0	0	0	0	0	0	0	0	0
Anacardiaceae	*Pistacia atlantica*	0	0	0	0	11	0	0	0	0	0	0	0	0	9	0	0	0
Lamiaceae	*Clinopodium vulgare*	0	0	0	0	0	0	0	79	0	0	0	0	0	0	0	0	0
Onagraceae	*Circaea lutetiana*	0	0	0	0	0	0	0	0	0	0	0	25	0	0	8	0	0
Hamamelidaceae	*Parrotia persica*	0	0	0	0	0	0	0	0	0	0	0	0	0	41	58	0	0
Lythraceae	*Lythrum salicaria*	0	0	0	0	0	0	0	0	0	0	0	0	0	0	0	0	61
Violaceae	*Viola odorata*	0	0	10	0	0	0	0	0	0	0	0	0	0	0	0	0	0
Bromeliaceae	*Ananas comosus*	0	0	0	0	0	0	0	0	0	0	49	87	0	80	0	0	0
Santalaceae	*Arceuthobium oxycedri*	0	0	0	0	20	0	0	110	0	0	0	0	0	12	0	0	0
Oleaceae	*Fraxinus excelsior*	0	0	0	57	0	0	9	0	0	0	0	104	0	0	0	0	0
Theaceae	*Camellia sinensis*	0	0	0	0	0	0	41	0	52	0	0	0	0	0	0	0	0
Malvaceae	*Tilia hyrcana*	0	0	0	0	0	0	0	0	5	0	0	22	0	37	130	0	0

Appendix II:

List of selected pollen, spores and Non-Pollen Palynomorphs (NPPs)

Picture No.	Pollen familiy	Pollen taxon
1	Betulaceae	*Alnus*
2	Amaranthaceae	Amaranthaceae-type
3	Asteraceae	*Ambrosia*
4	Apiaceae	Apiaceae-type
5	Asteraceae	*Artemisia*
6	Asteraceae	Asteraceae-type
7	Betulaceae	*Betula*
8	Brassicaceae	Brassicaceae-type
9	Buxaceae	*Buxus*
10	Campanulaceae	Campanulaceae-type
11	Cannabaceae	*Cannabis-Humulus*-type
12	Betulaceae	*Carpinus*
13	Caryophyllaceae	Caryophyllaceae
14	Poaceae	Cerealia-type
15	Asteraceae	Cichoroideae
16	Cyperaceae	Cyperaceae-type
17	Fabaceae	Fabaceae-type
18	Fagaceae	*Fagus*
19	Oleaceae	*Fraxinus*
20	Iridaceae	Iridaceae
21	Juglandaceae	*Juglans*
22	Juniperaceae	*Juniperus*
23	Lamiaceae	Lamiaceae-type
24	Oxalidaceae	*Oxalis*
25	Poaceae	Poaceae-type
26	Rosaceae	*Prunus*
27	Pinaceae	*Pinus*
28	Plantaginaceae	*Plantago lanceolata* - type
29	Juglandaceae	*Pterocarya*
30	Fagaceae	*Quercus*
31	Rosaceae	Rosaceae-type
32	Salicaceae	*Salix*
33	Ranunculaceae	*Thalictrum*
34	Malvaceae	*Tilia*
35	Ulmaceae	*Ulmus*
36	Lentibulariaceae	*Utricularia*
37	Ulmaceae	*Zelkova*
38		*Glomus*
39		*Pediastrum*
40		*Sordaria* - type
41		Trilete spore

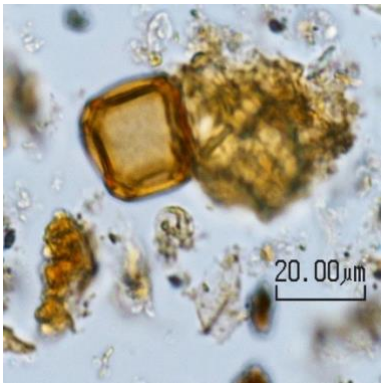

1. *Alnus* (4 pores)

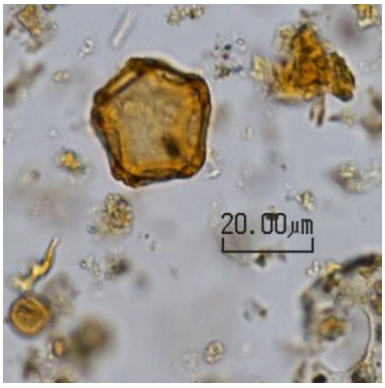

1. *Alnus* (5 pores)

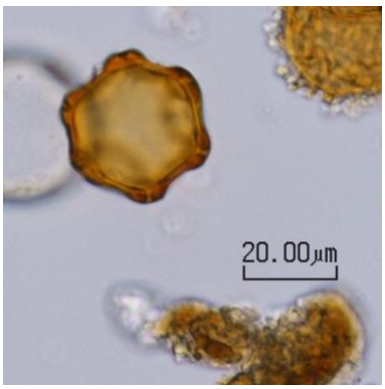

1. *Alnus* (6 pores)

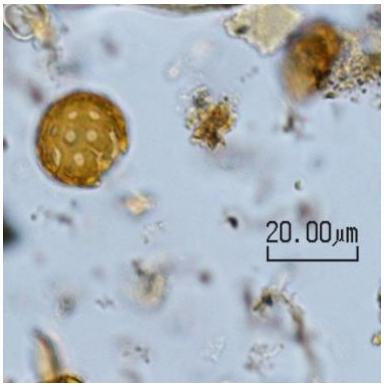

2. Amaranthaceae

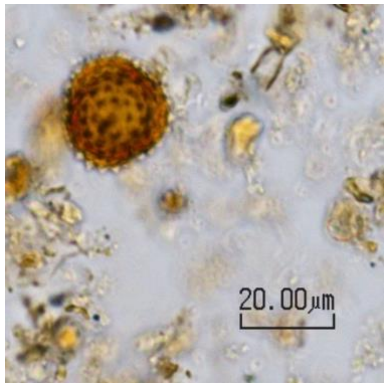

3. *Ambrosia*

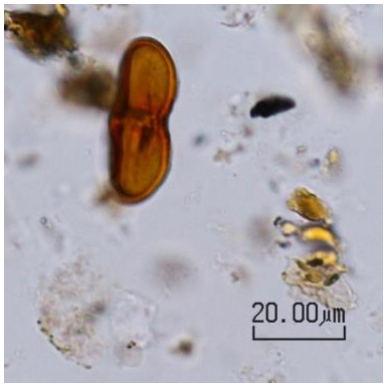

4. Apiaceae

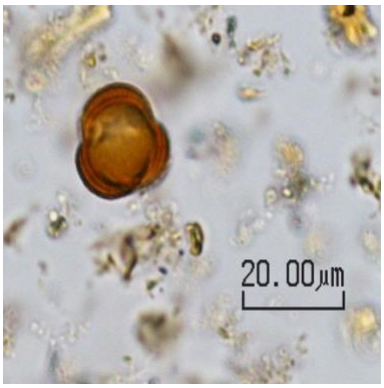

5. *Artemisia*

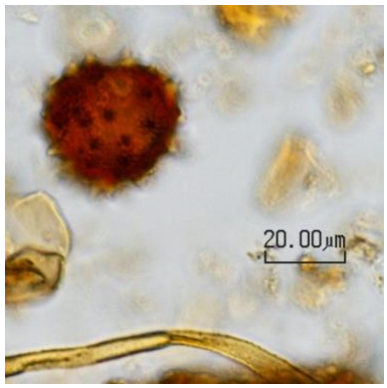

6. Asteraceae

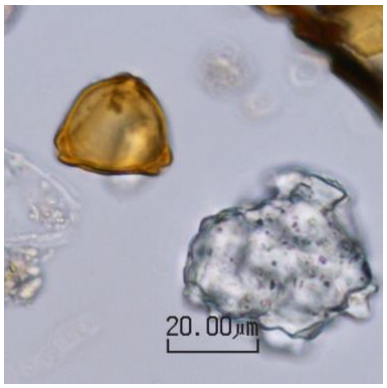

7. *Betula*

8. Brassicaceae

9. *Buxus*

10. Campanulaceae

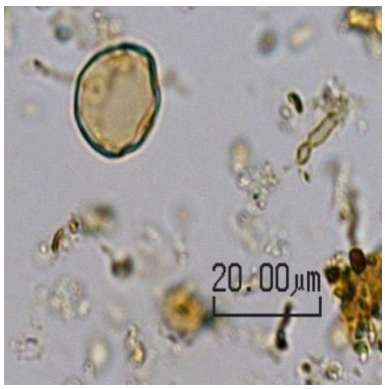

11. *Cannabis-Humulus*-type

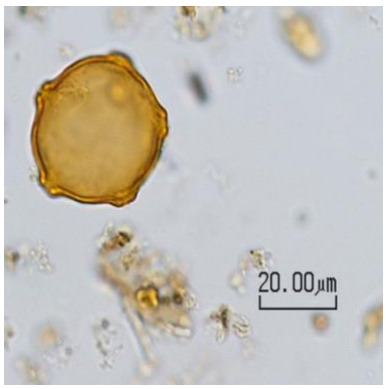

12. *Carpinus*

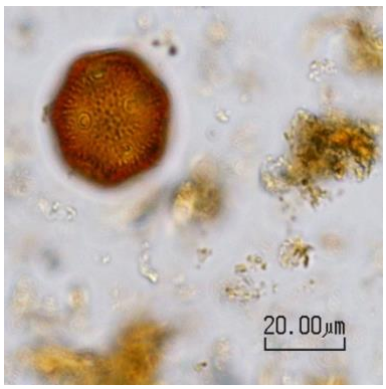

13. Caryophyllaceae

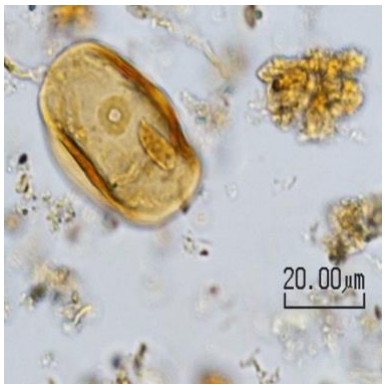

14. Cerealia-type

15. Cichorioideae

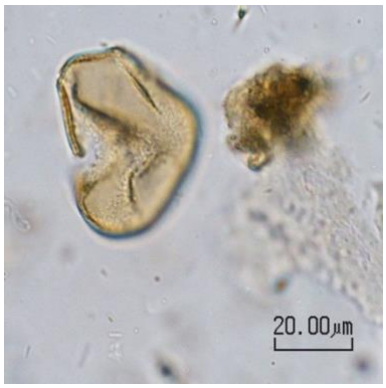

16. Cyperaceae

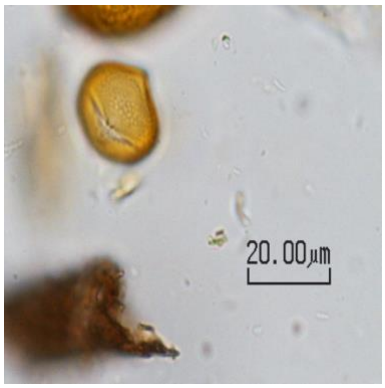

17. Fabaceae (reticulate)

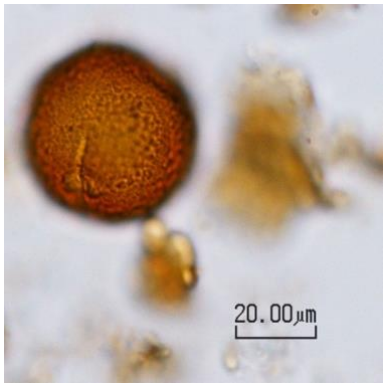

18. *Fagus*

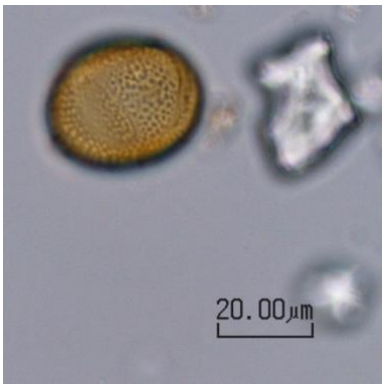

19. *Fraxinus*

20. Iridaceae

21. *Juglans*

22. *Juniperus*

23. Lamiaceae

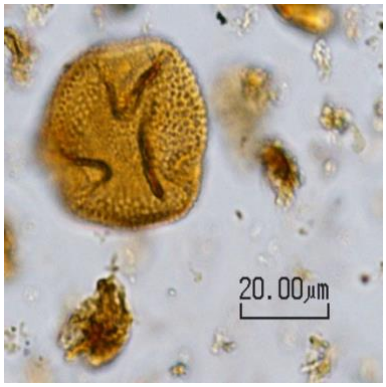

24. *Oxalis*

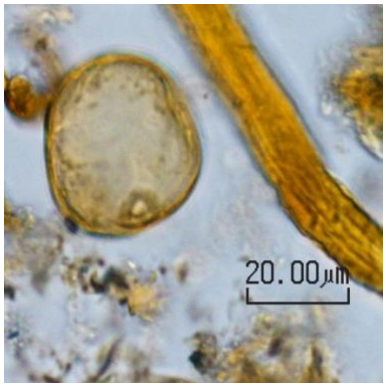

25. Poaceae

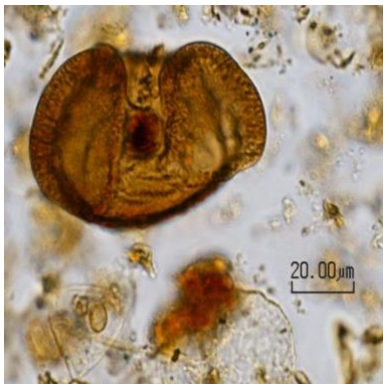

26. *Pinus*

27. *Plantago lanceolata*-type

28. *Prunus*

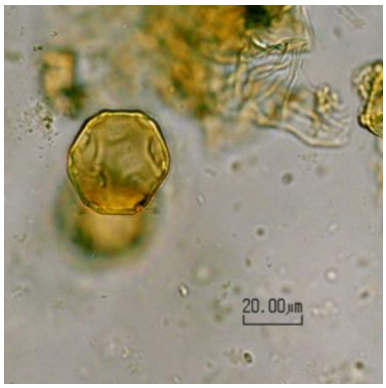

29. *Pterocarya*

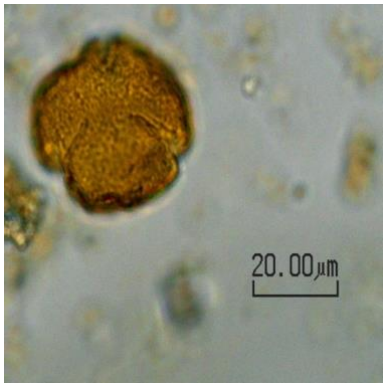

30. *Quercus*

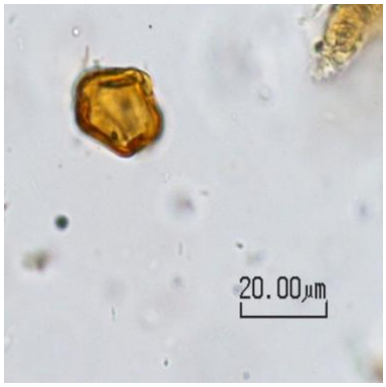

31. Rosaceae

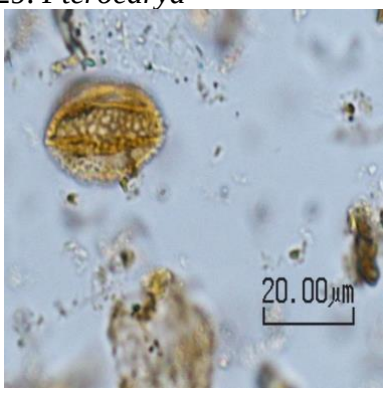

32. *Salix*

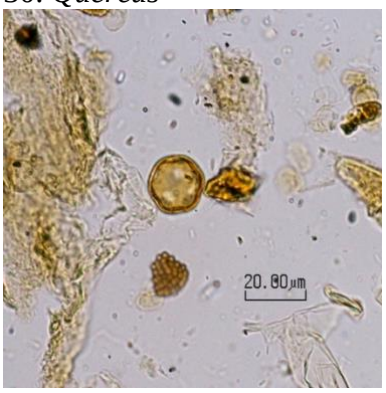

33. *Thalictrum*

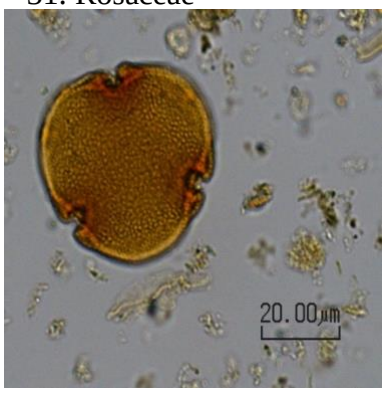

34. *Tilia*

35. *Ulmus*

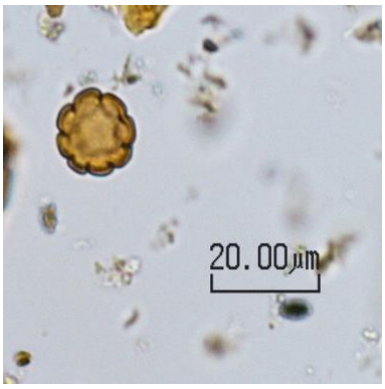

36. *Utricularia*

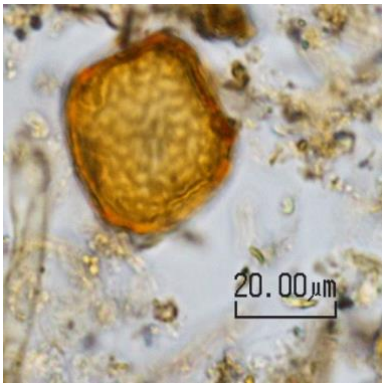

37. *Zelkova*

38. *Glomus*

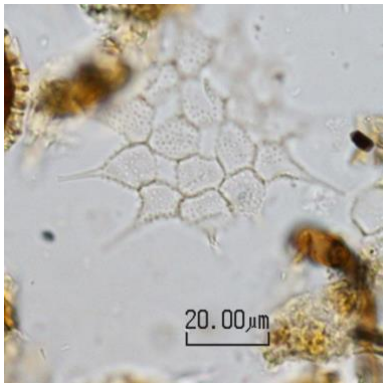

39. *Pediastrum*

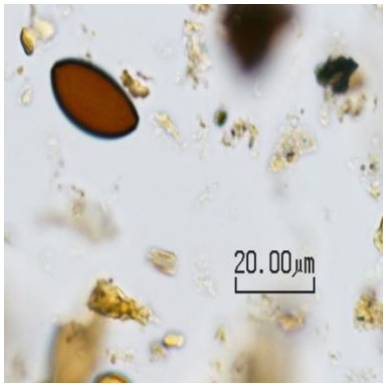

40. *Sordaria*

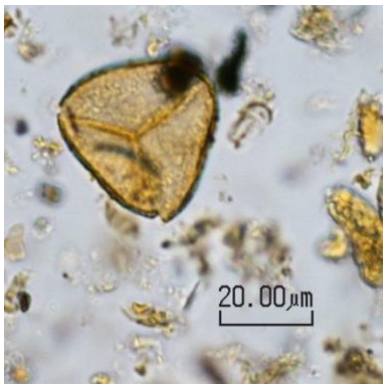

41. Trilete spore

Declaration of Academic Integrity

I hereby confirm that the present dissertation is solely the work of myself. All scientific collaborators appear as co-authors of the manuscripts. If any passages or figures/diagrams from books, papers, the Web or other sources have been copied or in any other way used, all references, including those found in electronic media, have been acknowledged and fully cited.

Leila Homami Totmaj